THE EFFECT OF AERATION RATE AND FREE-FLOATING CARRIER MEDIA ON THE EMISSION OF *BACILLUS GLOBIGII* IN BIOAEROSOLS

THESIS

Andrew J. Owens, Major, USA

AFIT-ENP-MS-20-M-110

DEPARTMENT OF THE AIR FORCE
AIR UNIVERSITY

AIR FORCE INSTITUTE OF TECHNOLOGY

Wright-Patterson Air Force Base, Ohio

AFIT-ENP-MS-20-M-110

THE EFFECT OF AERATION RATE AND FREE-FLOATING CARRIER MEDIA ON THE EMISSION OF *BACILLUS GLOBIGII* IN BIOAEROSOLS

THESIS

Presented to the Faculty

Department of Engineering Physics

Graduate School of Engineering and Management

Air Force Institute of Technology

Air University

Air Education and Training Command

In Partial Fulfillment of the Requirements for the

Degree of Master of Science in Nuclear Engineering

Andrew J. Owens, MS

Major, USA

March 2020

AFIT-ENP-MS-20-M-110

THE EFFECT OF AERATION RATE AND FREE-FLOATING CARRIER MEDIA ON THE EMISSION OF *BACILLUS GLOBIGII* IN BIOAEROSOLS

Andrew J. Owens, MS

Major, USA

Committee Membership:

Dr. Larry W. Burggraf
Chair

Dr. Willie F. Harper, Jr., P.E.
Member

Dr. Adam C. Burdsall
Member

Abstract

Aerosols produced by turbulent mechanical mixing and bubble aeration at Waste Water Treatment Plants (WWTPs) become bioaerosols with the entrainment of biological materials. Bioaerosols become a public health risk when human pathogens are present. This study evaluated bioaerosols containing *Bacillus globigii* (BG) spores, and the effects that aeration rate and the addition of Free-Floating Carrier Media (FFCM) had on the amount of BG spores collected following aerosolization. A series of laboratory-scale experiments investigated two different sizes of floating polystyrene spheres as FFCM and four different aeration rates. When the differences in compared aeration rates were sufficiently large, a positive correlation was observed between increasing aeration rate and increasing bioaerosol production. The maximum increase from 0.50 to 1.00 L/min resulted in a 97.58% increase in the percent of starting BG spores captured after aerosolization. The addition of FFCM of both sizes reduced the amount of BG spores captured when compared to the control. Smaller spheres (0.42 cm diameter) consistently attenuated BG bioaerosol emissions more effectively than those with larger (1.91 cm) diameters, with a mean control efficiency of 93.03% compared to 83.95%. Statistical analysis showed a significant increase in the ability of smaller diameter FFCM to attenuate bioaerosol production at the two higher investigated aeration rates. This study was the first, to the author's knowledge, to investigate multiple effects on bioaerosol production where the aerosol contained strictly bacterial endospores. As a part of a larger investigation, including laboratory scale and pilot-scale WWTP research, this study is the first in a series of studies intended to investigate the effect of experimental scale on

bioaerosol production. Results related to effects due to scale can be applied to better predict bioaerosol behaviors in operating treatment plants.

Acknowledgements

A substantial thank you goes out to Dr. Larry Burggraf for granting me the opportunity to perform research in an area more in-line with my educational background and academic interests, in the wake of the disappearance of my original degree plan. Another large thank you goes out to Dr. Willie Harper Jr., for framing out my research objectives and for his constant mentorship, instruction, and accountability. It was truly an honor for me to work with a great team of talented individuals.

Thank you to Dr. Adam Burdsall and Dr. Yun Xing, who taught me every technique and method utilized in the laboratory, and contributed so much to the experimental design. Their patience and guidance was much appreciated throughout numerous, unannounced office visits. Thank you to Dr. Nicholas Herr for hours and hours of instruction and assistance on the AFM. Thank you to Dr. Daniel Felker for a bevy of laboratory advice, and even more Army war stories. Thank you to Dr. Matthew Magnuson with the EPA for sponsoring this project. The US EPA, through its Office of Research and Development partially funded and collaborated in the research described here under Interagency Agreement DW-057-92440901-3.

To Lucas and Navy, thank you for showing me what things are most important and keeping me grounded during this process. You can accomplish any goal you set with hard work. And to Lisa, thank you for taking care of every aspect of our family during all of this coursework and research, all while maintaining your own career. I will be forever thankful for your love and sacrifices. Thank you for always being there.

Andrew J. Owens

Table of Contents

Page

List of Figures

Page

List of Tables

Page

THE EFFECT OF AERATION RATE AND FREE-FLOATING CARRIER MEDIA ON THE EMISSION OF *BACILLUS GLOBIGII* IN BIOAEROSOLS

I. Introduction

1.1 Introduction

The US Environmental Protection Agency (EPA) National Homeland Security Research Center (NHSRC) is working with environmental engineering professionals to improve water infrastructure security (Office of Research and Development Homeland Security Research Program, 2018). This includes the protection of the more than 14,000 Publicly Owned Treatment Works (POTWs) registered within the United States (US EPA, 2016). This research focused on varying conditions that resulted in changes in the number and concentration of bacterial spores collected following the generation of bioaerosols in lab-scale reactor vessel. The effects of aeration rate and exposed surface area, through the addition of free-floating carrier media (FFCM), on the emission of the spores were investigated. As a part of larger study involving smaller and larger experimental scales, this research contributes to the theoretical modeling for potential behavior in actual wastewater treatment plants (WWTPs). Numerous past studies have examined the extent of biological contamination due to the generation of bioaerosols at WWTPs, but these collective studies are the first focused specifically on bacterial spores. A significant public health threat exists in the event that water intentionally contaminated with *Bacillus anthracis* spores is aerosolized during water treatment processes.

Under the provisions of the 2002 Bioterrorism Act, the EPA-NHSRC and the American Water Works Association (AWWA) collaborated to develop publications and policies for the Planning for an Emergency Water Supply and Emergency Planning for Water and Water Utilities (*Roadmap to a Secure and Resilient Water and Wastewater Sector*, 2017). One critical

and ongoing initiative concerns biocontaminants containing high-consequence pathogens, which can be represented by a wide range of dangerous whole cells, viruses, proteins, and metabolites. These high-consequence pathogens are capable of causing disease in humans and animals and may be of a natural or genetically modified origin. These agents pose a serious health risk to the public when mobilized as weapons or when present in different forms of waste, such as wastewater or medical waste from medical treatment facilities (Tsai, Lai, & Lin, 1998). Given this threat, the EPA is interested in protecting the public and the environment from the harmful effects of such biocontaminants.

Biologically contaminated wastewater can come from medical treatment facilities (Han et al., 2018), accidental environmental introduction, or intentional terrorist attacks (J.-H. Lee & Wu, 2006). Water resource recovery facilities (WRRFs) may receive requests to accept biohazardous wastes for treatment, and before granting such requests, WRRF managers must carefully analyze the potential effects on plant operations. Guidance on the handling of such waste streams is needed to aid WRRFs in their decision to accept contaminated wastes (K. Lin & Marr, 2017). WRRF employees must also properly prepare for situations that involve the malicious and intentional introduction of biocontaminants into public wastewater collection systems (*EPA: Progress on Water Sector Decontamination Recommendations & Proposed Strategic Plan*, 2015). The policies and procedures needed must be based on scientifically-backed facts and research relating to the effect of the specific biocontaminants (if possible) on the treatment system and on public health.

One associated concern with this issue is the production of bioaerosols during the treatment of biologically contaminated wastewater. When biohazardous wastes are introduced into water reclamation facilities, plant managers may need to follow certain protocols in order to

ensure worker safety from the generated bioaerosols (Orsini et al., 2002). A viable exposure pathway (VEP) is defined by the EPA as a complete exposure pathway for a microorganism that includes routes of exposure with documented disease transmission potential (Office of Research and Development Homeland Security Research Program, 2018). The exposure pathway itself has five distinct parts: a source of contamination, an environmental media and transport mechanism, a point of exposure, a route of exposure and a receptor population (Office of Research and Development Homeland Security Research Program, 2018). To be considered viable, the biological contaminant must be capable of reaching the receptor and also able to retain its infectivity upon arrival to that receptor (Office of Research and Development Homeland Security Research Program, 2018). The EPA has identified bioaerosol release from WWTPs as a VEP when spores of *Bacillus anthracis* are present (Office of Research and Development Homeland Security Research Program, 2018).

One potential protective measure aimed at decreasing the overall amount of bioaerosols produced is the addition of free-floating carrier media (FFCM). These materials can vary greatly in size and composition, and have been added into activated sludge in order to promote biofilm growth and enhance biological treatment of the water (Abou-Elela, Ibrahim, Kamel, & Gouda, 2014; Arias, Martin, Matilde, Girotti, & Rodriguez-Cabello, 2009; Hung, Kuo, Chien, & Chen, 2010; Shreve & Brennan, 2019; Stensel & Reiber, 1983). These FFCM have been shown to decrease the rate of bioaerosol production by capturing biomass on the surface. The overarching goal of this research is to provide pertinent information that can be used as the foundation for science-based decisions and policy making for WWRFs.

1.2 Background

The Fall 2001 anthrax letter attacks resulted in five deaths and more than twenty reported cases of illness, and had an associated decontamination response cost in the hundreds of millions of dollars (Franco & Bouri, 2010). In the wake of 9-11, US policies set forth in documents such as Homeland Security Presidential Directive 7 (HSPD-7) (Critical Infrastructure Identification, Prioritization, and Protection), HSPD-9 (Defense of the United States Agriculture and Food), and HSPD-10 (Biodefense for the 21st Century) all identify the EPA as the lead federal agency for the protection of environmental resources, to include public water supplies (Franco & Bouri, 2010). HSPD-8 (National Preparedness), Annex 1 called for the development of fifteen National Planning Scenarios for use in national, federal, state, and local homeland security preparedness activities ("HSPD 8 Annex 1," 2017). Scenario 2 involves the release of 100 liters of aerosolized anthrax in a major US city, exposing more than 330,000 people to anthrax spores, and resulting in an approximated 13,000 casualties and injuries and economic losses (including decontamination costs) in the billions of dollars (*DHS' Progress in Federal Incident Management Planning*, 2010). The World Health Organization (WHO) estimated that the aerosolization of 50 kg of dried anthrax powder for two hours within an urban city with a population of 500,000 inhabitants would result in 95,000 deaths and 125,000 others incapacitated with illness (Spencer, 2003). The resulting strain on medical infrastructure and decontamination efforts would be immense. While perhaps these are worst-case scenarios with ideal aerosolized dissemination, it can be inferred that an intentional contamination of public water supplies would be detrimental to human health and elicit a technical response to the highest levels of local, state, and federal governments.

Bacillus anthracis (BA), often found naturally in soil, is a zoonotic pathogen that causes the disease anthrax, in which toxins from the bacteria cause septicemia in ruminant animals that is often fatal (Turner et al., 2016). While BA is found in soils worldwide, anthrax is most common in agricultural regions in Central and South America, sub-Saharan Africa, Eastern Europe, and central and southwest Asia, particularly in developing countries with little or no veterinary infrastructure to vaccinate animals (*Chemical , Biological , Radiological , and Nuclear Threats and Hazards (TM 3-11.91)*, 2017). In humans, the disease is manifested in cutaneous, gastrointestinal, or pulmonary (also called inhalation) forms of the disease, all dependent on the site of spore entry (Stewart, 2015). Aerosolization of anthrax spores is the most threatening method of dissemination to humans. The small size of spores, 1-2 μm in length, allow them to travel deep within the respiratory tract to the alveoli (Withers, 2014). Cutaneous anthrax has a mortality rate of only 5-20%, while inhalation anthrax (which would result from aerosolized spore inhalation) has a mortality rate of 80-90% (*Chemical , Biological , Radiological , and Nuclear Threats and Hazards (TM 3-11.91)*, 2017). The average incubation period for inhalation anthrax is seven days (with a range of 1 to 43 days), and symptoms of the disease typically persist for three to five days (*Chemical , Biological , Radiological , and Nuclear Threats and Hazards (TM 3-11.91)*, 2017).

The EPA has classified *Bacillus anthracis* (BA) as a High-Consequence Pathogen (HCP) in wastewater systems (Office of Research and Development Homeland Security Research Program, 2018). Anthrax is listed by the US Centers for Disease Control and Prevention (CDC) as a Category A Agent (along with Smallpox, Plague, and Viral Hemorrhagic Fevers) because it can be easily disseminated, can result in high mortality rate, and requires special action for public health preparedness (“Bioterrorism Agents/Disease,” 2018). The most likely routes of BA

entering waste water treatment facilities (WWTFs) were identified to be through intentional and illicit contamination, collected wastewater from a decontamination event, or through surface water runoff (Office of Research and Development Homeland Security Research Program, 2018).

The weaponization of anthrax spores typically involves a method for aerosolizing the spores. Aerosolized spores are capable of being inhaled and causing pulmonary anthrax, the most lethal of the three forms of anthrax. Numerous methods of sampling and identification exist to investigate bioaerosols. Sampling techniques include impaction, impingement, filtration, suction sampling, and electrostatic precipitation (Mandal & Brandl, 2011). Once sampled and collected, multiple techniques can be applied to identify the microorganisms, including microscopy methods, cultivation methods, flow cytometry, Polymerase Chain Reaction (PCR), ATP-bioluminescence, Raman spectroscopy, or Laser-induced fluorescence (Mandal & Brandl, 2011). In the cultivation method, colony-forming units (CFUs) are counted visually after incubation on solid growth media. Temperature variations and nutritionally selective agars can be used to selectively grow organisms of interest, if existing in mixed populations. The cultivation method itself reflects surviving and viable organisms, as organisms no longer living would fail to grow on the nutrient media. Other identification methods, such as PCR (which is also popularly used in published studies), do not distinguish between living and dead organisms. A variety of factors related to the specific bioaerosol study being conducted influence the selection of sampling and identification methods.

Another limitation of the cultivation method mentioned above is the fact that one CFU does not necessarily indicate the presence of a single spore. Clumps of spores could result in fewer formed colonies than the actual number of spores present. In her research, Hawkins (2008)

worked on designing a micro-etched cover slip platform with 3µm x 3 µm wells for individual spores to settle in so that heat treatments could be applied to individual spores (Hawkins, 2008). Separation of spores into a one-spore, one-well orientation proved challenging and was acknowledged to decrease the overall statistical results of the study (Hawkins, 2008). Wet spores tend to clump together more than dry spores. Methods to dry and sonicate (Berger & Marr, 1960) bacterial spores have resulted in reduced clumping. Spores were not treated to enhance individual separation in these experiments, but the correlations between spores and CFUs were noted. BA spores only were analyzed by Hawkins and by Berger and Marr, where spore clumping is more present than in some surrogates, such as BG. A qualitative assessment of BG spores from these experiments using phase contrast microscopy revealed relatively low amounts of spore clumping and a high purity of BG spores (approximately less than 5% vegetative cells).

Published literature often reported bioaerosol concentrations in terms of CFU per volume of air (typically in units of CFU/m^3 or CFU/L). The use of CFUs allows for comparisons to be made, for instance, when Li et al., 2016, found that the sludge thickening basin at a WWTP had higher bioaerosol concentrations (1697 CFU/m^3) compared to other parts of the plant such as the grit chamber (460 CFU/m^3) or even the downwind plant offices in a separate building (450 CFU/m^3) (J. Li et al., 2016). CFUs were never translated into total numbers of bacterial cells, bacterial spores, or fungal spores. This distinction is important, as results from this research are presented in terms of CFUs or CFUs per volume, but the consequences of a dose of inhaled spores largely depends on a total number of spores.

The threat of intentionally contaminating a public water supply is not farfetched, and bioterrorism is not a new threat to the United States. In the fall of 1984, members a religious commune referred to as the Rajneeshees intentionally contaminated 10 salad bars in the town of

The Dalles, Oregon, with *Salmonella typhimurium* in an attempt to influence local elections (Torok et al., 1997). A total of 751 people were diagnosed with *Salmonella* gastroenteritis in a four-week span (Torok et al., 1997). A biological agent used in bioterrorism does not even have to be lethal to spread disease, panic, and fear against a targeted population. Historical case studies have established an interest and willingness of foreign and domestic adversaries to use biological agents as weapons. A threat against vulnerable public water supplies is credible and protection efforts for national infrastructure and personnel are warranted.

1.3 Problem Statement

The EPA is greatly concerned about the protection of the nation's water supply and infrastructure. In particular, the accidental or intentional contamination of water supplies can cause serious health risks to WWTF workers when high-consequence pathogens are aerosolized from turbulent mixing and aeration of water tanks. Due to their survivability and optimally-small size, BA spores are a particularly dangerous health concern whenever aerosolized in the vicinity of unprotected human populations. As mentioned, inhalation anthrax is the most lethal of the three forms of the disease. Additionally, post-decontamination wastewater and medical waste from medical treatment facilities can also introduce pathogens into a WWTF. Due to the presence of such potential contaminants, it is important to understand how bioaerosols are released and to determine the scientific basis for any potential effective intervention. Franco and Bouri (2010) acknowledged a limited number of laboratory and field studies have been conducted to evaluate re-aerosolization of anthrax spores from a variety of surfaces and to determine their viability, as well as an overall underfunding of pertinent research in bioaerosols and decontamination (Franco & Bouri, 2010). FFCM has been proposed as a water surface additive capable of decreasing bioaerosol emissions. Further research is also needed to determine

the effects of aeration rate and the addition of FFCM on the aerosolization of BG spores in conditions mimicking those of WWTFs.

1.4 Research Objectives

The purpose of this research is to determine the effect of the mixing regime of a laboratory-scale aeration system on bacterial spore-containing bioaerosol production. The first objective is to examine the effect of increasing the mixing intensity (in the form of aeration rate), as bubble-aeration is often used in various locations within a WWTP. The second objective is to determine the effect of utilizing FFCM as mean to limit the surface area of treated wastewater exposed to the air on bioaerosol production. The third objective is to determine the effect of experimental scale on the production of bioaerosols. This research will serve as the medium-scale contribution to a more expansive research effort, including small-scale contributions at the Air Force Institute of Technology and large-scale contributions at the EPA's National Homeland Security Research Center's (NHSRC's) WWTP Pilot Scale Facility in Cincinnati, Ohio. BG spores were used in the experiments, simulating an intentional nefarious contamination of a public water supply with BA spores. Qualitative analysis will be performed to determine the effect of aerosolization on the physical properties of BG spores.

1.5 Hypothesis

The test hypothesis is that aeration rate in reactor bottle and the amount of BG captured in the BioSampler impinger are proportional. It is hypothesized that FFCM added to the water surface within the reactor bottle will decrease the amount of BG captured in the BioSampler impinger across all evaluated aeration rates. The procedures of the small-scale research and this medium-scale research are similar, and it is hypothesized that similar trends and relationships

between factors will exist between these two scales. It is theorized that the trends and relationships regarding changes in aeration rates and the addition of FFCM will be observed in the large-scale research as well. Establishing such relationships in the large-scale system could potentially influence plant operations regarding the aeration rates utilized and if a type of FFCM would be beneficial to water surfaces as a means of decreasing BA spores in produced bioaerosols. Differences with the large-scale experiments will still be expected as they will be conducted in an actual pilot-scale water treatment facility, and thus more susceptible to the effects of environmental changes and potential contamination.

1.6 Scope and Approach

Only the endospores from *B. globigii* were utilized and introduced to the water in the reactor bottle to form bioaerosols. Pure stocks of this microorganism were available and regarded as a health-safe surrogate for the biowarfare agent BA. The BG surrogate was prepared as to only introduce harvested spores to the experimental apparatus; BG vegetative cells, other bacteria, and viruses were not included as a part of this investigation.

Many of the experimental conditions were selected to best allow this research to serve as the middle size of a series of three different scaled experiments between AFIT and the EPA. The microorganism being subjected to aerosolization required that experimental apparatus remain contained within the biosafety cabinet, a factor that limited the size at which these medium-scale laboratory experiments could be conducted.

A total of twelve experiments were conducted focused on investigating aeration rate and the addition of FFCM. One additional experiment investigated the effect of increasing the initial amount of BG spores in the reactor bottle. Each experiment focused on one changed parameter and completed in triplicate to allow for statistical analysis. Sample sizes for this scoping study

were still relatively small, but unavoidable due to time-intensive preparation of the BG spores, and the lengthy setup and execution of each independent experiment.

II. Literature Review

2.1 Properties of BG Spores

2.1.1 Bacteriology

Bacillus globigii (BG) is a gram-positive, aerobic, motile, endospore-forming, rod-shaped, bacterium, historically utilized as a research surrogate for *Bacillus anthracis* (BA), an established biowarfare agent (Carrera, Zandomeni, Fitzgibbon, & Sagripanti, 2007; Zolock, Li, Bleckmann, Burggraf, & Fuller, 2006). Genetically similar to *Bacillus subtilis*, the species of *B. globigii* and the specific variant *B. subtilis* var *niger* were both eventually reclassified as *Bacillus atrophaeus* (Nakamura, 1989). Figure 1 pictures colonies of BG grown on a DIFCO broth and LB agar mixed-medium plate, showing characteristic irregular borders and reddish-brown pigmentation. Due largely to its prevalence in documented military research, BG remains a common reference in literature (Bishop & Stapleton, 2016; Buttner, Cruz-Perez, & Stetzenbach, 2001; Plomp, Leighton, Wheeler, & Malkin, 2005a; Reponen, Willeke, Grinshpun, & Nevalainen, 2011; White, Popovici, Lytle, & Rice, 2014; Wiencek, Klapes, & Foegedingl, 1990). *Bacillus* species, to include BG, are also commonly used as a surrogate during the evaluation of water treatment facilities' ability to remove bacteria (White et al., 2014). BG was used as a simulant for BA in a 2003 study examining the efficacy of selected hand hygiene agents, which allowed human participants to be used and avoided medical and ethical conflicts (Weber, Sickbert-Bennett, Gergen, & Rutala, 2003). Mwilu et al. studied lower detection limits of BG spores in water utilizing two different detection strategies in attempts to more rapidly identify BA (Mwilu et al., 2009). Farrell et al. also utilized BG in their study using immunoassays for rapid identification techniques, with the results intended to be applied to identifying BA (Farrell, Halsall, & Heineman, 2005).

Figure 1. BG vegetative cells on DIFCO/LB agar plate

Certain gram-positive (but no gram-negative species) are capable of producing endospores. When *Bacillus* species are subjected to environments causing the organism metabolic distress, ellipsoidal endospores are centrally or paracentrally formed in the unswollen sporangia (Nakamura, 1989). These endospores (commonly referenced as "spores") contain the bacterial cell's genomic information and enhance the organism's ability to survive. Spores are resistant to damage from heat, radiation, changes in pH, and toxic chemicals (Setlow, Cowan, and Setlow, 2003), significantly more so than the vegetative cells from which they arise (Szabo, Muhammad, Heckman, Rice, & Hall, 2012). BA spores have been shown to survive heat at 120°C for 15 minutes, chemical disinfection (0.05% sodium hypochlorite for 30 minutes, 500 mg/L ethylene oxide for 30 minutes, or 0.88 mol/L hydrogen peroxide for 30 minutes), and low-dose gamma radiation of less than 10 kGy (Fiester, Helfinstine, Redfearn, Uribe, & Woolverton, 2012). BA spores can remain in their dormant state for extended periods of time, and have been shown to survive in soil for decades (Spencer, 2003). From inner to outer, an endospore consists of a core containing supercoiled DNA, an inner membrane, germ cell wall, cortex, outer

membrane, and spore coat (Fiester et al., 2012). Figure 2 depicts an example *Bacillus* endospore with an exosporium present as the outermost layer.

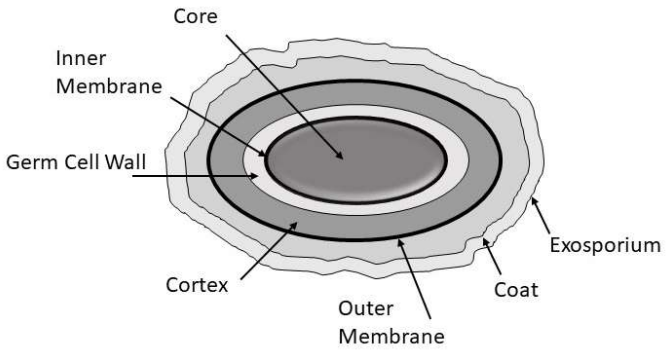

Figure 2. Example structure of a *Bacillus sp.* Endospore

The spore's genetic information is protected by the presence of a high concentration of calcium bound to dipicolinic acid (pyridine -2,6-dicarboxylic acid or DPA) and the presence of small acid-soluble proteins (SASPs) in the core (Spencer, 2003). The volume of the core varies by species and is relatively large, occupying approximately 42% of the total spore volume in *B. cereus* spores (Zolock et al., 2006). The core is relatively dehydrated and metabolically dormant (A. G. Li, Burggraf, & Xing, 2016). Layers of cytoplasmic membranes and cross-linked peptidoglycan, and a tough, keratin-like protein coat comprise the remaining spore structure (Murray, Patrick R.; Rosenthal, Ken S.; Pfaller, 2005).

The inner membrane, germ cell wall, and the cortex help provide the high heat resistance for the spore, and help maintain the dehydrated state of the core (Carrera et al., 2007). The term "germ cell wall" is often used to describe the inner layer of the cortex. Using AFM analysis, a range of cortex thicknesses of 90 to 150 nm were measured in BA spores, with thinner amounts at the poles of the long axis and the thicker amounts at the poles on the short axis of the spores (A. G. Li et al., 2016). The germ cell wall and cortex are both made up of peptidoglycan, a

polymer consisting of sugars (glycans) and amino acid chains (peptides) that forms a major component of the cell wall in vegetative bacterial cells. The germ cell wall is structurally similar to the vegetative cell wall, consisting of a large number of glycan chains that cross-link between peptides (A. G. Li et al., 2016). The cortex peptidoglycan is significantly less cross-linked, allowing the cortex to be flexible and have the ability to shrivel or swell in response to pH or ionic changes (Ghosh et al., 2008). During germination, the cortex is rapidly degraded by peptidoglycan lytic enzymes, and the germ cell wall forms the actual cell wall of the resulting vegetative cell (A. G. Li et al., 2016).

Encasing the cortex of the spore is the spore coat, a structural and reactive barrier that protects more the inner spore components (Plomp, Leighton, Wheeler, & Malkin, 2005b). The coat is comprised of a multilayered protein structure and considered to be critical to germination as well as to heat and toxic chemical resistance (Carrera et al., 2007). The thickness of the coat, number of layers and surface characteristics of the coat can all vary between species (Zolock et al., 2006). The spore coat plays a role in the spore's resistance to chemicals, enzymes, and to mechanical forces and disruptions (Sahin, Yong, Driks, & Mahadevan, 2012). The spore coat is the outermost detectable layer of spores for BG and *B. subtilis*.

A protein-based honeycomb lattice with hair-like projections called the exosporium is present as the outermost layer in many *Bacillus* species, including *B. anthracis*, *B. cereus* (BC), and *B. thuringiensis* (BT), but not found in BG and *B. subtilis* (Stewart, 2015). The function of the exosporium is relatively poorly understood, although studies have shown that its presence affects interactions with surfaces and cells in the environment, forms early interactions with the host upon infection, provides some stress resistance, and has a role in assembling more interior spore layers (Boone et al., 2018). It is also relatively poorly understood how the presence of

exosporium influences hydrophobicity (A. G. Li et al., 2016). Wiencek et al. determined that *Bacillus* spores (including BG) were more hydrophobic than their corresponding vegetative cells, a result linked to the relative abundance of protein in the outer layers and exosporium of the spore compared to the peptidoglycan on the vegetative cell wall (Wiencek et al., 1990). The cortex is largely responsible for maintaining the state of dehydration of the spore since it provides a hydrophobic layer that can hinder water diffusion in and out of the spore core (A. G. Li et al., 2016).

The exosporium is relatively fragile, and a damaged or missing exosporium may decrease adhesion or increase resistance to surface removal (Tufts et al., 2014). However, exosporium damage or removal has not been shown to negatively impact the pathogenicity of BA (Boone et al., 2018). While the presence of an exosporium is acknowledged as a difference between BA and BG, the delicate exosporium is unlikely to survive wet or dry aerosolization (Carrera et al., 2007). This strengthens the argument for the use of BG as a simulant for BA in bioaerosol research.

The lifecycle of spore-forming *Bacillus* species is divided into three categories: vegetative cell growth, sporulation, and germination (Sella, Vandenberghe, & Soccol, 2014). The transition between each stage is driven predominately by the availability of nutrients to the organism. A complete consumption of metabolized carbon or nitrogen nutrient resources induces sporulation in *Bacillus* and other endospore-forming species as a survival mechanism. Sella et al., 2014, mentions several additional environmental signals capable of initiating sporulation, including the presence of high mineral composition, neutral pH, temperature, and high cell density. It is worthwhile to state that even under optimal conditions for sporulation, the formation of spores in vegetative cells is still considered stochastic (Sella et al., 2014).

The term endospore itself refers to the fact that generated spore originates within the mother cell (T. Boone & Driks, 2016). Some references describe sporulation in eight stages (T. Boone & Driks, 2016), while others describe the process in 7 stages (Sella et al., 2014). The difference is accounted for in the enumeration (or not) of the chromosomal replication into two identical nucleoids as a step (Zolock et al., 2006). Once this has taken place, Stage 1 occurs when the identical nuclear material is arranged axially into filaments (Sella et al., 2014). Stage 2 fully segregates the nuclear material when the invagination of the plasma membrane of the cell occurs asymmetrically near one pole of the cell, forming a double-membrane septum (Sella et al., 2014). This provides separation between the mother cell and forespore (T. Boone & Driks, 2016). In Stage 3, the septum curves and eventually the forespore is fully engulfed by the mother cell in a phagocytotic-like process (Sella et al., 2014). Whereas prior stages are non-obligatory, the completion of Stage 3 commits the cell to sporulation (T. Boone & Driks, 2016).

In Stage 4, the mother cell mediates the transformation of the forespore into the completed endospore (Sella et al., 2014). The peptidoglycan-based cortex is formed between the inner and outer spore membranes, and associated proteins are synthesized (Sella et al., 2014). Dehydration within the spore core begins in accordance with the accumulation of calcium dipicolinate (T. Boone & Driks, 2016). Stage 5 consists of the mother cell depositing around 80 proteins into two layers, forming the spore coat (Sella et al., 2014). These proteinaceous layers contribute to the spore's chemical and γ-radiation resistance (T. Boone & Driks, 2016), and the number and type of these protein layers vary amongst *Bacillus* species (Zolock et al., 2006). Dehydration of the core continues as the spore continues to mature in Stage 6, acquiring all of its DPA synthesized by the mother cell (T. Boone & Driks, 2016). Large amounts of divalent cations, to include Ca^{+2}, Mg^{+2}, and Mn^{+2} are absorbed in parallel with the DPA, and the spore

reaches its maximum state of dehydration (T. Boone & Driks, 2016). Resistance to heat and organic solvents is enhanced (Sella et al., 2014). Finally in Stage 7, lytic enzymes disrupt the membranes and cell wall of the mother cell, allowing for the release of the mature endospore (Sella et al., 2014). Stage 7 marks the conclusion of the sporulation process. Figure 3 shows a light microscopy image taken at 1000x magnification and shows a vegetative BG cell, released BG endospores, and one example of a vegetative cell in the process of sporulation.

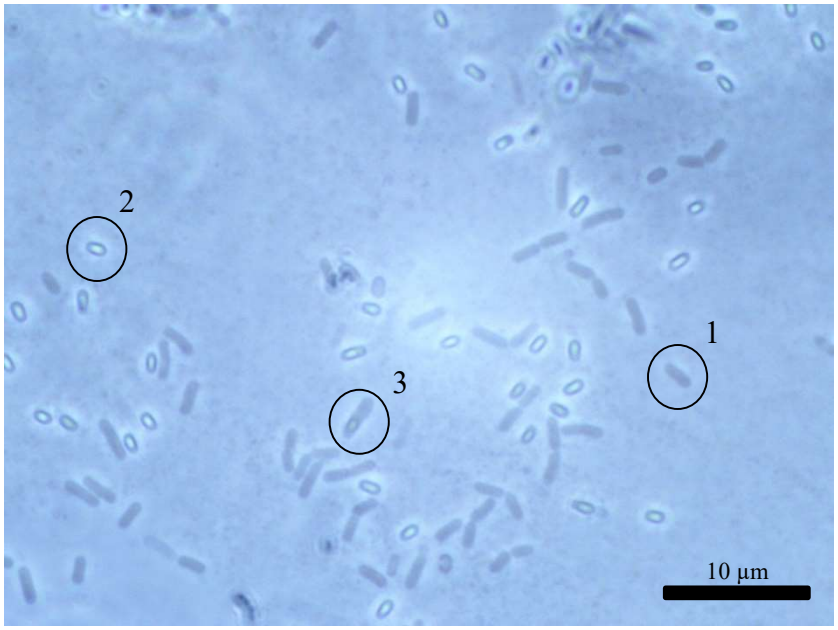

Figure 3. Phase Contrast Microscopy Image (1000x oil-immersion) of BG: 1. Vegetative Cells, 2. Endospores, and 3. Sporulating Cells

Germination is essentially the reverse process of sporulation, in which bacterial spores form vegetative cells. Despite their relative dormancy, spores remain able to sense environmental changes. Germination itself is divided into three categories, with the first being activation (Sella et al., 2014). Germination of spores is activated by germinants, which can be nutrient in nature and include amino acids, purine nucleosides, and sugars, or chemical in nature and include

cationic surfactants such as dodecylamine (Setlow et al., 2003). The germinants are sensed by germination receptors (GRs) located in the spore's inner membrane (Sella et al., 2014). Activation is a reversible process and does not fully commit the spore to germination (Stewart, 2015).

The second stage of germination is rehydration. In this stage, the DPA is degraded and released, ultimately resulting in the rehydration of the core (Sella et al., 2014). Rehydration allows for increased protein mobility and the reactivation of biochemical processes later in cellular outgrowth (Paidhungat et al., 2002). The third stage of germination is spore coat hydrolysis. The spore coat is broken down, allowing for the development of the vegetative cell (Sella et al., 2014). This marks the transition from a germinating spore to a developing vegetative cell. This transition is referred to as outgrowth, and cellular division is initiated (Sella et al., 2014). The cells remain in their vegetative state, metabolizing nutrients and reproducing cells, until a time where stress is once again imparted, and spores may once again be produced.

2.1.2 Pathogenesis

BG spores typically range between 1.00 and 2.00 μm in length and between 0.50 and 0.75 μm in width (Carrera et al., 2007; Plomp et al., 2005b). This sizing makes them an ideal particulate size for a bioweapon. Once inhaled, the spores are deposited in the lung's alveoli, where they are transported via the body's lymphatic system to the mediastinal lymph nodes and induce hemorrhage (Spencer, 2003). Particles of less than one micrometer in diameter are often readily exhaled and unable to settle deep inside the lungs. Particles, and in this case spores, of greater than 5 μm pose little threat to humans since they are normally cleared from the lungs via the cilia on the mucosal linings (Spencer, 2003).

Disease is induced by toxins carried on two virulent plasmids, pXO1 and pXO2 (Spencer, 2003). The pXO1 plasmid codes for three toxins responsible for hemorrhage, edema, and necrosis (Spencer, 2003). The smaller pXO2 plasmid encodes three genes responsible for the production of a polyglutamyl capsule that inhibits phagocytosis by the host organism on the vegetative BA cells (Spencer, 2003). These virulence factors originate in vegetative BA cells, not the BA spores themselves. Germination must take place within the host organism, a process which can take up to 60 days after exposure to the spores (Spencer, 2003). An outbreak of anthrax in the Soviet town of Sverdlovsk in 1979 from a bioweapons production facility resulted in 77 documented cases of disease, resulting in at least 66 deaths (Omotade et al., 2014). Human fatalities were all reported within a distance of 4.5 km of the site of the release, and livestock fatalities were reported to range at distances from 2 to 67 km from the release site (Coleman, Thran, Morse, Hugh-Jones, & Massulik, 2008). All of the cases occurred within 6 weeks of the agent's release (Spencer, 2003). Such a delay in the presentation of symptoms and subsequent diagnosis, caused by the need of spores to germinate and reproduce, enhances the escaping of perpetrators using BA to contaminate a city or public environmental resource.

2.1.3 Pathogenic Concentration

A target concentration of BG spores in the reactor bottle was required to conduct the experiments composing this research. The concentration of 2.19×10^6 CFU/mL was used throughout the research to best match the procedure utilized in the small-scale research completed in parallel that compliments the larger, multi-scale research desired by the US EPA. The literature supports the utilization of a concentration on this order of magnitude. It should be

noted that factors such as the pathogen of interest, the host organism being studied, respiration rates, and a multitude of other factors result in a variety of values for concentrations of interest.

B. thuringiensis (BT) is commonly used as an insecticide since select proteins are toxic to insects but not harmful to mammals. Garcia and DesRochers reported a 100% mortality rate in a Californian species of mosquito using insecticide with a BT concentration of $1x10^5$ bacilli/mL (Garcia & DesRochers, 1979). Korsten and Jager investigated the use of *B. subtilis* as an antagonist against fruit diseases in avocados using concentrations that they varied between 10^8 and 10^5 bacilli/mL (Korsten & De Jager, 1995). Campbell and Mutharasan investigated the identification of small concentrations of BA within a mixture of BT and BC with a concentration of $3.33x10^5$ spores/mL (Campbell & Mutharasan, 2007). Marti et al., 2011, used a *Clostridium* spore concentration on the order of 10^4 CFU/mL in contaminated influent wastewater while studying removal properties of membrane bioreactors (Marti et al., 2011). In one example using BG, Smith et al., 2019, utilized a range from $2x10^1$ to $2x10^7$ CFU/mL of BG spores while examining the functional resilience of activated sludge exposed to the contaminant (Smith et al., 2019). The handwashing study conducted by Weber et al. contaminated each participant's hands with 5 mL of a liquid inoculum containing approximately $2.2x10^6$ BG spores per mL (Weber et al., 2003).

Specific to BA, the US Army Research Institute of Infectious Diseases (USAMRIID) reports that a human LD_{50} for BA is between $8x10^3$ and $5x10^4$ aerosolized spores (Withers, 2014). Coleman et al., reports a slightly lower human LD_{50} for inhalation anthrax of 10^3 aerosolized BA spores (Coleman et al., 2008). Bartrand et al. reported that an LD_{50} for laboratory rabbits was $1.1x10^5$ spores (Bartrand, Weir, & Haas, 2008), and Haas reported a range of LD_{50} for Anthrax in primates between $7.07x10^4$ and $1.36x10^5$ spores (Haas, 2002). The greatest risk to

the host organism, regardless of species, is when the spores are deposited deep into the lungs. In analyzing pre-Biological Weapons Convention (BWC) research, Haas compared dose response data for BA and concluded that inhalation anthrax dose response in primates can be described by the exponential dose-response model (Haas, 2002). This fit was done for low doses of BA spores, ranging from 10^0 to 10^4 inhaled BA spores.

The lethal doses of pure spores mentioned previously differ, in definition, from lethal concentrations of spores suspended in a media such as air or water. In 1953, when more research was conducted on animal models for the research and development of biological warfare agents, Druett et al. collected dose-response data from exposing rhesus monkeys to BA. Druett et al. reported 100% lethality in tested monkeys with concentrations of BA between $1x10^5$ and $1.66x10^5$ spores/L (of air), exposing the monkeys for one minute and assuming a respiration rate of 2.4 L/min (Druett, Henderson, Packman, & Peacock, 1953). This would amount to an inhaled dose of between $2.4x10^5$ and $3.98x10^5$ spores. Mwilu et al. reported values for a human infectious dose for BA of $2.5x10^5$ spores/mL while investigating detection strategies for BG as a BA simulant (Mwilu et al., 2009). Turner et al. concluded that environmental exposures of up to $1x10^{10}$ BA spores is possible, with the highest natural concentrations typically found in the decaying carcasses of livestock animals infected with anthrax (Turner et al., 2016). Following the death of the animal, the thriving BA vegetative cells exhaust their metabolic resources and sporulate, resulting in the potentially high number of spores around the carcass. It is not possible to select one single concentration of BG spores that would be more appropriate than another for the purpose of this research. It is believed that the literature supports the concentration used as an appropriate value.

2.2 Bioaerosols

2.2.1 Bioaerosol Characteristics

An aerosol is generally defined as a small solid or liquid particle suspended in air and is more specifically defined as a bioaerosol when the small particle is an individual microorganism, an aggregate of multiple microorganisms, or a combination of microorganisms and non-living materials. These microorganisms can include viruses, bacterial cells, fungi, pollen, and protozoa. Bioaerosols vary in size, but nearly all range in diameter between 20 nm and 100 μm (Mandal & Brandl, 2011). With this size range, diseases associated with biological materials ranging between 50 nm and 10 μm are expected to be related to bioaerosols in cases where such materials are transported through the air (B. U. Lee, 2011). The EPA describes a two-part process that is necessary for the generation of a viable bioaerosol: the release of microbiological particles through an aerosol producing mechanism in an aqueous medium, such as bubble aeration, and the subsequent survival of the microorganism in the environment following aerosolization (Office of Research and Development Homeland Security Research Program, 2018). Spores, to include BG and BA, are hardy and well-suited to survive in various water treatment conditions and turbulent-mixing processes.

The most relevant mechanism for describing bioaerosol formation in wastewater treatment processes is the bubble-burst mechanism, where the movement of air through a volume of water results in the bursting of the traveling bubble at the air-water interface (Sánchez-Monedero, Aguilar, Fenoll, & Roig, 2008). Submerged aeration produces air bubbles at the bottom of a volume of water and float upward until they burst at the surface, as the surface tension is insufficient. The bursting bubble results in a spray of aerosols in approximately 180° on top of the water surface. Smaller bursting bubbles result in film droplet formation, while

larger bursting bubbles, often caused by wave-like movement in larger volumes of water, result in jet droplet formation (Office of Research and Development Homeland Security Research Program, 2018). Aeration systems in WWTPs supply an ongoing flow of air bubbles capable of combining and thus forming larger air bubbles.

Diseases caused by biological materials and microorganisms between 50 nm and 10 µm in diameter are able to be associated with bioaerosols when conditions exist that introduce and transport these particles in the air (B. U. Lee, 2011). In the specific case of spores, the term "droplet-nuclei" describes the condensed liquid surrounding the spore present in the bioaerosol, which is then capable of travel particularly along air currents or prevailing winds in the case of an open-air WWTP (Cooper, Aithinne, Floyd, Stevenson, & Johnson, 2019). Gravitational settling is considered insignificant for endospores due to their small aerodynamic diameter range of 0.5 to 3.0 µm (Reponen et al., 2011).

Various methods have been used to collect and study bioaerosols from the ambient air. These methods include the use of an impactor, impinger, filtration, or settle-plates (Cooper et al., 2019; Morawska, 2001). Resulting sample analysis can be performed via direct counting of bioaerosol particles (using light microscopy or epifluorescence microscopy) or by culturing onto nutrient plates and counting resulting colonies. Non-counting techniques, including the use of PCR (Xu et al., 2011) or UV-APS, a particle time of flight counter between two laser beams, (Morawska, 2001) have also been used. However, these non-counting techniques do not allow for the determination of viability, whereas the culture method requires viable microorganisms to grow and be counted.

An SKC BioSampler is a glass impinger that is used to sample bioaerosols. Designed to mimic the human nose, the airflow in the BioSampler is accelerated through three angled nozzles

that impinge tangentially on the inner wall of the collection vessel (Kesavan, Schepers, & Mcfarland, 2010). The angled ejection of particles reduce particle bounce, and the centrifugal airflow causes the collection liquid to swirl and gently remove collected particles with minimal re-aerosolization (in comparison with other impinger designs) (Willeke, Lin, & Grinshpun, 2007). This action also assists in reducing evaporation of the liquid in the collection vessel (Zheng & Yao, 2017). During the collection process, the aerosols are converted to hydrosols and available molecular or biochemical techniques can applied for sample analysis (Zheng & Yao, 2017). A number of studies have utilized SKC BioSamplers (Cooper et al., 2019; Han, Li, & Liu, 2013; Jung, Lee, Lee, Kim, & Lee, 2009; Kesavan et al., 2010; Reponen et al., 2011; Willeke et al., 2007; Zhen, Han, Fennell, & Mainelis, 2014) or discussed the use of SKC BioSamplers in the study of bioaerosols (B. U. Lee, 2011; Mandal & Brandl, 2011; Xu et al., 2011; Zheng & Yao, 2017).

The stated efficiency for the SKC BioSampler for particle sizes of 1.0 µm is approximately 100% ("SKC BioSampler Specification Sheet," 2019), and Willeke et al. reported a sampling efficiency of 96% for inert particles of the same particle size (Willeke et al., 2007). Factors such as the volume of the collection liquid, the target particle size, and the flow rate on the attached vacuum pump were discovered in prior research to effect the overall biological collection efficiency of the BioSampler (Zheng & Yao, 2017). Zheng and Yao determined in their investigation that efficiencies decreased with decreasing the volume of the collection liquid (Zheng & Yao, 2017). The experiments in this research employed the BioSampler with maximum volume of 20 mL, recommended by the manufacturer. Using the same collection volume of 20 mL of deionized water, Zheng and Yao calculated an overall collection efficiency of 83% for aerosols containing vegetative *B. subtilis* cells with an average diameter of

approximately 1.0 μm (Zheng & Yao, 2017). Kesavan et al. calculated a higher average collection efficiency specifically for BG spores of 96% for three different SKC BioSamplers (Kesavan et al., 2010). The SKC BioSampler was selected as a bioaerosol sampler in this research due to its availability, ease of use, comparability to other experiments, and that collection liquid was easily transferred to agar plates for culturing and colony counting.

The density of spores varies based on whether the spore is hydrated or not, also referred to as wet and dry aerosols. Carrera et al., 2007, reported a wet density for BG spores of 1.201 ± 0.0030 g/mL and a dry density for BG spores of 1.45 ± 0.02 g/mL, values slightly greater than for BA spores. The concept of particle density plays a role in the gravitational force pulling down on a bioaerosol, with the equation (in Newtons):

$$F_{grav} = \frac{\pi}{6} * d_p^3 * \rho_p * \mathrm{g}$$

In this equation, d_p respresents the physical particle diameter, ρ_p is the particle density and g is the acceleration constant due to gravity (9.81 m/s^2) (Morawska, 2001). For particles with a radius of less than 10 μm, the initial acceleration from the moment of stabilization in the air is negligible, and it is assumed that the particles instantaneously fall at their terminal velocity. Stokes' Law can therefore be used to determine the particle gravitational settling velocity (v_{grav}) by the equation (in m/s):

$$v_{grav} = 0.003 * \rho_p * d_p^2$$

In this equation, 0.003 is an approximated constant used under conditions with normal temperature and pressure (NTP), where temperature is 20°C (or 293.15 K) and pressure is 1 atm (or 760 torr) (Morawska, 2001). The time an aerosolized particle remains airborne can be determined by integrating over the height of stabilization for the aerosol. Spores were determined

to have higher wet density values than their vegetative cells (Carrera et al., 2007). The spores in these experiments were hydrated in DI water, and thus the wet density was considered.

In a system generating bioaerosols that is open to the environment, factors such as temperature, relative humidity, and wind speed would all affect how far a particle could travel (Zhen et al., 2014). Factors such as aeration rate would influence the height of stabilization that the particles would reach following aerosolization (Zhen et al., 2014). The settling velocity and time the aerosol remains airborne were not necessarily applicable in the small and medium-scale experiments based on the experimental setups. However, these factors would apply partially to the large-scale experiments in which environmental conditions have more of an impact, and most certainly apply when aspects of this research are applied to bioaerosol behavior in actual WWTPs.

2.2.2 The Presence of Bioaerosols in Water and Wastewater Treatment Plants

Bioaerosol emission at various operational sites within a WWTP have been studied where turbulent mixing, stirring, or aeration occurs (Bauer, Fuerhacker, Zibuschka, Schmid, & Puxbaum, 2002; Fannin, Vana, & Jakubowski, 1985; J. Li et al., 2016; Y. Li, Zhang, Qiu, Zhang, & Wang, 2013; T. H. Lin, Chiang, Lin, & Tsai, 2016; Michałkiewicz, 2018; Pascual et al., 2003; Sánchez-Monedero et al., 2008). While direct correlations between factors such as proximity to wastewater or duration of exposure by WWTP workers and pathogenic infection have not been fully established, authors have documented a form of illness characterized by fever, muscle weakness, general malaise, and acute rhinitis, a condition colloquially referred to as “sewage worker’s syndrome” (Clark, 1984; Fannin et al., 1985; Lundholm & Rylander, 1983). Concerns surrounding the spread of pathogens via the intentional contamination of public water supplies

are thus evidently validated. Li et al. identified approximately 300 unique bacterial species collected from bioaerosols produced by the biological reaction basin, and concluded their study stating that three WWTP sites (the screen room, the sludge thickening basin, and the biological reaction basin) presented significant microbial exposure risks (J. Li et al., 2016). Pathogens in wastewater from normal treatment operations have been documented to result in human disease, and certainly intentional contamination of particularly virulent pathogens would assuredly result in manifested disease.

Wastewater treatment plants can have a number of configurations, but most have at a minimum a primary and secondary stage (Sánchez-Monedero et al., 2008). In primary treatment, influent wastewater passes through screens and grit chambers and ultimately to a sedimentation tank where minute particles gradually settle to the bottom and effluent water is passed on to the next stage (*EPA: How Wastewater Treatment Works... The Basics*, 1998). In the secondary stage, organic material is removed through the use of trickling filters in some older designs or more increasingly common activated sludge, in which bacteria breakdown the organic material into harmless by-products (*EPA: How Wastewater Treatment Works... The Basics*, 1998). Aeration tanks are often present in secondary stages allowing for air and activated sludge to be mixed with the wastewater (*EPA: How Wastewater Treatment Works... The Basics*, 1998). Additional sedimentation tanks, clarifiers, and chemical (i.e. chlorine) treatments complete the remainder of the wastewater treatment process. In some cases, additional stages may be added ahead of the primary stage (often called preliminary stage or treatment) or after the secondary stage (often called tertiary stage or treatment) (Office of Research and Development Homeland Security Research Program, 2018).

Bioaerosols at WWTPs typically occur where moving mechanisms are present or where forced aeration is performed (Pascual et al., 2003). Secondary stages where activated sludge is mixed with wastewater, as well as other locations were aeration is used such as in the influent to the primary stage, the grit tanks, or in the final settling tanks are all documented locations of bioaerosol emissions (Sánchez-Monedero et al., 2008). With different designs and configurations, there is no specific location which contains the highest level of bioaerosols present at all WWTPs. Maintenance operations, such as the spraying of grit chambers or the spraying of the sludge screw pump, can also generate bioaerosols (Office of Research and Development Homeland Security Research Program, 2018). Efforts to reduce emitted odors from WWTPs (such as physical covers over outdoor grit tanks and/or primary settling tanks) have shown the ability to reduce bioaerosols (Fernando & Fedorak, 2005), but still present potential health risks to WWTP workers as the covers require cleaning and maintenance.

Results from previous studies discovered emitted bioaerosols traveled at great enough heights and distances to implicate potential health concerns for WWTP workers and even nearby residents. Li et al., 2013 detected an average concentration of airborne viable bacteria of 4168 ± 263 CFU/m^3 at a distance of 2 meters and an average concentration of airborne viable bacteria of 1929 ± 98 CFU/m^3 at a distance of 10 meters downwind of an oxidation ditch utilizing rotating brush aerators (Y. Li et al., 2013). Sánchez-Monedero et al., 2008, determined that mechanical agitation of wastewater at WWTP created more bioaerosol emissions than more passive methods such as the use of air diffusers. Their study detected mesophilic bacteria in concentrations up to 4580 CFU/m^3 at a distance of 2 m downwind of mechanical agitators at WWTPs, and a reduced concentration of up to 57 CFU/m^3 at a distance of 2 m downwind of air diffusion systems (Sánchez-Monedero et al., 2008). Carducci et al., 2000, likewise concluded that areas in the

vicinity of moving mechanical equipment or mechanisms performing wastewater aeration yielded the highest concentrations of bacteria in their survey of three wastewater treatment sites over the course of eleven months (Carducci et al., 2000).

Lin et al., 2016, investigated the effects of adding two different small-sized suspended solids (SS) on resultant bioaerosol emissions of *E. coli* in a lab-scale wastewater treatment system. Bioaerosol collection occurred at the top of the sludge treatment tester container, with *E. coli* concentrations peaking at approximately 4250 CFU/m^3 at the highest aeration rate of 15 L/min when the SS was activated sludge, and concentrations peaking at 21250 CFU/m^3 at 15 L/min when the SS was kaolin clay (T. H. Lin et al., 2016). Overall, it was determined that concentrations of collected *E. coli* via aerosolization increased as concentrations of kaolin clay increased in the sludge treatment tester container, and that concentrations of bacteria collected due to aerosolization decreased as the concentration of activated sludge was increased. Lin et al., 2016 also make mention that environmental conditions, such as varying air velocity, would add complexity when applying and comparing laboratory data to bioaerosol concentrations at real WWTPs.

Michalkiewicz, 2018 conducted a year-long survey on bioaerosol emissions from eleven different WWTPs, with research collection stations at sites on each WWTP where intense mixing, transfer or aeration occurs (Michałkiewicz, 2018). The highest concentration collected from any single WWTP for mesophilic bacteria was 195,000 CFU/m^3, and the median values oscillated between 160 to 1300 CFU/m^3 across all eleven plants. One research station per WWTP, positioned at a distance of 150-200 m on the windward side relative to the WWTP border, was established as a control to confirm that the mixing sites within the WWTP were the sources of the bioaerosols. While Michalkiewicz, 2018 evaluated the collection of a variety of

microorganisms (fungi, psychrophilic bacteria, coliform bacteria, mesophilic bacteria, etc.), the research was not focused on bacterial endospores.

The EPA's report on exposure pathways of high-consequence pathogens in 2018 (Office of Research and Development Homeland Security Research Program, 2018) consolidated different results of locations of bioaerosol concentrations from previous studies. The findings can be found recreated in Table 1.

Table 1. Range of High and Low Bacterial Bioaerosol Concentrations from WWTP Proccesses

WWTP Process or Activity	High Bioaerosol Concentration (CFU/m^3)	Low Bioaerosol Concentration (CFU/m^3)
Raw Waste Influent	$1.78x10^6$ Source: (Medema, Wullings, Roeleveld, & van der Kooij, 2004)	$5.81x10^1$ Source: (Heinonen-Tanski et al. 2009)
Pretreatment/Primary Treatment	$3.73x10^3$ Source: (Fracchia, Pietronave, Rinaldi, & Giovanna, 2006)	$2.80x10^1$ Source: (Karra & Katsivela, 2007)
Sludge Management (Secondary Treatment)	$1.70x10^4$ Source: (Bauer et al., 2002)	$2.20x10^1$ Source: (Sánchez-Monedero et al. 2008)
Tertiary Treatment	$2.70x10^3$ Source: (Sánchez-Monedero et al. 2008)	$2.70x10^3$ Source: (Sánchez-Monedero et al. 2008)
Maintenance Activities	$3.16x10^4$ Source: (Medema et al., 2004)	$1.27x10^1$ Source: (Heinonen-Tanski et al. 2009)

Recreated from (Office of Research and Development Homeland Security Research Program, 2018)

The results from Table 1 show a range in concentrations from approximately $1x10^6$ CFU/m^3 to $1x10^1$ CFU/m^3. It should be noted that the experimental conditions in the referenced studies differed in terms of configuration of WWTP, environmental conditions, and bacterial organism observed. The data presented highlights the fact that bioaerosol concentrations tend to differ at

different areas of a WWTP, with the highest concentrations typically found at the initial wastewater influence, operations with sludge management, and with maintenance activities. A graphical representation of the locations within a WWTP where previous research efforts have reported above-background levels of microorganism concentrations due to bioaerosol production can be found in Figure 34 within Appendix C: Literature Review WWTP Summary.

Bioaerosol research was not restricted to wastewater applications in the literature. Zheng and Yao (2017) conducted a study on the collection efficiency of the SKC BioSampler, the same liquid impinger utilized in this research. In their laboratory-scale setup, the optimal conditions for most efficiently collecting aerosolized vegetative cells of *B. subtilis* included a BioSampler Collection Vessel volume of 20mL and a vacuum pump flow rate of 12.5 L/min (Zheng & Yao, 2017). The culturing method was used to determine the transport of viable *B. subtilis* cells in the created bioaerosols, and under the aforementioned optimal conditions, a maximum concentration of approximately 950 CFU/L was observed. This value occurred with the bacterial solution was subjected to a constant aeration rate of 2.5 L/min (Zheng & Yao, 2017). The study determined that the sampling flow rate significantly influences the collection efficiency of the BioSampler, and that the Collection Vessel volume has an impact on the viability of the collected aerosolized particles.

Lee et al., 2019 examined bioaerosol concentrations at urban, mountainous, and seaside locations between the months of February and April, analyzing the role that geography/altitude, temperature, and relative humidity contributed to bioaerosol emissions (B. U. Lee, Lee, Heo, & Jung, 2019). Maximum bioaerosol concentrations at all three sampling sites occurred during the month of April (for the three evaluated months), with the highest concentration of 775 ± 361 CFU/m^3 detected at the mountain site. The next highest concentration of 232 ± 133 CFU/m^3 was

measured at the urban site, and the lowest concentration at 150 ± 40 CFU/m^3 was measured at the seashore site (B. U. Lee et al., 2019). Decreases to these amounts by eleven-times or more was observed when comparing the concentrations from the month of February, although the mountain site still recorded the highest bacterial concentrations, followed by the urban site and then the seashore site. Bioaerosols are present and detectable in the environment, even without the introduction of turbulent, mechanical mixing or aeration. Kang et al., 2015 investigated culturable bioaerosol release from a 200 m^2 large manmade water fountain. It was found that culturable bacterial bioaerosol concentrations were nearly identical before and during an hour long operation of the fountain, pumping water at 100 L/second at 25 ± 10 CFU/m^3 and 23 ± 6 CFU/m^3, respectively (Kang, Heo, & Lee, 2015). After the fountain ran for one hour, it was discovered that culturable bacterial bioaerosol concentrations were over twice as high at 52 ± 8 CFU/m^3. This second example again demonstrated methods of producing bioaerosols not directly linked to the mechanical mixing or aeration of a WWTP.

An overall lack of comparative data in published literature prevents direct comparisons to the results presented in this document. Still, many studies provide important and applicable findings. Wang et al. varied aeration rate from 0.3 m^3/hr to 1.2 m^3/hr in an indoor, laboratory-scale wastewater treatment device (Wang, Li, Xiong, Guo, & Liu, 2019). Submerged aeration supplied air bubbles that through activated sludge and wastewater in the biochemical reaction tank and bioaerosol amounts (measured in CFU/m^3) were collected and calculated at 0.1 m and 1.5 m above the water surface. For the 4x increase in aeration rate, an increase of 2.23x in CFU/m^3 (for total bacteria) and 4.60x in CFU/m^3 (for intestinal bacteria) was observed (Wang et al., 2019). It should be noted that vegetative cells of multiple bacteria were collected and cultured in this study, as opposed to focusing on spores.

2.3 Free-Floating Carrier Media in Water and Wastewater

Free-floating carrier media (FFCM) have previously been introduced into wastewater treatment systems as a means of affixing and cultivating biofilms. Bauer et al., 2002, recommended that reducing the surface area of the aeration basin could reduce the flux of bioaerosol emissions. A wide variety of materials have been utilized as FFCM in an array of studies, including high-density polyethylene (HDPE) (Shreve & Brennan, 2019), highly-porous elastic foams (Arias et al., 2009), gravel (El-Serehy et al., 2014), polyester fabric (Abou-Elela et al., 2014), clay (Stensel & Reiber, 1983), and polystyrene (Hung et al., 2010). Khan et al. documented a positive correlation with biofilm mass, nitrification, and estrogen removal, establishing that higher surface energy plastics demonstrated an increase in biofilm mass attachment (Khan, Chapman, Cochran, & Schuler, 2013). Materials with the highest surface energy were the most hydrophobic, and materials with the lowest surface energy values were the most hydrophilic (Khan et al., 2013). Shreve and Brennan, 2019, showed that wastewater treatment systems incorporating FFCM made of HDPE showed greater removal efficiencies of trace organic contaminants when compared to traditional setups lacking the FFCM (Shreve & Brennan, 2019). Because of a FFCM's direct placement in wastewater and potential ability to absorb microbiological material, the possibility exists that FFCM could also be utilized to reduce bioaerosol emissions.

Hung et al. used floating polystyrene balls as a means of reducing bacterial bioaerosol emissions from a lab-scale aeration system to replicate the aeration in wastewater treatment processes (Hung et al., 2010). Commercially available polystyrene balls (diameters of 1.9 cm, 2.9 cm, 3.4 cm, and 4.8 cm) were threaded together to make cross-linked webs that would maintain positioning on top of the water layer during aeration at rates of either 40 $Lmin^{-1}$ or 60

$Lmin^{-1}$. *E. coli* was inoculated into the aeration tank containing approximately 48 L of water. Results were measured in terms of control efficiency, the ratio of the difference between the airborne *E. coli* concentration without surface additives and the *E. coli* concentration with surface additives to the airborne *E. coli* concentration without surface additives. While this research used BG instead of vegetative *E. coli*, the same principles could be applied to calculating control efficiencies. This study determined that decreasing the diameter of the polystyrene balls increased the control efficiency of the FFCM, and thereby established this type of additive as an economic means of decreasing bioaerosol emissions.

2.4 Atomic Force Microscopy (AFM)

AFM is readily used for creating high-quality, two and three-dimensional images with resolution of a fraction of a nanometer. AFM is the most widely used method of Scanning Probe Microscopy (SPM), a technique used to examine materials with a solid, surface-scanning probe (Miles, 1997). In the case of AFM, the force caused by the interaction between a sharpened tip located a cantilever and the sample surface is measured. The AFM used in this research was a Bruker Dimension Icon with Scan Asyst, located inside of a MBRAUN MB200B glovebox filled with nitrogen gas. The operation of the AFM was done using Bruker NanoScope (Version 9.4) software. AFM has been used in a multitude of microbiological applications, and has specifically been used to examine bacterial endospores (A. G. Li, Burggraf, and Xing 2016; Zolock et al. 2006; Zhao, Schaefer, and Marten 2005; Plomp et al. 2005)

The AFM probe tip is typically made from SiO_2 or Si_3N_4 and mounted on a cantilever spring with a known spring constant reported by the manufacturer. Samples are mounted on a piezoelectric scanner that can move in the x, y, and z directions to maintain contact with the probe. Piezoelectric materials produce an electrical voltage in response to an applied force,

changing shape in the presence of an electric field or conversely generating an electric field due to a change in shape. The near-field forces (i.e. electron cloud overlap, Van der Waals forces, capillary forces, and electrostatic forces) between the tip and sample detected by a laser deflection system are used to sense the spacing of the tip in the AFM. The laser deflection off of the cantilever is detected on a four-quadrant photodiode, and changes to the location of the laser spot due to bending in the cantilever as it scans the sample surface generates a measurable electrical signal. The properties and dimensions of the cantilever are important for determining the sensitivity and resolution of the AFM.

There are three common AFM operating modes: contact mode, non-contact mode, and tapping mode. In contact mode, the tip is constantly in contact with the sample's surface. In non-contact mode, the tip oscillates sinusoidally with small amplitude and maintains a fixed distance between the tip and the surface of the sample. The amplitude of tip oscillation is larger in tapping mode when the tip repetitively contacts and raises above the surface.

Tapping mode was used to image *Bacillus* species spores in Zolock et al., 2006 and Li et al., 2016, and was also utilized in this research. Tapping mode is relatively uninfluenced by frictional forces, which can cause distortions to images taken in contact mode. The intermittent contacting with the sample's surface at a sufficient amplitude prevents the tip from being stuck by adhesive meniscal forces of a water contaminant layer (if present). The NanoScope software had a preset mode labeled Scan Asyst Air, which automatically optimized settings for imaging. This preset mode operated the AFM in tapping mode, and was utilized in the majority of the AFM analysis in this research.

III. Methodology

3.1 Overview

BG spores in a deionized water solution were bubble aerated and the resulting bioaerosols collected with a liquid impinger collection system. Experiments were laboratory-scale tests fully enclosed within a biosafety cabinet and completed in triplicate. Aeration rates and the size of expanded polystyrene free-floating carrier media were varied. Collection times were standardized at 30 minutes for all experiments. Initial BG spore concentrations and collected spore concentrations from the production of bioaerosols were compared using the cultivation method and counting CFUs. Two-tailed, Student T-Tests were used to determine statistical significance amongst variables at the 95% ($\alpha = 0.05$) confidence level. Light microscopy and Atomic Force Microscopy were used to verify spore purity, compare physical measurements, and observe spore surface characteristics.

3.2 Preparation of BG Stock

The original *B. globigii* stock used in these experiments was provided in-kind by the US EPA. To create a new BG stock solution, 1mL of deionized (DI) water was added to 50 µL of BG stock. The mixture was homogenized using the Vortexer (Daigger Vortex Genie 2, Catalogue Number 22220A) for approximately three seconds, and then 100 µL was placed onto each of ten DIFCO/LB agar plates. The mixture was spread around each plate using a plastic L-shaped spreader before being incubated for one week at 35°C. To harvest the BG following the one-week incubation, an L-shaped spreader was used to scrape colonies off of the agar surface and into centrifuge tubes. One centrifuge tube was used for the colonies of approximately 5 of the agar plates. A 100 µL pipette tip was utilized to aid in the removal of colonies and vegetative

cells from the L-shaped spreader. A centrifuge tube was utilized to hold the pipette tip while not in use. One milliliter of DI water was added to each centrifuge tube and vortexed to suspend the BG colonies.

The centrifuge tubes were spun in a centrifuge for 20 minutes at a spin rate of 4000 rpm at a temperature of 5°C. The centrifuge was previously cooled with an empty 20-minute run at the above spin rate. The tubes were carefully removed, the supernatant was removed and discarded, and another 1mL of DI water was added to each tube. Each tube was vortexed again to break apart the pellet. This process of spinning the tubes and discarding the supernatant was repeated for a total of four iterations. The last batch was stored overnight and refrigerated. Twenty-four hours later, the centrifuge tubes were vortexed to re-dissolve any pellets that formed overnight. A fifth spin was conducted in the centrifuge under the same conditions as before. The supernatant was removed, and 1mL of DI water was added to the pellet. The centrifuge tubes were stored in the refrigerator for four additional days.

After four days, the centrifuge tubes were spun for 20 minutes at a spin rate of 4000 rpm at a temperature of 5°C. The supernatant was discarded, leaving the pellet intact. A solution of 40% Ethanol was prepared, and 1mL of the 40% Ethanol was added to the pellets in the centrifuge tubes. Each tube was vortexed to dissolve the pellet. The contents of all the centrifuge tubes were then combined into one 10mL conical tube. An additional 1mL of 40% Ethanol was added to complete the stock solution. A 10^6 serial dilution was performed prior to using the new stock solution.

3.3 Preparation of Agar Media

Agar media was prepared as needed and poured into plastic Fisherbrand petri dishes (100mm by 15mm) (Catalogue Number FB0875712). One liter of liquid agar media produced

approximately 40 agar plates. This solution consisted of 8 grams of Difco Powder Nutrient Broth (Becton, Dickinson and Company (BD), Catalogue Number 90002-660) and 15 grams of LB Agar (Fisherbrand, Catalogue Number BP1425-500). The solution was thoroughly mixed with DI water to create 1 Liter of solution and autoclaved. Once cool enough to handle, the sterile solution was poured into the petri dishes and allowed to solidify. Once the agar was properly set, the agar plates were stored in the laboratory refrigerator. Plates were visually inspected prior to use in experiments to ensure the agar remained intact and was not overly dried.

3.4 Field Rotameter Calibration

The field rotameter was calibrated through the use of a primary standard. The primary standard utilized was Bios Defender 510 (MesaLabs, Catalogue Number 200-510-M). This instrument was used to conduct a volumetric flow calibration, with a stated error of ±1% for the readings. The lowest reading possible on the field rotameter was 0.40 L/min, and the lowest aeration rate utilized during the course of the experiments was 0.50 L/min. To ensure the resultant calibration curve encompassed the entire range of aeration rates to be used during all experiments, the first aeration rate the field rotameter was set at was 0.45 L/min. The calibration curve is included in Figure 33. SKC Field Rotameter Calibration CurFigure 33 of Appendix B. The field rotameter was then disconnected from the aquarium pump, and the Bios Defender 510 was attached. At the same aeration rate from the aquarium pump, five readings were taken and recorded using the Bios Defender 510. The mean of the five values was calculated and compared to the aeration rate measured on the field rotameter. The standard deviation was used to analyze the error associated with the Bios Defender 510 measurements. The values of the standard deviations were all in the thousandths place, ranging from 0.001 to 0.005. The same procedure was repeated at a 0.55 L/min aeration rate, a 0.80 L/min aeration rate, a 1.05 L/min aeration rate,

and a 1.25 L/min aeration rate. To ensure the utility of the calibration curve, the highest calibration aeration rate on the Bios Defender 510 was higher than the highest aeration rate from the experiments (1.00 L/min). The calibration curve was plotted using the aeration rate values from the Bios Defender 510 as the independent variable and the aeration rate values from the SKC Field Rotameter as the dependent variable. The R-squared (R^2) value for the resulting linear regression line was calculated to be 0.9945, indicating a strong linear correlation.

In general, the aeration rate measurements agreed between the two measurement devices at the higher aeration rates. At a target aeration rate of 1.00 L/min, the field rotameter and Bios Defender 510 measurements differed by only 1.15%. At lower aeration rates, the variance increased, reaching at maximum at the 0.50 L/min aeration rate where the two measurements differed by 16.97%. As a result, the field rotameter was needed to be set to a aeration rate of 0.57 L/min in order to achieve a true aeration rate of 0.50 L/min. The field rotameter was set to a aeration rate of 0.70 L/min to achieve a true aeration rate of 0.65 L/min and 0.88 L/min to achieve a true aeration rate of 0.85 L/min. No adjustment was necessary on the field rotameter in order to achieve a true aeration rate of 1.00 L/min.

3.5 Experimental Setup

Submerged aeration is often used in WWTPs to provide mixing and to provide oxygen for wastewater treatment. Aeration to the experimental setup was provided from a commercially available aquarium pump (Eheim Air Pump 200). This pump had a stated power consumption of 3.5 Watts and a maximum pump output of 200 liters/hour. The pump contained a HEPA filter to reduce airborne contaminants from being drawn into the pump. A dial located on top of the pump controlled the pump output, which ranged between 0 and 2.4 liters/minute when measured with the field rotameter. Bioaerosol emissions were investigated in these experiments by varying

the aeration rate in this manner. Commercially available airline tubing (Lee's Aquarium Products, Catalogue Number 14507) with an inner diameter of 5 mm was connected to one of the output nozzles on the air pump. An in-line activated carbon filter was created to provide secondary filtering of contaminants pumped through the air pump. This in-line filter was made in the laboratory by removing the flange inside the valve housing of an Eheim-brand check valve. This in-line filter is depicted below in Figure 4.

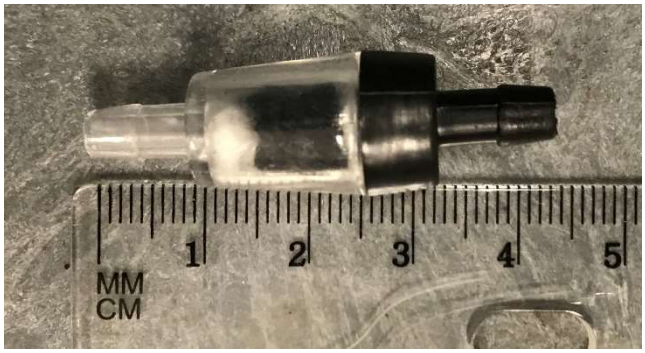

Figure 4. In-line activated carbon filter with fiberglass plugs

A fiberglass layer of approximately 0.013 grams was inserted into the valve, followed by approximately 0.155 grams of activated carbon, and finally a second layer of approximately 0.011 grams of fiberglass to keep the activated carbon in place. A second length of airline tubing was attached to the output end of this filter. The tubing was passed through the plastic cap of a one-liter Pyrex glass bottle. The cap was prepared with two holes drilled on top. A waterproof and air-tight seal was created by sealing the tubing and the two holes in the cap with silicone-based adhesive (GE brand). At the end of the tubing, a commercially available aeration stone (approximately 4 cm in length and 1.5 cm in diameter) was attached. The bottle was filled with approximately 240 mL of DI water. A second length of tubing was passed through the second hole in the plastic cap, with approximately 2 cm of tubing extending downward from the cap into

the bottle. The tubing was sealed in place with the same silicone-based adhesive. The far end of the tubing ended with the attachment of a two-way plastic connector.

During the experimental setup, the two-way connector was positioned at the opening of the biosafety cabinet. A length of airline tubing (approximately 72 cm) was attached to the two-way connector and passed through the plastic cap of the one-liter Pyrex glass bottle that served as the bioreactor bottle for the experiments. A second, 4 cm long aeration stone was attached to the end of this length of tubing and submerged in the solution contained in the bioreactor. A plastic adapter fitting was placed into the second hole of the plastic cap of the bioreactor.

Attached to the plastic adapter fitting was a length (approximately 24 cm) of platinum-cured silicone tubing. This tubing (Cole Parmer, Catalogue Number F01499) had an inside diameter of 0.500 inches, an outside diameter of 0.750 inches, and a wall thickness of 0.125 inches. This tubing was attached to the inlet piece of the SKC BioSampler (SKC Inc., Eighty-Four, PA, Catalogue Number 225-9595). The SKC BioSampler is composed of three pieces of glassware: the top inlet section, the middle outlet section with three tangential nozzles, and the bottom collection vessel.

The BioSampler was secured to a mounting rod attached to the top of the BioSampler field case. To level the height of the BioSampler to the appropriate height next to the bioreactor bottle, the BioSampler field case was placed on a standard 96-well microcentrifuge tube rack (Cole Parmer, Catalogue Number 06736-09). The nozzle on the middle outlet section was connected to a length of platinum-cured silicon tubing (Cole Parmer, Catalogue Number F01307) which had an inside diameter of 0.250 inches, an outside diameter of 0.500 inches, and a wall thickness of 0.125 inches. The length of this tubing was approximately 36 cm. The tubing was connected to the outlet valve of a 120 V air sampler vacuum pump (SKC Inc, Catalogue

Number 228-9605). The sonic flow vacuum pump was plugged into the power outlet located inside the biosafety cabinet.

Prior to starting an experiment, a $1x10^6$ serial dilution of the BG stock was performed. In a microcentrifuge tube, 10 µL of BG stock was added to 990 µL of DI water. This resulted in a $1x10^2$ serial dilution, and 10 µL of this solution was added to another microcentrifuge tube containing 990 µL of DI water. This resulted in a 10^4 serial dilution, and finally 10 µL of this solution was added to a third microcentrifuge tube containing 990 µL of DI water. The final result in the microcentrifuge tube was a 10^6 serial dilution. After vortexing the solution, 100 µL was transferred and spread onto each of three agar plates. Following 24 hours of incubation at 35°C, the colonies on each plate were counted to determine the number of CFU's per plate. A total number of CFU's in the BG stock was calculated, and then divided by the volume of the BG stock solution to determine the concentration of the BG stock solution (in CFU/mL). This process was used to determine the amount of BG stock that was necessary to add to the reactor bottle to achieve a target concentration of $2.19x10^6$ CFU/mL. Subtracting this volume from 240 mL thus determined the amount DI water to add to the reactor bottle. This volume plus the calculated volume of BG stock solution (that would result in approximately the desired CFU/mL concentration) would therefore equal a total volume of 240 mL. This reactor bottle volume was kept consistent across all experiments.

Before being utilized in the experiment, all glassware and silicone tubing to be used was autoclaved. Once cooled, the sterilized silicone tubing and glassware was transferred to the biosafety cabinet. The calculated amount of DI water was added to the reactor bottle using the Pipet-Aid pipetter. The calculated amount of BG stock solution was added to the reactor bottle

using the Fisherbrand 1000 µL pipette. The solution was mixed by swirling the reactor bottle by hand.

Experiments utilizing FFCM in the form of the small or large diameter polystyrene spheres had those spheres added to reactor bottle after the BG stock solution was added. The polystyrene balls could not be autoclaved prior to use and were washed with 70% ethanol and triple-rinsed with DI water prior to addition to the reactor bottle. A sterilized metal spatula was utilized to aid in adding the polystyrene spheres into the reactor bottle and to aid in maneuvering the spheres into a monolayer along the fluid surface. In these experiments, the term "monolayer" indicated a single layer of polystyrene spheres on top of the BG liquid solution in the reactor bottle in which every sphere was in contact with the solution.

A $1x10^4$ serial dilution was performed to verify the concentration of BG within the reactor bottle. For each experiment, two microcentrifuge tubes were filled with 990 µL of DI water. A Fisherbrand 10 µL pipette was used to extract 10 µL of inoculated solution from the reactor bottle, which was then added to the first microcentrifuge tube containing 990 µL of DI water to create a $1x10^2$ serial dilution. The microcentrifuge tube was vortexed for 3 seconds and labeled. The 10 µL pipette was used to extract 10µL from the $1x10^2$ serial dilution microcentrifuge tube and the new aliquot was added to the second microcentrifuge tube containing 990 µL of DI water to create a $1x10^4$ serial dilution. The microcentrifuge tube was vortexed for 3 seconds, labeled, and placed inside the biosafety cabinet. The Fisherbrand 100 µL pipette was used to add 100 µL to each of three agar plates. The plates were labelled and incubated at 35°C for 24 hours.

Next, the SKC-brand BioSampler was set up inside the biosafety cabinet. The bottom of the three pieces was the 20 mL BioSampler Collection Vessel (Catalogue Number 225-9596)

and this was placed on the BioSampler field case and secured to the mounting rod with the attached hook-and-loop fastener strap. The Outlet Section (Catalogue Number 225-9593) with the three tangential nozzles was set inside the Collection Vessel. The third piece, the Inlet Section (paired with the Outlet Section catalogue number), was set inside the top of the Outlet Section. The length of smaller diameter silicone tubing (inside diameter of 0.250 inches) was connected between the outlet nozzle on the Outlet Section to the nozzle on the air sampler vacuum pump. The air sampler vacuum pump was set to a vacuum pressure of approximately 2.0 inches of Mercury (inHg).

Outside of the biosafety cabinet, the commercially available aquarium pump was set on the flat, level surface of a laboratory cart. A 5.0 cm of airline tubing was connected to the outlet nozzle of the pump. Connected to the other end of the airline tubing was the inlet of the custom-made in-line activated carbon filter. Airline tubing was attached to outlet of the activated carbon filter and ran to the water trap. The cap on the water trap bottle was tightened as much as possible by hand to help create an airtight seal in conjunction with the use of the silicone-based adhesive. The water trap bottle was filled with 240mL of DI water, the same amount of fluid as the reactor bottle inside the biosafety cabinet. A 2cm long aeration stone provided the bubbling inside the water trap. The airline tubing from the exit port of the water trap led to the sash of the biosafety cabinet, where it terminated with a two-way plastic connector.

The aeration rate was set at one of four different rates for all of the experiments: 0.50 L/min, 0.65 L/min, 0.85 L/min, and 1.00 L/min. This rate was set by turning the manual dial on top of the aquarium pump and verified using a field rotameter. The SKC Field Rotameter (SKC, Catalogue Number 320-4A5) was used to verify the aeration rate from the aquarium pump prior to each experiment. The air flow rate was measured by removing the two-way plastic connector

that connects the tubing from the water trap to the tubing that runs into the biosafety cabinet. The end of the tubing running out of the water trap was connected to the field rotameter. This ensured that the air from the pump had already traveled through the pump's internal HEPA filter, the activated carbon filter, and the water trap. The field rotameter measurement was obtained visually when any vertical movement in the measurement ball had ceased. The measurement took place along the largest width of the measurement ball. The field rotameter was disconnected and the tubing for the experiment was reconnected at the two-way plastic connector.

A section of airline tubing approximately 72 cm long was cut and decontaminated by wiping it down with 70% ethanol. This section of tubing was connected to the two-way plastic connector and passed through one of the two holes in the cap of the reactor bottle. The cap of the reactor bottle had two 0.65 cm-diameter holes drilled in the middle of the top surface. Once passed through, a second 2 cm long sterile aeration stone, that had been autoclaved with the tubing and glassware, was attached to the airline tubing. The aeration stone and tubing were pushed downward into the reactor bottle until the aeration stone reached the bottom of the bottle. As best as possible, the aeration stone was positioned in the center of the bottle, lying horizontally. Due to pre-existing bends in the airline tubing and the design of the reactor bottle and cap, this positioning was not always possible. Nevertheless, the aeration stone was always completely submerged in the fluid inside the reactor bottle.

The desired effect was for the bubbles to originate in the bottom of the reactor bottle and float upwards to the surface of the BG solution. A Straight Barbed Reducing Fitting (Cole Parmer, Catalogue Number UX-06458-10) was placed into the second hole in the cap of the reactor bottle. The length of larger diameter silicone tubing (inside diameter of 0.500 inches) was connected between the Inlet Nozzle of the BioSampler and the reducing fitting on top of the

reactor bottle. This aspect of the experimental setup varied from previous setups using SKC BioSamplers mentioned in literature. The Inlet Nozzle in these experiments was connected to the reactor bottle with tubing, whereas other studies have not attached any tubing to the Inlet Nozzle. The open nozzle drew in air in the vicinity of the opening, dependent on the draw from the vacuum pump. Other experiments confined the BioSampler in a chamber to reduce outside contamination, but still left the nozzle open. Impacts on the BioSampler's efficiency were possible due to this experimental design, however, the same setup was used consistently throughout all of the performed experiments. Loss of BG spores being aerosolized in the reactor bottle but not arriving in the collection liquid of the BioSampler were therefore expected to be similar across all experiments with similar parameters.

Once the aeration stone was properly submerged, the cap of the reactor bottle was hand-tightened. Once tight, the cap was loosened one-half turn. A pre-made mark on the cap aided in determining the one-half turn. The glass Pyrex bottle had vertical seams in the glass on both sides of the bottle, 180° apart. The mark on the cap was made to align with one of the seams when fully tightened. To loosen by half a turn, the cap was rotated until it matched up with the seam on the opposite side. Placing the cap in this position ensured consistency across all experiments. It also allowed for airflow to exist while the vacuum pump was drawing in air on the opposite side of the apparatus. Wastewater treatment plants do not operate in sealed, air-tight environments. Having the reactor bottle cap loosened served to allow for the functioning of the apparatus by providing airflow for the vacuum pump to continuously cycle out, and to more closely replicate real-life wastewater treatment plant conditions.

Once the apparatus was properly setup, the vacuum pump was turned on, followed immediately by turning on the aquarium pump. The start time was annotated, and a timer set for thirty minutes. Figure 5 shows a complete experimental setup inside the biosafety cabinet.

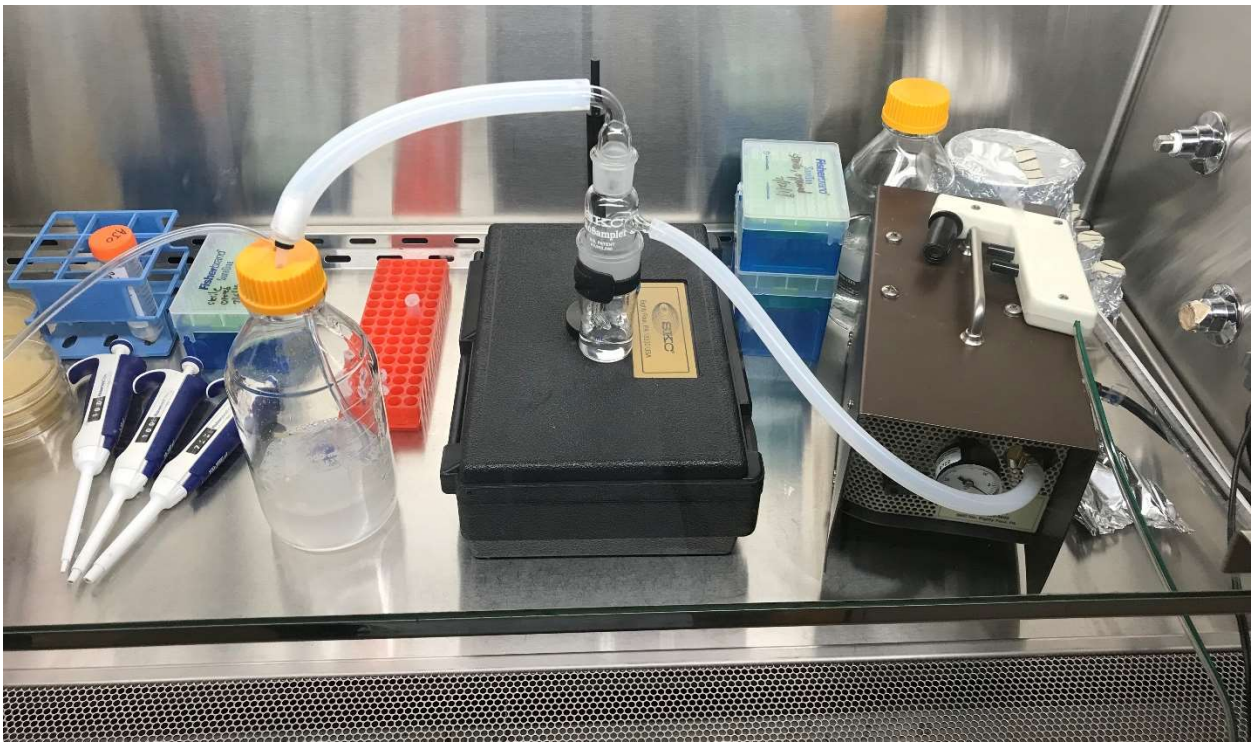

Figure 5. Experimental setup inside the biosafety cabinet for Experiment BGA12

Digital pictures and video were taken for documentation purposes. Following the thirty-minute collection, the aquarium pump was turned off, followed immediately by the vacuum pump. The tubing connected between the vacuum pump and Outlet Nozzle of the BioSampler was disconnected and placed in a biohazard bag for post-experiment autoclaving. The silicone tubing connected between the Inlet Nozzle of the BioSampler and the plastic reducing fitting on top of the reactor bottle was also disconnected and placed in the same biohazard bag. The top two portions of the BioSampler (the Inlet Nozzle and the Outlet Nozzle) were removed and placed in a 600mL beaker for eventual autoclaving. Emitted bioaerosols from the reactor bottle were

captured in the DI water in the Collection Vessel of the BioSampler. One milliliter of the solution from the bottom of the Collection Vessel was removed using the Fisherbrand 1000µL pipet and placed in a microcentrifuge tube. The microcentrifuge tube was then vortexed for three seconds, and 100µL was pipetted on one of each of five agar plates. An L-shaped spreader (Fisherbrand, Catalogue Number 14-665-230) was used to spread the fluid evenly across the surface of each plate. A new, sterile L-shaped spreader was used for each individual plate. The five plates were labelled and incubated at 35°C for 24 hours. The colonies formed on the plates after 24 hours were counted as CFUs, and the values for each plate was recorded.

A typical experiment was conducted in triplicate. The reactor bottle, polystyrene spheres (if added), and airline tubing connected to the aquarium pump were all kept the same. Silicone tubing and the BioSampler were replaced for each of the triplicates. Prior to setting up the BioSampler, a serial dilution was always performed to verify the concentration of the reactor bottle. The process for the serial dilution was the same as previously described. Setup of the BioSampler and running the aquarium pump and vacuum pump for thirty minutes was also always kept constant. For each triplicate, five agar plates from the BioSampler and three agar plates from the serial dilution were inoculated and incubated at 35°C for 24 hours.

The quantity of CFUs present on each agar plate was important. Plates with high numbers of colonies on them were difficult to count by hand and too many colonies within a given space could inhibit germination from otherwise viable spores. No set number of CFUs could be set as a threshold for being “too many,” but CFU counts above 850 CFUs or higher became difficult to accurately count and inhibited growth appeared possible based on how close colonies were to one another. In cases where high CFU counts were present or suspected, an additional 10x dilution was performed by adding 100 µL of swirled liquid from the BioSampler to 900 µL of DI

water. This mixture was vortexed for three seconds, and 100 µL was transferred to each of five agar plates and spread evenly across the surface with an L-shaped spreader.

Similarly, low CFU counts (typically of 25 CFUs or lower) presented statistical challenges. Applying the Central Limit Theorem, larger population sizes reduce the variance, or the dispersion about the mean, and thus also lowers the standard deviation. Low CFU counts contributed to higher variances within the data. When too few CFU counts were present or suspected, an additional 10x concentration was performed by transferring 10 mL of collection liquid from the BioSampler using a glass pipette to a plastic 15 mL-capacity conical vial. The tube was placed in the centrifuge for 20 minutes at a rotational velocity of 4,000 rpm. Once complete, the conical vial was carefully transferred back to the biosafety cabinet and the top 9 mL of liquid were removed and discarded with a pipette. The remaining 1 mL was then mixed by vortexing for three seconds, and 100 µL was transferred to each of five agar plates and spread evenly across the surface with an L-shaped spreader.

Once all triplicate experiments were completed for a given set of conditions, the equipment was either decontaminated or sterilized and disposed of in accordance with safety protocols. The silicone tubing, plastic reducing fitting, BioSampler pieces, reactor bottle, and biohazard trash bag were all autoclaved. Prior to removing the reactor bottle from the biosafety cabinet, the airline tubing was disconnected at the two-way connector. The tubing that was in the biosafety cabinet and that ran through the reactor bottle (including the connected aeration stone) was disposed of in the biohazard trash bag. Polystyrene spheres were left in the reactor bottle and removed after running the autoclave. Reusable equipment from the experiment was rinsed with 70% ethanol once removed from the biosafety cabinet before being properly stored. The biosafety cabinet itself was wiped out and cleaned with 70% ethanol prior to turning off the

laminar flow inside the biosafety cabinet. Silicone tubing and glassware was autoclaved, double-washed in the laboratory sink and dried prior to use in a subsequent experiment.

3.6 Data Analysis Techniques

Inferential statistical analysis is necessary in order to make predictions based on the data collected in these experiments. Such analysis will be required so that predictions in other experimental and real-world applications may have statistical backing. Hypothesis testing is a form of inferential statistics where sample data is used to answer research questions. A hypothesis can be posed that states a variable has an impact on the collected data (or that it does not have an impact). When comparing variables such as flowrate and the presence (or not) of floating additives, a null hypothesis was established to state that no statistically significant change in spore collection in the BioSampler would be observed with the presence of the variable. The alternate hypothesis, in this case, stated that the statistically significant change in spore collection in the BioSampler would be observed with the presence of the variable. A variety of statistical tools and models can be used for hypothesis testing.

A Student's T-test (or just "T-test") can be used as a hypothesis testing tool that analyzes two sets of data. The T-test is capable of calculating the likelihood that the cause of data being similar (or different) is due to chance, and thus the likelihood that the reason is due to the presence (or absence) of the variable. The T-test requires the establishment of a significance level or alpha-value (α). The alpha-value is defined as the probability of accepting the alternate hypothesis when the null hypothesis is, in fact, true. In statistics, such an occurrence is known as a Type I error. In scientific experimentation, an alpha-value of 0.05 is generally acceptable. This alpha-value represents a 5% likelihood of committing a Type I error.

Different types of T-tests exist for different forms of data distribution and for different hypotheses. T-tests can be paired or unpaired, depending on whether the two sets of data being compared are paired or unpaired. The data compared in these experiments was unpaired. The nature of the hypotheses being posed will determine whether the T-test is one-tailed or two-tailed. The terms refer to the normal distribution curve model upon which the T-test is based. A hypothesis asking whether a set of data is only greater in value (or only less in value) than the second would require a one-tail T-test. A hypothesis asking whether a set of data is significantly different in value (either greater or less) than a second set of value would require a two-tail T-test. In these experiments, just the presence of statistically significant difference was being investigated. It did not matter whether one data set was higher or lower in value than another, just whether or not they were significantly different. A two-tailed, unpaired T-test was therefore selected for this statistical analysis.

This established alpha-value is compared to the p-value obtained from running the T-test. If the calculated p-value is larger than the alpha-value, a significant difference is not observed between the two data sets. If the calculated p-value is smaller than the alpha-value, a significant difference is observed between the two data sets. Microsoft Excel 2016 was used to perform the T-test analysis in these experiments. The displayed results included the calculated p-value. The p-value was then compared to the alpha-value of 0.05 to determine statistical significance.

3.7 Scale-Up

With applications of research results intended for large volumes of water in WWTP's, the influence of scale was an additionally studied factor. This research represented the medium-scale contribution to a series of experiments also comprised of small and large-scale efforts. The small-scale was conducted in the same biosafety cabinet as the medium-scale, as this was the

only location at the Air Force Institute of Technology where bioaerosol experiments could be conducted. The large-scale experiments were conducted in Cincinnati, OH at the EPA's WWTP Pilot Scale Facility.

The medium-scale experiments utilized a reactor bottle that was four times larger in volume, 1.00 L versus the small-scale experiment's 250 mL reactor bottle volume. Not all aspects of the experimental scale-up followed a four-times increase. The surface area of the DI water within the small-scale reactor bottle was 31.25 cm^2 and 71.42 cm^2 in the medium-scale reactor bottle, a 57% increase. The average diameter of the expanded polystyrene FFCM used in the small-scale experiments was 2.24 mm compared to a diameter of 4.23 mm in the medium-scale experiments, a 47% increase. These measurements were made available through the unpublished results for an ongoing investigation (Burdsall et al., 2020). The pumps providing airflow into the reactor bottle as well as the mechanism responsible for producing bubbles under the surface of the water within the reactor bottle were different in the two experimental scales. However, aeration rates of 0.50 L/min and 0.85 L/min were utilized in both the small and medium-scale experiments. Experiments at both scales were conducted with and without FFCM, allowing for further comparison.

At the time of writing this document, one initial large-scale experiment, and the unpublished data was still being analyzed. The pilot-scale wastewater treatment system was located at the EPA's Test and Evaluation (T&E) Facility in Cincinnati, Ohio. The system contained a 25 L primary clarifier, a 213 L aeration basin, and a 52 L secondary clarifier. The aeration basin was separated into six independent compartments (labeled A through F), each receiving submerged bubble aeration at a rate of 3.5 L/min, and each having an approximate volume of 35.5 L. Figure 6 shows the six compartments comprising the aeration basin.

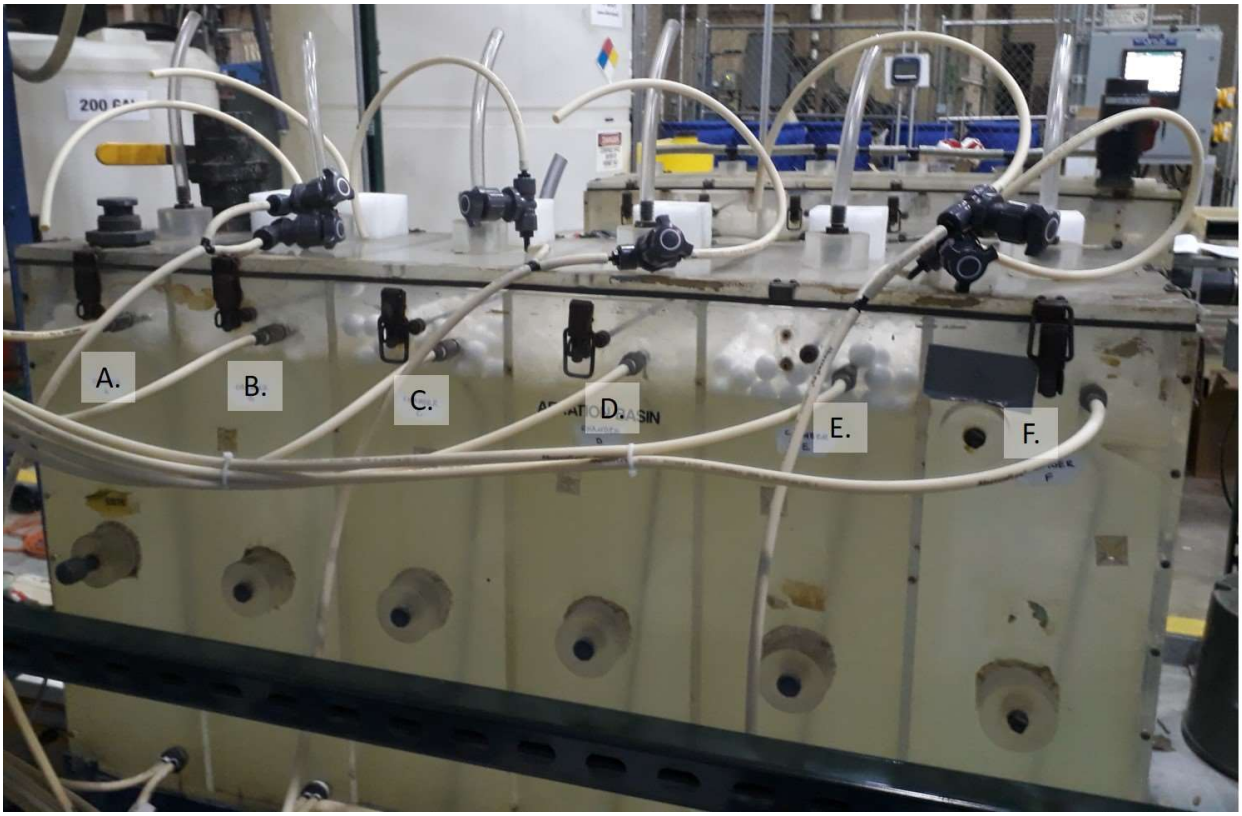

Figure 6. Aeration basin for the large-scale experimental setup composed of six separate compartments labelled A through F.

The estimated amount of actual liquid volume in each compartment was 31.28 L. The surface area of each compartment was calculated to be approximately 586.42 cm^2. A stock of BG spores was created to a concentration of $1.1x10^8$ CFU/mL, and this stock of BG spores was fed into the system at a rate of 3 mL/min. SKC BioSamplers collected bioaerosols generated from each of the six compartments, and the sampling rates were planned to be set at 8.5 L/min. Compartments A and D contained 1.27 cm (0.5 inch) diameter hollow, low-density polyethylene (LDPE) spheres arranged in two layers for the added FFCM. Compartments C and E contained 1.27 cm diameter polystyrene spheres arranged in two layers for the added FFCM. With both material types, the bilayer was composed of 185 spheres. Compartments B and F did not contain any added FFCM and served as the experimental controls. Bioaerosol collection times were 30 minutes in duration,

the same as the small and medium-scale experiments conducted at AFIT. Samples were also collected from each compartment of the aeration basin when bioaerosol samples were taken, so the concentrations could be compared. Sampling from the water and the bioaerosols was planned to be taken at 1, 7, and 24 hours following startup of the pilot-scale wastewater treatment system.

The large-scale setup is 148-times larger than the medium-scale, based on total volume of the reactor bottle or aeration basin compartment that holds the water being aerated. The medium-scale was four times larger than the small-scale experiments in this same way. The small and medium-scale experiments were conducted in a controlled environment: inside a laminar-flow biosafety cabinet located inside a temperature-controlled laboratory room. The large-scale setup is an open system, although still indoors. Contamination is a concern, particularly contaminants that would decrease sporulation or otherwise inhibit BG colonies from growing once plated. The samples plated from the initial large-scale experiment were heat-shocked prior to plating in order to mitigate contamination. Environmental factors such as temperature and relative humidity will be more variable than in the laboratory setting. While some of the future experiments are planned to contain just water in the aeration basin, the initial experiment had synthetic wastewater added by researchers at the EPA, resulting in additional variables when compared to the small and medium-scale bioaerosol experiments.

3.8 OD 600 for Spore Concentration Verification

Calculating accurate values for the concentration of BG spores in the reactor bottle prior to the start of the bubble aeration and in the BioSampler following the collection of generated bioaerosols was of paramount importance. In addition to cultivation methods used to count CFUs on incubated agar plates, the Biomate 3 spectrophotometer (Fisher Scientific) was used to measure the optical density at 600 nm (OD 600) values as a secondary confirmation of reported

concentration values. Bacteria in natural conditions rarely produce pigments in the green visible light section of the electromagnetic spectrum, meaning that scattered light at a wavelength of approximately 600 nm is most likely scattered by the bacterial cells. OD 600 has been widely used in microbiological research as a rapid way of determining concentrations of organisms based on turbidity of a solution analyzed in a cuvette with less investment of human resources. The Biomate 3 operated with Eppendorf UVette (Catalog Number 952010051) cuvettes with a transmission range of 220 to 1600 nm. Prior to taking measurements, a blank sample was prepared by filling a cuvette with 100 µL of DI water, and then 100 µL of the sample was added to a second cuvette. The cuvettes were loaded into the spectrophotometer using the 2 mm optical path length orientation. The blank cuvette was loaded first, and the "Measure Blank" option was selected on the spectrophotometer. Once the baseline reading was collected, the blank cuvette was removed, and the sample cuvette was loaded. The "Measure Sample" option was selected, and an OD 600 value was provided on the digital screen. Five readings were typically recorded, and the values averaged.

To use OD 600 values, the culture method must first be used to determine CFUs at various concentrations. Undiluted, the stock solution for BGA3 had an OD 600 value of 1.3844, with the CFU counting results equating this value to a concentration of 2.38×10^9 CFU/mL. A one-tenth dilution (2.38×10^8 CFU/mL) of the stock solution resulted in an OD 600 value of 0.4584. The one-hundredth dilution (2.38×10^7 CFU/mL) resulted in an OD 600 value of 0.0862, and the one-thousandth dilution (2.38×10^6 CFU/mL) had an OD 600 value of 0.0036. Figure 7 shows the resulting plot of the BG concentration and OD 600 values, with a superimposed regression line. Error bars represent the standard deviation calculated from five different

measurements for each data point. In the case of the smaller OD 600 values, the error bars are too small to be observed in Figure 7.

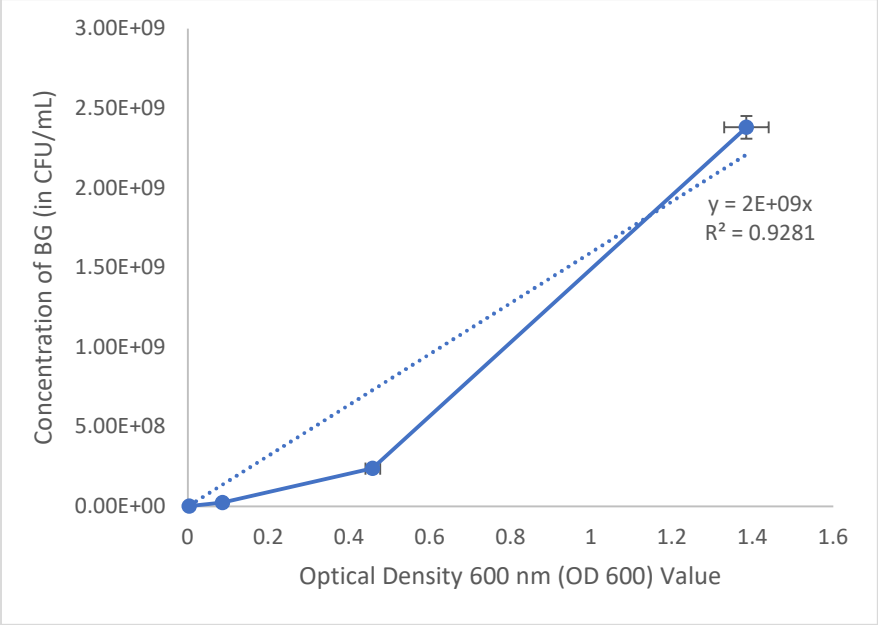

Figure 7. Equivalent OD 600 values for concentrations of BG spores (CFU/mL) from the BGA3 stock

The R^2 value of 0.9281 suggests a relatively strong linear fit. The resulting equation can be utilized to approximate a concentration of BG in CFU/mL with any obtained OD 600 value.

An OD 600 value of 1.00 would equate to a BG spore concentration of $2x10^9$ CFU/mL using the regression line equation from Figure 7. Nagler and Moeller, 2015, investigated *B. subtilis* with an OD 600 of 0.5 equating to a concentration of $1.67x10^8$ spores/mL (Nagler & Moeller, 2015). Paidhungat et al., 2002, calculated a different value for *B. subtilis* spores, equating an OD 600 value of 1.0 to $1x10^8$ CFU/mL (Paidhungat et al., 2002). Vegetative cells of *B. cereus*, not their spores, were studied by Biesta-Peters et al., 2010, and they observed an OD 600 value of 0.5 equating to approximately $1x10^9$ CFU/mL. These values reinforce the use of OD 600 as a complimentary secondary method for verifying BG spore concentrations.

3.9 AFM Sample Preparation

Samples from the BG stock solution and collected in the BioSampler were prepared for viewing in the Bruker Dimension Icon Atomic Force Microscope (AFM). The AFM is housed within an oxygen-free, nitrogen-filled MBraun Glovebox. The nitrogen gas environment facilitated a consistent measurement environment with little relative humidity to interact with the spores. Experimental samples were mounted on 1 cm diameter stock specimen disks. The BG stock solution contained 40% ethanol, and this was removed by washing with DI water. A total of 100 µL of BG stock solution was added to 900 µL of DI water and centrifuged at 4,000 rpm at a temperature of 5°C for 20 minutes. The top 900 µL of supernatant was removed with a micropipette, and another 900 µL of DI water was added. The solution was mixed by using the Vortexer for 3 seconds and centrifuged for another 20 minutes under the same conditions. The top 900 µL of the supernatant was removed, and a separate micropipette was used to remove the top 80 µL of the resulting supernatant. Around 20 µL remained in the microcentrifuge tube, and this volume was pipetted onto a mica specimen disk and allowed to dry.

A similar procedure was followed for samples taken from the BioSampler, except the steps for washing the ethanol were not required. Ten milliliters from the BioSampler was centrifuged at 4,000 rpm at a temperature of 5°C for 20 minutes. The top 9 mL of the supernatant was removed, and the resulting 1 mL was mixed by using the Vortexer for 3 seconds and centrifuged for another 20 minutes under the same conditions. The top 900 µL of the supernatant was removed, resulting in 100 µL of solution at a 100x concentration from the starting BG concentration. Around 20 µL remained in the microcentrifuge tube, and this volume was pipetted onto a mica specimen disk and allowed to dry.

3.10 AFM Setup

The AFM was operated using NanoScope Analysis Version 1.4 software (Bruker Corporation). A SCANASYST-AIR tip (silicon tip on a nitride lever) was used. The cantilever had a resonance frequency (f_o) of 70 kHz, a length of 115 µm, a thickness of 650 nm, a width of 25 µm, and a spring constant (k) of 0.4 N/m. The tip had a radius of 2 nm. The AFM was operated in the SCANASYST mode, a proprietary setting from the manufacturer (Bruker). In this modality, image quality was continuously monitored, and parameter adjustments were made automatically during the process of a scan. Automatically optimized scan parameters allowed for faster scans, increased consistency between scans, and protection of the delicate tip from damage. Once calibrated and aligned, the microscope view was utilized to identify areas where spores, appearing as small, black flecks, existed on the mica disks. Images of groups of spores or individual spores could be obtained by using both the Height Sensor and Peak Force Error results.

3.11 Phase Contrast Microscopy

Phase contrast microscopy was utilized throughout the experiments to measure BG spore dimensions and to confirm that the BG spore stock solution preparation did not contain vegetative cells or contaminants. A Zeiss Axioskop 50 was used, with both 40x and 100x oil-immersion objectives. Heat-fixing aided in keeping BG cells and spores stationary on the slide. OMAX Troup View (Version 3.7) software was used for taking digital images, and ImageJ (version 1.52a from the National Institutes of Health (NIH)) software for digital image analysis. A picture of a 10 µm ruler standard was taken, and using ImageJ, the number of pixels in the 10 µm standard was determined. Spore dimensions were then measured in pixels and converted to micrometers.

IV. Results and Discussion

4.1 Bioaerosol Capture

Experiments examining twelve different experimental conditions were conducted to evaluate the factors of aeration rate and the presence of FFCM and those factors' impact on bioaerosol production. Four different aeration rates (0.50, 0.65, 0.85, and 1.00 L/min) were used in experiments with either no FFCM added (controls), the small expanded polystyrene spheres added in a monolayer, or the large expanded polystyrene spheres added in a monolayer. As these experiments represent the medium-scale of a much larger set of experiments conducted between AFIT and the EPA, these medium-scale results were also analyzed with the results of Dr. Adam Burdsall's unpublished small-scale experiments.

Table 2 provides a summary of the averaged experimental data collected in the twelve aforementioned experiments.

Table 2. Summary of Averaged Experimental Data

Experiment Number	Aeration Rate (L/min)	Average BG in Rx (CFU)	Average Standard Deviation	Average CFU Captured in BioSampler (CFU)	Average Standard Deviation	Average Percent of Reactor Bottle Captured in BioSampler (%)	Average Standard Deviation
BGA13	0.50	5.520e8	1.528e8	4.727e4	4.475e3	8.753e-3	1.839e-3
BGA14	0.50	3.680e8	8.285e7	8.778e2	1.532e2	4.209e-4	1.983e-4
BGA31	0.65	3.640e9	1.252e8	2.259e5	9.668e3	6.267e-3	1.044e-3
BGA32	0.65	4.304e9	2.584e8	3.349e4	2.965e3	7.690e-4	2.718e-4
BGA33	0.85	2.141e9	3.610e8	2.791e5	3.260e4	1.320e-2	1.703e-3
BGA34	0.85	2.589e9	1.610e8	1.903e4	3.629e3	6.866e-4	4.517e-4
BGA35	1.00	2.029e9	1.733e8	3.441e5	7.521e4	1.730e-2	2.548e-3

BGA36	1.00	1.104e9	1.608e8	1.093e4	1.206e3	9.662e-4	2.886e-4
BGA37	0.50	1.261e9	2.195e8	1.003e4	1.447e3	7.611e-4	4.418e-4
BGA38	0.65	1.077e9	1.837e8	1.325e4	2.525e3	1.260e-3	5.252e-4
BGA39	0.85	6.453e8	8.980e7	1.299e4	1.753e3	2.042e-3	3.018e-4
BGA41	1.00	3.635e9	2.764e8	1.261e5	1.323e4	3.445e-3	7.776e-4

Each condition was run in triplicate, and each value in Table 2 represents the mean of the three triplicate values.

Figure 8 graphically shows the results from the twelve experiments listed in Table 2, with each experiment represented by three dots of the same color, and each dot representing one of the triplicate experiments for each experimental condition. The independent variable along the x-axis was the amount of BG spores inside the reactor bottle, expressed in terms of 10^7 CFU's. The dependent variable along the y-axis is the resultant percent obtained by dividing the amount of CFU's captured in the BioSampler by the starting amount of CFU's in the reactor bottle and multiplying by one hundred. The collection efficiency of the BioSampler was suggested to be 100% by the manufacturer and calculated at approximately 96% for BG spores in previously published studies (Kesavan et al., 2010). The operating conditions of the BioSamplers were kept standardized across all experiments, limiting any change in collection efficiency of the BioSamplers between experiments. The capture data is normalized to the starting BG concentration within the reactor bottle.

Horizontal error bars represent the standard deviation calculated for the starting BG concentration in the reactor bottle for each experiment. The range indicated by the horizontal error bar for each individual experiment and the overall range in x-axis values for the groupings of experimental parameters demonstrate a degree of variability in attempting to reach a

consistent BG spore concentration. While the same target concentration was utilized in calculations, it was not possible to consistently reach this target BG spore concentration in every experiment. Vertical error bars were not present in this figure, as the percent of BG spores captured in the BioSampler was the per experiment was the result of one individual calculation. Vertical error bars are included in later figures in which a single icon is used to represent the average of the triplicate experiments. Low CFU counts on agar plates may have also contributed to larger than expected variances in the analyzed data.

In general, the data collected in triplicate formed relatively close clusters. The four clusters with the highest values of the percent of reactor captured represented the four control experiments where no FFCM was added to the reactor bottle solution. The control experiments had a percent of reactor captured on the order of approximately 10^{-2}%, while the experiments in which FFCM of any size was added had a percent of reactor captured on the order of approximately 10^{-3}%. Further analysis will break down this overall representation of experimental data into more specific topics.

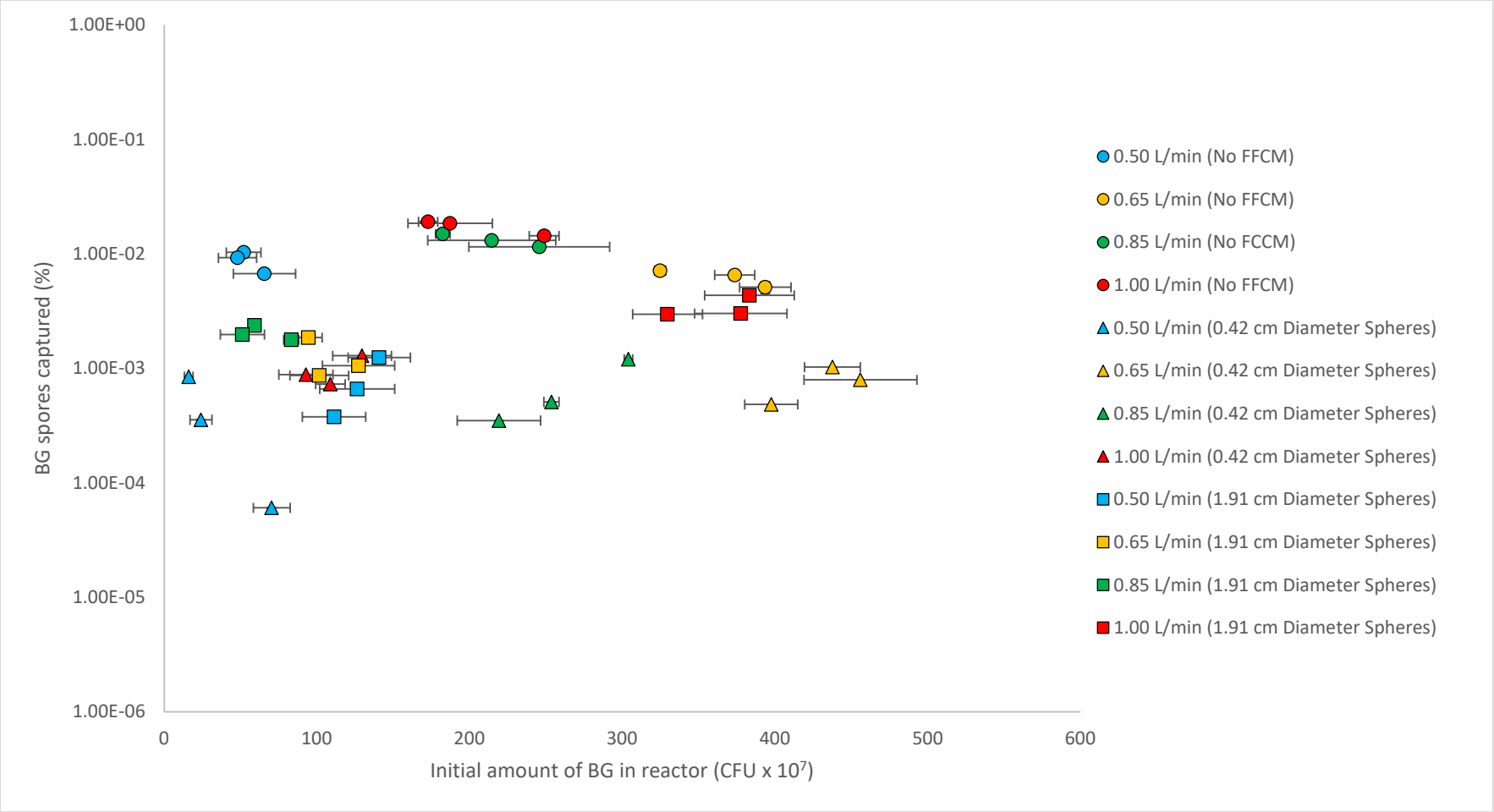

Figure 8. Percent of reactor captured in the BioSampler vs starting amount of BG in the reactor bottle (all data)

4.2 Effect of Increasing Aeration Rate on Bioaerosol Capture

The first variable analyzed was the effect of varying the aeration between 0.50, 0.65, 0.85, and 1.00 L/min in the reactor bottle. Aeration rates of 0.50 and 0.85 L/min were utilized in the small-scale experiments and were selected for inclusion in these experiments to allow for comparability. Aeration rates were selected at bubbling intensities that allowed for large numbers of bubbles to be created, but that were also low enough to have bubble aeration as the only mixing mechanism. High aeration rates through the aeration stone led to sloshing of the liquid inside the reactor bottle, and therefore introduced additional forms of turbulent mixing to the system. Figure 9 shows the effect of aeration rate on the percent of the reactor bottle captured in the BioSampler, separated into three groups based on the presence or lack of FFCM. It was hypothesized that aeration rate and percent of the reactor bottle captured would be proportional, and the plotted data for each additive condition would for a stair-step like arrangement. This was only true for when the larger (1.91 cm diameter) polystyrene spheres were added to the reactor bottle. In all three groupings, the largest percent of BG captured occurred when the aeration rate was at its highest value of 1.00 L/min.

Additionally, in all three groupings, the lowest percent of BG captured occurred when the aeration rate was at one of its two lowest values, either 0.50 or 0.65 L/min. With no FFCM added, the percent increase in the percent of BG spores captured was 97.58% when increasing from 0.50 to 1.00 L/min. For the same increase in aeration rate, the percent increase of in the percent of BG spores captured was 129.57% when the 0.42 cm diameter spheres were present and 352.60% when the 1.91 cm diameter spheres were present in the reactor bottle.

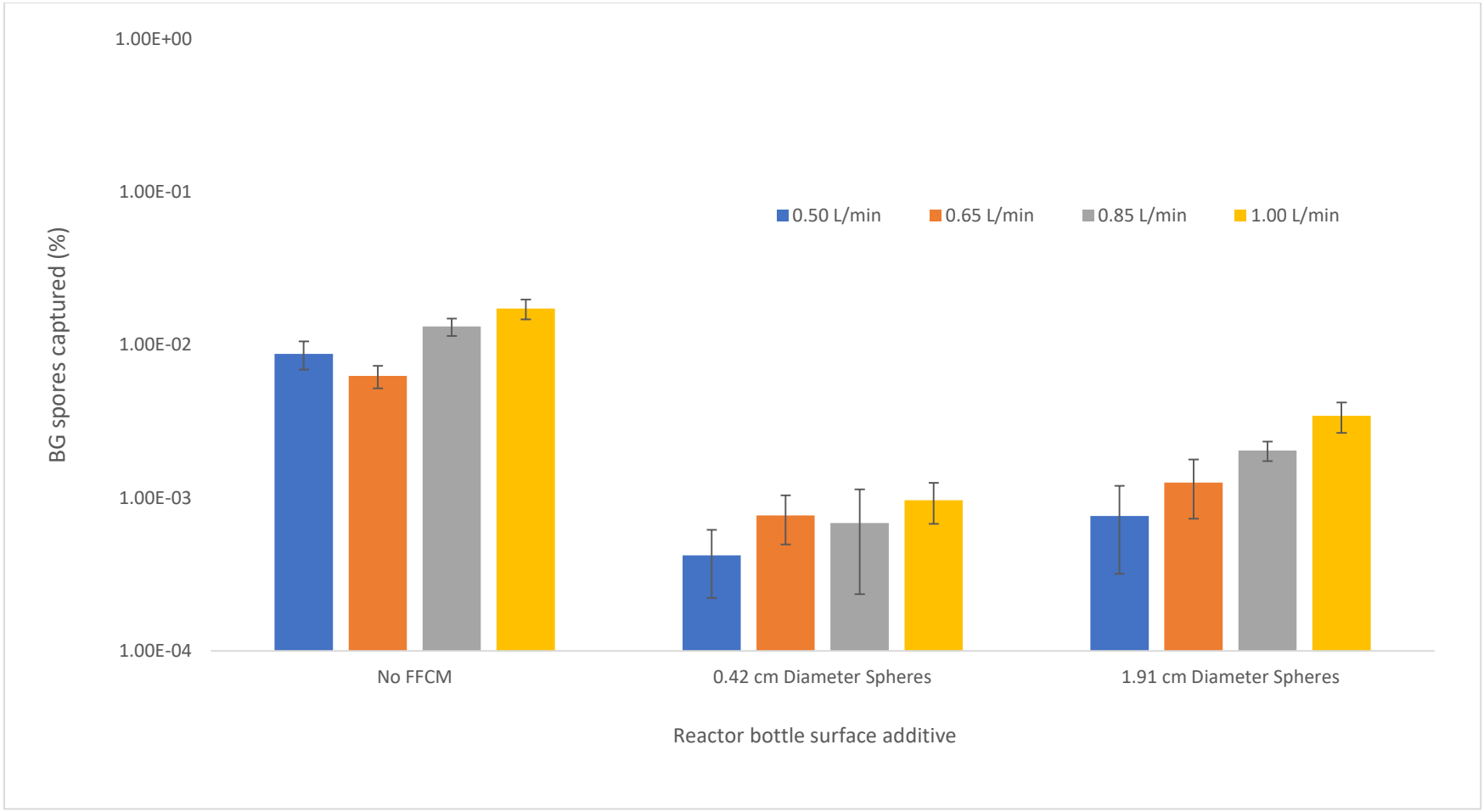

Figure 9. Average percent of BG from the reactor bottle captured in the BioSampler with three reactor surface conditions

For each group of data in Figure 9, a linear regression line was applied and the resulting coefficient of determination (R^2 value) was calculated. The grouping of data of aeration rates investigated when 1.91 cm diameter spheres were added to the reactor bottle possessed an R^2 value of 0.9489, suggesting a strong linear fit between increasing aeration rate and a resulting increase in the percent of BG spores captured. The other two groups of data have lower R^2 values assigned to their linear regression lines. The R^2 value corresponding to the group of data when 0.42 cm diameter spheres were added was 0.7874, and the corresponding R^2 value to the group of data when no FFCM was present was 0.7429. All three groups of data show an overall positive correlation over the range of investigated aeration rates.

A weak overall correlation could be made upon graphical inspection that higher aeration rates tend to result in higher percentages of BG collected in the BioSampler following aerosolization in the reactor bottle. Statistical analysis will be provided to better quantify the correlation between these two factors.

4.2.1 Effect of Increasing Aeration Rate on Bioaerosol Capture with Increased Reactor Concentration

The concentration of BG spores in the reactor bottle was not always the same for every experiment, although a target concentration of 2.19×10^6 CFU/mL was always intended for the first twelve experiments. Reasons for these variations vary widely. Small differences inevitably occurred in each batch of agar media plates generated, although the same formula and techniques were employed at the creation of every batch. Temperatures and relative humidity within the lab and incubator could have fluctuated somewhat. Serial dilutions were utilized to obtain countable CFUs on agar plates, but low enough numbers to prevent high numbers of colonies from self-

suppressing growth of more colonies. A more likely source of variation is how the BG spores are distributed inside the stock solution vial prior to plating and prior to addition to the reactor bottle. While the tube was always vortexed for three seconds, spores had some available time to start settling out, congregating in higher numbers, or just in general move through the liquid media. These differences would have been fully or partially responsible for the variation in the amount of BG spores in the reactor bottle at the start of each experiment.

A separate experiment was conducted that tripled the target concentration to 6.57×10^{6} CFU/mL. All other experimental conditions were kept the same to maintain comparability. Figure 10 displays the average of the triplicate data collected from each experiment. The x-axis shows the amount of BG spores in the reactor bottle at the start of each experiment, and the y-axis shows the percent of BG spores from the starting amount that were collected in the BioSampler. Circle graphical markers denote experiments in which no FFCM was added to the reactor bottle, triangle graphical markers denote experiments in which 0.42 cm diameter polystyrene spheres were added to the reactor bottle, square graphical markers denote experiments in which 1.91 cm diameter polystyrene spheres were added, and the diamond graphical marker denotes the experiment conducted with a tripled amount of BG spores in the reactor bottle. Blue, yellow, green, and red marker colors indicate experiments conducted with aeration rates of 0.50, 0.65, 0.85, and 1.00 L/min, respectively. At control conditions (no added FFCM), an average percent of BG spores captured was 8.753×10^{-3}% at an aeration rate of 0.50 L/min. At the same aeration rate and no FFCM added, the experiments with a tripled starting amount of BG spores in the reactor (blue diamond graphical marker) had an average percent of BG spores capture of 2.762×10^{-3}%. The values differ within an order of magnitude and represents a 68.45% decrease in values with the tripled amount of added BG spores. Overall, it is

not believed that variations within the starting amount of BG spores in the reactor bottle have much of an effect on the percent of BG spores captured.

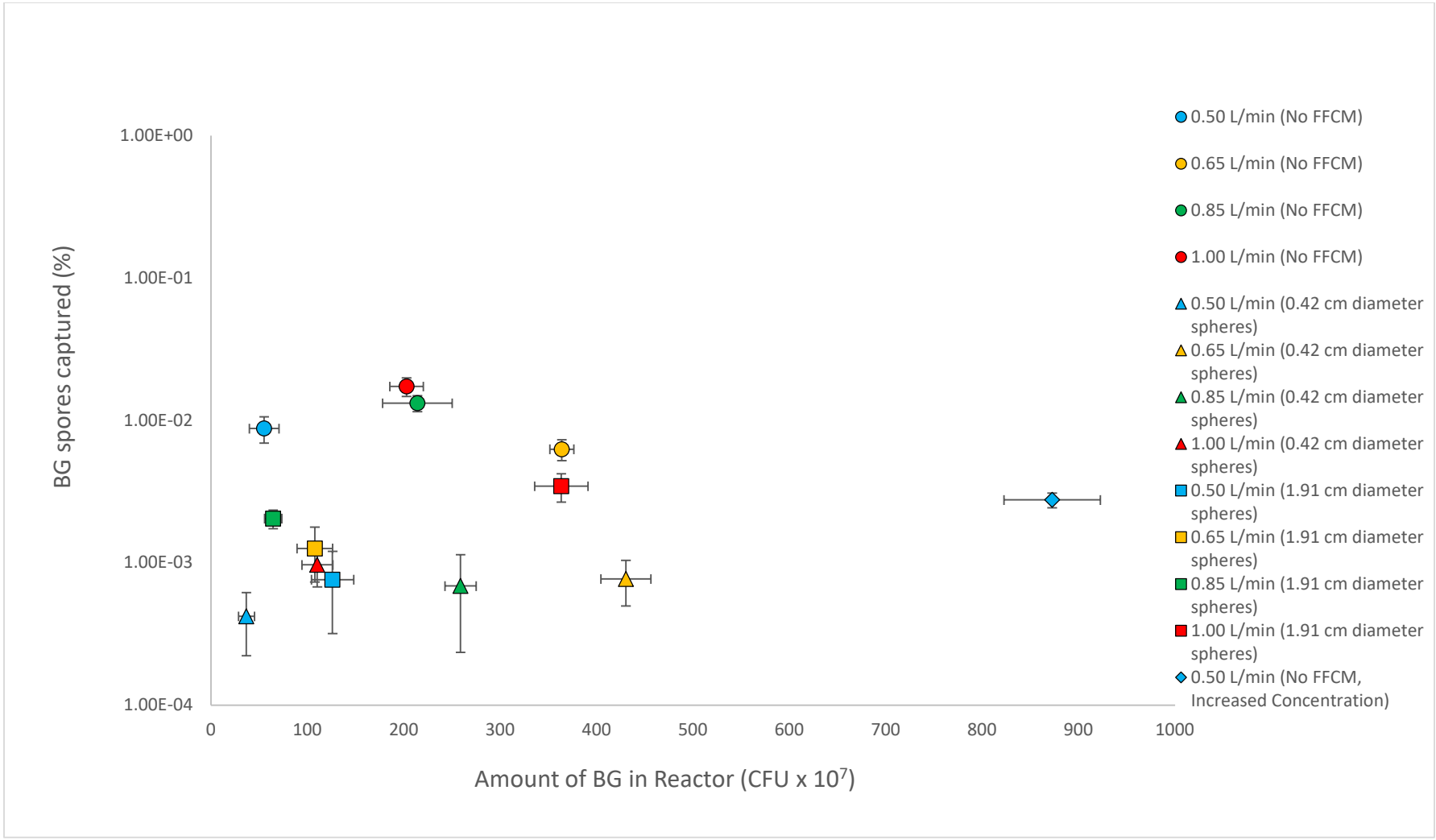

Figure 10. Averaged percent of BG spores captured in the BioSampler compared to the starting amount of BG in the reactor (in CFUs)

4.2.2 Statistical Analysis for the Effect of Aeration Rate on Percent Capture

Hypothesis testing through the use of a two-tailed, unpaired T-Test was utilized to compare the percentage of the BG in the reactor captured in the BioSampler at the four aeration rates. Hypotheses were made that stated that a difference in percent capture of BG in BioSampler would be different if the aeration rate within the reactor bottle was increased between the four rates measured during these experiments. Table 3 summarizes the hypothesis testing conditions and results.

Table 3. Statistical Analysis of Variation of Aeration Rate

Test Performed: Two-tailed, unpaired T-Test on the percent of BG from the reactor bottle captured in the BioSampler						
Surface Additive (diameter reported)	**Condition 1 (L/min)**	**Condition 2 (L/min)**	**Percent Increase (%)**	**p-value**	**Compared α-value**	**Statistically Significant Difference**
No FFCM	0.50	0.65	30.00	0.1345	0.05	No
0.42 cm spheres	0.50	0.65	30.00	0.2781	0.05	No
1.91 cm spheres	0.50	0.65	30.00	0.2769	0.05	No
No FFCM	0.65	0.85	30.77	0.0092	0.05	Yes
0.42 cm spheres	0.65	0.85	30.77	0.8041	0.05	No
1.91 cm spheres	0.65	0.85	30.77	0.1111	0.05	No
No FFCM	0.85	1.00	17.65	0.1036	0.05	No
0.42 cm spheres	0.85	1.00	17.65	0.4328	0.05	No
1.91 cm spheres	0.85	1.00	17.65	0.0619	0.05	No
No FFCM	0.50	0.85	70.00	0.0372	0.05	Yes
0.42 cm spheres	0.50	0.85	70.00	0.4866	0.05	No
1.91 cm spheres	0.50	0.85	70.00	0.0143	0.05	Yes
No FFCM	0.65	1.00	53.85	0.0061	0.05	Yes
0.42 cm spheres	0.65	1.00	53.85	0.4375	0.05	No
1.91 cm spheres	0.65	1.00	53.85	0.0157	0.05	Yes
No FFCM	0.50	1.00	100.00	0.0092	0.05	Yes
0.42 cm spheres	0.50	1.00	100.00	0.1265	0.05	No
1.91 cm spheres	0.50	1.00	100.00	0.0138	0.05	Yes

The T-Test calculations produced a P-value. The P-value was compared to the set α-value of 0.05, which acted as the threshold for statistical significance. Aeration rates were compared with all three variations on surface additives (no FFCM, small polystyrene spheres, and large polystyrene spheres). All combinations of increase in aeration rate were analyzed, a total of six comparisons, not only changes from one aeration rate to the next highest, and all differences were reported in Table 3 with the percent increase they represented. It was additionally hypothesized that larger percent increases in aeration rate would be more likely to cause a statistically significant difference in percent of BG captured in the BioSampler.

The lowest percent increase in aeration rate, 17.65%, occurred between the comparison of the 0.85 and 1.00 L/min aeration rates. No statistically significant difference was calculated under any of the surface additive configurations. The second lowest percent increase in aeration rate, 30.00%, occurred when the aeration rate was increased from 0.50 to 0.65 L/min, and no statistically significant difference was calculated under any of the surface additive configurations. When the aeration rate was increased from 0.65 to 0.85 L/min, a 30.77% increase, a statistically significant difference in percent of BG captured in the BioSampler was calculated when no FFCM was added. Comparisons when the small and large spheres were added resulted in no determined statistical significance.

The final three statistical comparisons were calculated for larger changes in aeration rate. At aeration rate percent increases of 53.85% (0.65 to 1.00 L/min), 70.00% (0.50 to 0.85 L/min), and 100.00% (0.50 to 1.00 L/min), statistically significant differences in the percent of BG captured in the BioSampler were determined when no FFCM was added and when the large polystyrene spheres were added to the reactor bottle. No statistically significant differences were calculated under any of the changes in aeration rate when the small polystyrene spheres were

present. These results reinforce the previous conclusions regarding the effect of aeration rate on the percent of BG captured in the BioSampler from the reactor bottle.

Overall, higher aeration rates resulted in higher percentages of BG captured. However, this was observed when higher differences in aeration rates were compared. When the percent increase in aeration rate was 30.77% or less, only 1 out of 9 comparisons resulted in a statistically significant increase in BG spore concentration collected in the BioSampler. Such percent increases in aeration rate occurred when comparing one interval to the next highest (0.50 to 0.65 L/min, 0.65 to 0.85 L/min, etc.). When the percent increase in aeration rate was 53.85% or greater, 6 out 9 comparisons resulted in a statistically significant increase in BG spore concentration collected in the BioSampler. These percent increases occurred when comparing larger gaps in intervals, for example 0.50 to 0.85 L/min. Correlation between increasing aeration rate and increasing BG spore concentrations collected in the BioSampler was most clearly observed at higher percentages of increase in aeration rate and particularly when no FFCM or the large spheres were present in the reactor bottle. The ability of the small spheres to best reduce the percentage of BG captured in the BioSampler likely contributed to the fact that statistically significant differences were not observed during any comparison with the small spheres present, regardless of how much of an increase in aeration rate occurred.

4.2.3 Analysis of Comparative Studies on the Effect of Aeration Rate on Percent Capture

Figure 11 compares trends observed when analyzing the effects of aeration rate on the amount of bioaerosol capture for this experimental data and data collected a study conducted by Wang et al., 2019. Across the x-axis are the three experimental conditions: the control group (no added FFCM to the reactor bottle), the data collected by Wang et al., 2019 for total airborne

bacteria, and the data collected in the same study by Wang et al., 2019 for intestinal bacteria specifically. The y-axis represents the percent increase in bioaerosol concentration. Wang et al., 2019 increased the aeration rate in their experiment utilizing actual wastewater from 0.3 to 1.2 m^3/hr. With comparative units, the aeration rate increase corresponding to the control groups from this study was significantly lower, from 0.03 to 0.06 m^3/hr. The percent increase in bioaerosol concentration was calculated in all three experimental conditions when the aeration rate was doubled. When considering all bacteria, the data from Wang et al., 2019, shows a 61.34% increase in bioaerosol concentration when the aeration rate is doubled, and a percent increase of 179.55% was observed when the aeration rate was doubled and intestinal bacteria was selected for and counted. In comparison to the data from the literature, the data from this study's control group experiments shows a 97.59% increase in bioaerosol concentration when the aeration rate is doubled.

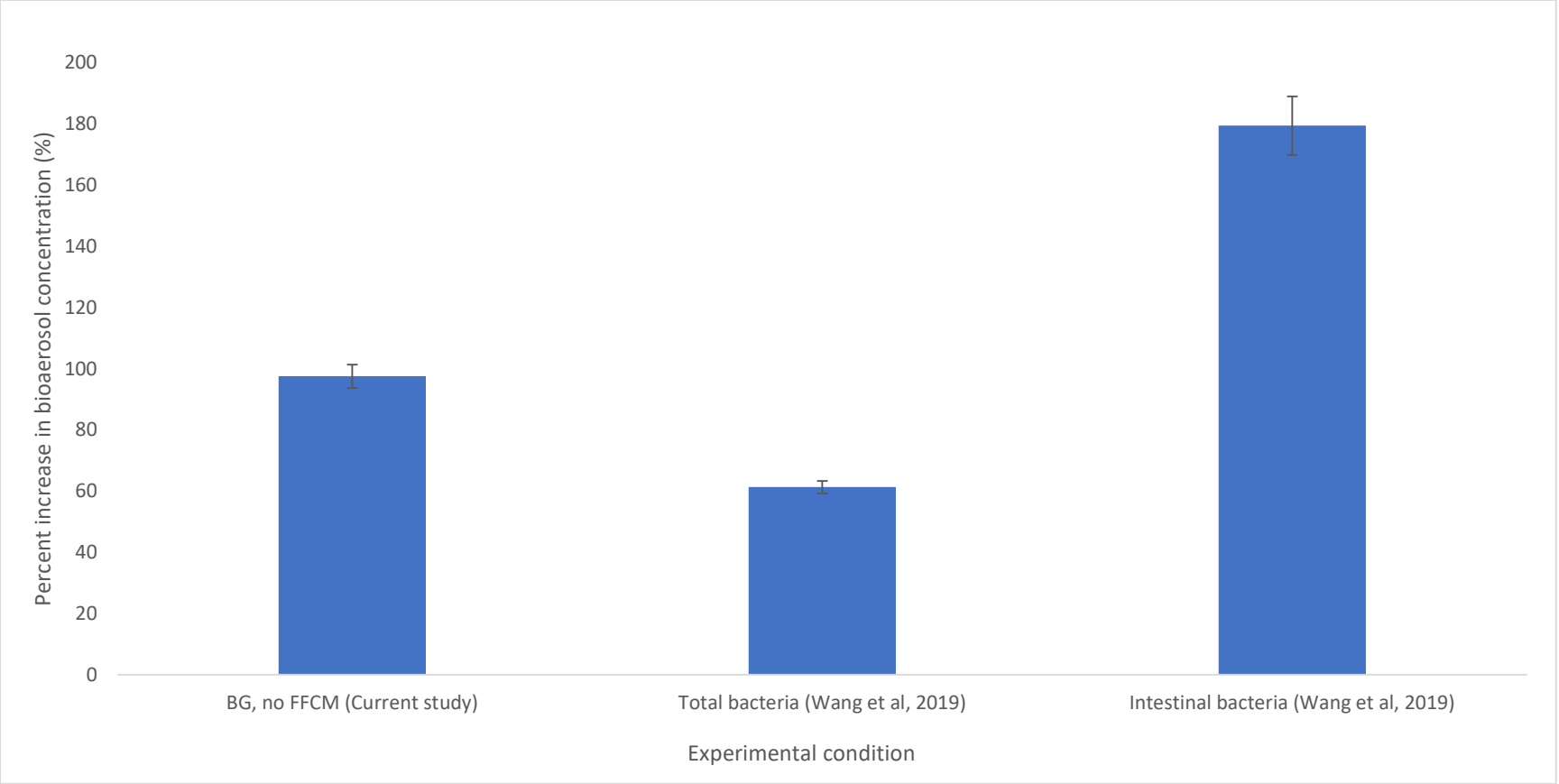

Figure 11. Percent increase in measured bioaerosol concentration when aeration rate in reactor vessel is doubled

Differences in the study exist. Wang et al., 2019 utilized actual wastewater with a reactor tank volume of $5x10^5$ mL, and qualitatively had low starting bacterial concentrations since the reactor tank was not intentionally inoculated with bacteria. This differs from the bioaerosol experiments conducted at AFIT since only BG spores were used in an intentional inoculation of water in the reactor bottle with a volume of 240 mL. Analyzing percent increase in bioaerosol concentration when experimental aeration rates were doubled allows for comparison. The control group data shows that increasing aeration rate did increase the collected bioaerosol concentration, matching the trend observed by Wang et al., 2019, as well as Hung et al., 2009. The value (97.59% increase) would fit in between the values (61.34% and 179.55%) calculated from the data by Wang. Collections were taken at two different heights by Wang et al., 2019: 0.1 m and 1.5 m above the water surface. When considering the larger scale of the $5x10^5$ mL reaction tank used by Wang compared to the 240 mL reactor bottle used in these experiments, the 1.5 m collection site in the Wang et al., 2019 investigation was more appropriately scaled to the collection height of approximately 15 cm in these experiments.

The range of aeration rates in the current research is postulated to be a factor causing a relatively weak relationship between increasing aeration rate and increased percent of bioaerosols captured to be observed. Wang et al. quadrupled the normalized aeration rate to surface area from 0.25 to 1.00 $cm^2\,(L/min)^{-1}$, while the current research doubled the normalized aeration rate from 71.42 to 142.84 $cm^2\,(L/min)^{-1}$. Lin et al., 2016, also observed a correlation between increased aeration rate and increased bacterial bioaerosol concentrations when increasing the normalized aeration rate in three intervals to a thirty-times increase, from 7.93 to 238.00 $cm^2\,(L/min)^{-1}$ (T. H. Lin et al., 2016). In the current research data, the percent of BG captured in the bioaerosol at a 1.00 L/min aeration rate was always larger than at 0.50 L/min.

Inconsistencies were observed at the 0.65 L/min aeration rate in the control experiments and at the 0.85 L/min aeration rate in the experiments with adding the 0.42 cm diameter FFCM, suggesting that the relatively small intervals of change in aeration rate did not provide enough distinction in the data. A larger range of aeration rate values, including a larger range between each interval, would have likely resulted in a stronger correlation between aeration rate and the percent of BG emitted in the collected bioaerosol.

4.3 Effect of Adding FFCM on Bioaerosol Capture

A second factor investigated in this research was the effect of adding FFCM to the surface of the BG solution in the reactor bottle. Figure 12 shows four groups along the x-axis, organized by increasing normalized aeration rate (in L/L/min). Each group shows the control condition (no added FFCM), and the effect on the percent of the reactor bottle captured in the BioSampler with the addition of the small or large polystyrene spheres. Similar trends were observed in all four groups with the varying aeration rates. In all four groups, the percent of the reactor bottle captured was highest when no FFCM was present (the control condition). In all four cases, the next highest value for percent of the reactor bottle captured, which was approximately an order of magnitude lower than the control conditions, occurred when large polystyrene spheres were added as FFCM. Lastly, in all four cases, the lowest value for percent of the reactor bottle capture occurred when the small polystyrene spheres were added as FFCM. While still approximately an order of magnitude lower than the values under the control conditions, the smaller radii polystyrene spheres performed the best at depressing values of emitted bioaerosols. Statistical analysis will be provided to better quantify the correlation between these two factors.

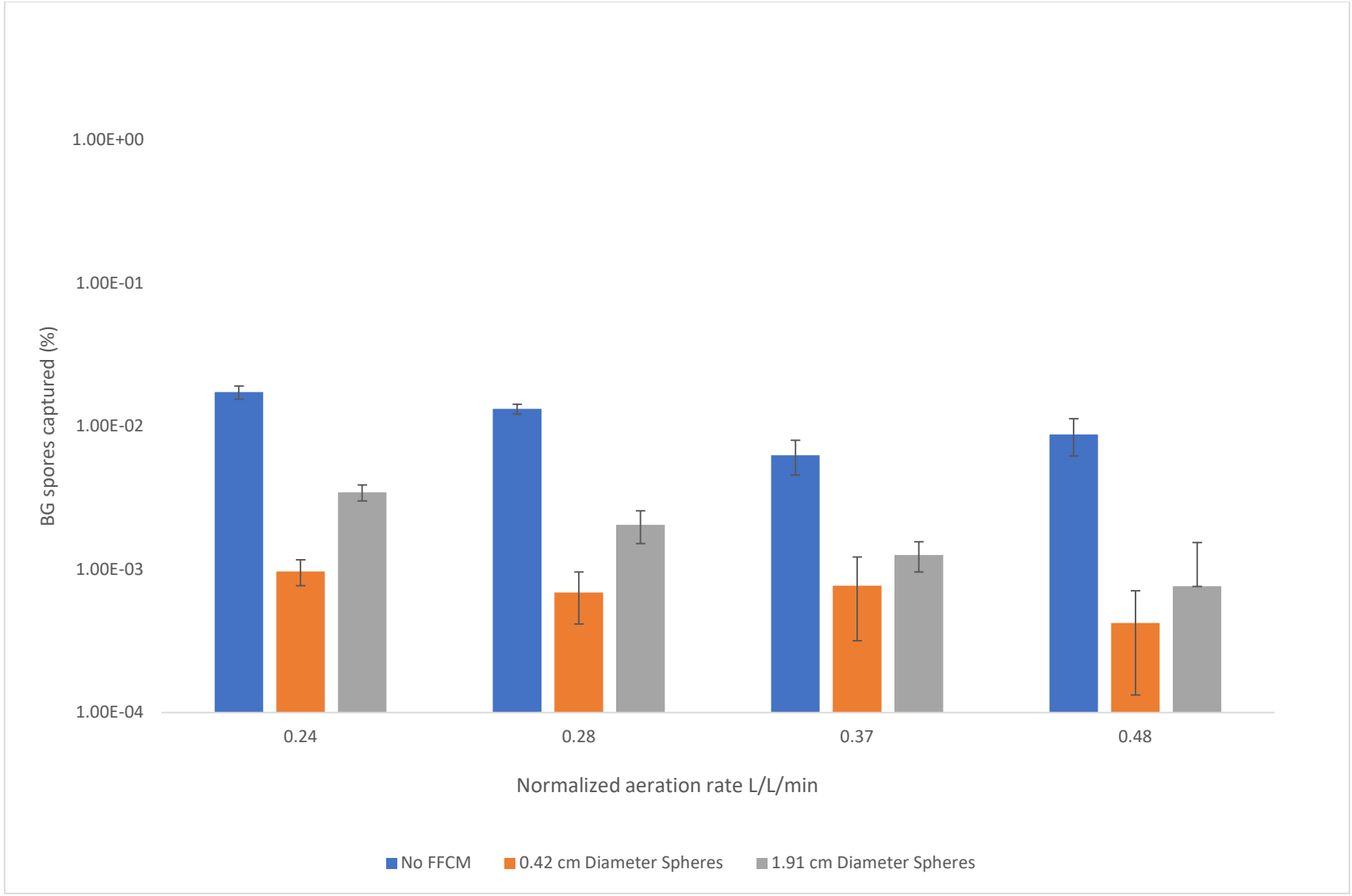

Figure 12. Average percent of BG from the reactor bottle captured in the BioSampler at varying normalized aeration rates L/L/min

In Figure 12, aeration rates were normalized to the volume of the reactor bottle. This allowed for comparisons to other sources of data in which different volumes of water were studied. The same pump and aeration stone would provide different aeration capabilities to 60 mL of water in a reactor bottle as compared to 240 mL of water in a reactor bottle (or any significant change in volume). The values ranged from 0.24 to 4.48 L/L/min. Wang et al. completed their study using normalized aeration rates ranging from 0.4 to 2.2 L/L/min (Wang et al., 2019). The observed overall increase in bioaerosol production with increasing aeration rate in these experiments support observations made by Wang et al. that increasing the number of bubbles generated (per unit time) results in increasing bioaerosol production.

Wastewater treatment plants maintain constant aeration rates at areas requiring bubble or mechanical aeration. Reference values for normalized aeration rates provided by Metcalf & Eddy Inc. included 20-30 L/L/min for a spiral roll designed coarse bubble diffuser configuration and 10-15 L/L/min for coarse or fine bubble aeration using a grid system (Metcalf & Eddy, 2013). It is noted that the experimental normalized aeration rates in this study and those utilized by Wang et al. were considerably lower than the normalized aeration rates offered as reference values. Matching the normalized aeration rates in the experiments to known reference values at WWTPs was not necessarily an initial requirement of this research, but it is an important consideration when proceeding forward with potential applications of this work to real-life treatment facilities.

4.3.1 Statistical Analysis for the Effect of Adding FFCM on Percent Capture

Hypothesis testing using a two-tailed, unpaired T-Test was utilized to compare the percentage of the BG in the reactor captured in the BioSampler with and without the addition of FFCM. Hypotheses were made that stated that a difference in percent capture of BG in the

BioSampler would be lower if FFCM was present versus when it was absent, and that a difference would be observable between the two different diameter sizes of the polystyrene spheres. Table 4 summarizes the hypothesis testing conditions and results, with the α-value again set to 0.05.

Table 4. Statistical Analysis of Addition of FFCM

Test Performed: Two-tailed, unpaired T-Test on the percent of BG from the reactor bottle captured in the BioSampler					
Aeration Rate (L/min)	**Condition 1 (diameter reported)**	**Condition 2 (diameter reported)**	**p-value**	**Compared α-value**	**Statistically Significant Difference**
0.50	No FFCM	0.42 cm spheres	0.0166	0.05	Yes
0.50	No FFCM	1.91 cm spheres	0.0182	0.05	Yes
0.50	0.42 cm spheres	1.91 cm spheres	0.3771	0.05	No
0.65	No FFCM	0.42 cm spheres	0.0126	0.05	Yes
0.65	No FFCM	1.91 cm spheres	0.0051	0.05	Yes
0.65	0.42 cm spheres	1.91 cm spheres	0.2463	0.05	No
0.85	No FFCM	0.42 cm spheres	0.0065	0.05	Yes
0.85	No FFCM	1.91 cm spheres	0.0079	0.05	Yes
0.85	0.42 cm spheres	1.91 cm spheres	0.0228	0.05	Yes
1.00	No FFCM	0.42 cm spheres	0.0081	0.05	Yes
1.00	No FFCM	1.91 cm spheres	0.0121	0.05	Yes
1.00	0.42 cm spheres	1.91 cm spheres	0.0140	0.05	Yes

For experiments utilizing all four aeration rates, the differences in percentage of BG captured in the BioSampler between experiments with no surface additives and experiments with FFCM were all determined to be statistically significant. This held true whether the FFCM was the small or large polystyrene spheres. The results of this hypothesis testing further indicated a relationship between the presence of FFCM and the reduction of BG from the reactor bottle captured in the BioSampler.

This statistical analysis was also utilized to compare the effects of the small polystyrene spheres to the large polystyrene spheres. The T-Test was used to determine if the percentages of

BG captured in the BioSampler were significantly different depending on the diameter of the FFCM. At an aeration rate of 0.50 L/min, the calculated P-value was 0.3771. This value was much larger than the α-value of 0.05, and therefore the difference was not considered to be statistically significant. At an aeration rate of 0.65 L/min, the calculated P-value was 0.2463. This value was much larger than the α-value of 0.05, and therefore the difference was not considered to be statistically significant.

However, at higher aeration rates, the differences were observed to be statistically significant. At an aeration rate of 0.85 L/min, the calculated P-value was 0.0228. This value was smaller than the α-value of 0.05, and therefore the difference was considered to be statistically significant. At the highest aeration rate of 1.00 L/min, the calculated P-value was 0.0140. This value was smaller than the α-value of 0.05, and therefore the difference was considered to be statistically significant. The calculated P-values decreased in all experiments where the aeration rate was increased. This suggested that the diameter size of the FFCM had an effect on the amount of BG collected in the BioSampler following aeration, a relationship more evident at the higher of the tested aeration rates.

4.3.2 Analysis of Comparative Studies on the Effect of Adding FFCM on Percent Capture

Figure 13 introduces the method of analyzing the effect of adding FFCM on the emission of bioaerosols from the aerated reactor bottle through the calculation of control efficiency, a method used by Hung et al., 2009. Control efficiency was calculated by dividing the difference between the airborne bacterial (*E. coli* in the case of Hung, BG endospores in these experiments) concentration without any added FFCM and that with added FFCM by the airborne bacterial concentration without any added FFCM. In Figure 13, the dependent variable is the control

efficiency, and groups along the x-axis were organized by aeration rate, including 0.50, 0.65, 0.85, and 1.00 L/min for these experiments and the significantly higher 60 L/min from Hung et al. Each aeration rate grouping contained bars corresponding to FFCM diameter size (small and large for the first four groups and four different FFCM sizes for the data from Hung et al.). Also included was unpublished data from Burdsall et al., 2020, which provided the small-scale data in this series of experiments. Burdsall et al. used the smallest diameter of FFCM (mean diameter of 0.22 cm). Since different reactor vessels were utilized in the three different groups of experiments, the data was normalized with regards to surface area (presented in units of cm^2 $(L/min)^{-1}$) to allow for accurate comparisons.

All of the groups in which FFCM diameter size was varied demonstrated the same trend that increasing FFCM diameter size is proportional to decreasing control efficiency. All of the experimental procedures arranged the FFCM into monolayers on top of the reactor vessel water surface. The large polystyrene spheres in this research had an average diameter of 1.91 ± 0.56 cm, nearly identical to the smallest polystyrene balls size used by Hung et al. reported at 1.9 cm. Even at significantly different normalized aeration rates, the control efficiencies were very similar, with the average control efficiency for the first four groups calculated at 83.95%, compared to 91.3% from Hung's data. The experiments from Burdsall et al. utilized one size of polystyrene spheres for FFCM (FFCM composed of other materials was not included for comparative purposes). The FFCM was also added based on mass (approximately 0.3 g of polystyrene spheres). This mass of polystyrene spheres formed a partially complete bilayer, with some patches along the surface having more or fewer spheres. However, the data is still presented as the FFCM had a very small diameter and the control efficiencies calculated at two different normalized aeration rates were both above 90% (92.58% at 32.76 cm^2 $(L/min)^{-1}$ and

92.74% at 62.50 cm^2 $(L/min)^{-1}$). The current study reported a range of control efficiencies between 87.73% and 95.19%, with normalized aeration rates ranging between 71.42 and 142.84 cm^2 $(L/min)^{-1}$. Regardless of which study the data was from, experiments using FFCM with a diameter of 0.42 cm or less all had a control efficiency of 87.73% or higher. When the FFCM diameter was 1.91 cm or less, all of the experiments had a control efficiency calculated at 79.9% or higher. The addition of FFCM proved effective at attenuating BG bioaerosol release at a wide range of normalized aeration rates and experimental scale.

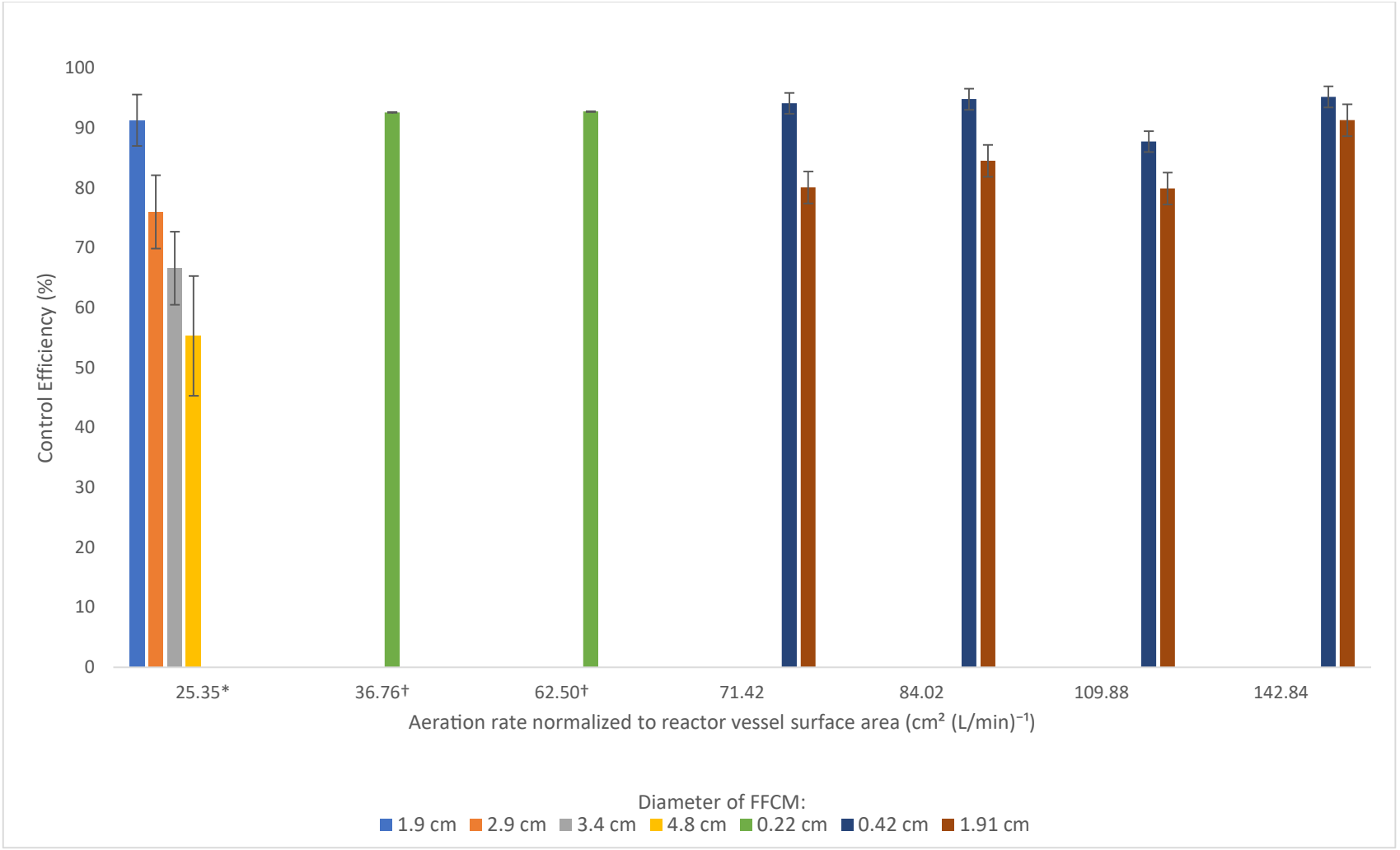

Figure 13. Control Efficiency (%) of added FFCM with varying diameters at investigated normalized aeration rates (*Data from Hung et al. (2010), †Data from Burdsall et al. (2020))

In an effort to explain why smaller diameter FFCMs result in higher control efficiencies, the arrangement of the additives was examined. Polystyrene spheres were added so that a monolayer was formed on the surface of the BG and water solution inside the reactor bottle. The definition of a monolayer, as used in this experiment, was that every added polystyrene sphere was in contact with the surface of the water. The spheres were completely free-floating and could be moved once the bubble aeration began. In the investigation by Hung et al., 2009, the added balls were threaded together to form net-like arrays that prevented movement of the balls during the aeration process. Images of the monolayers formed inside the reactor bottle of the small and large diameter polystyrene spheres can be seen in Figure 14.

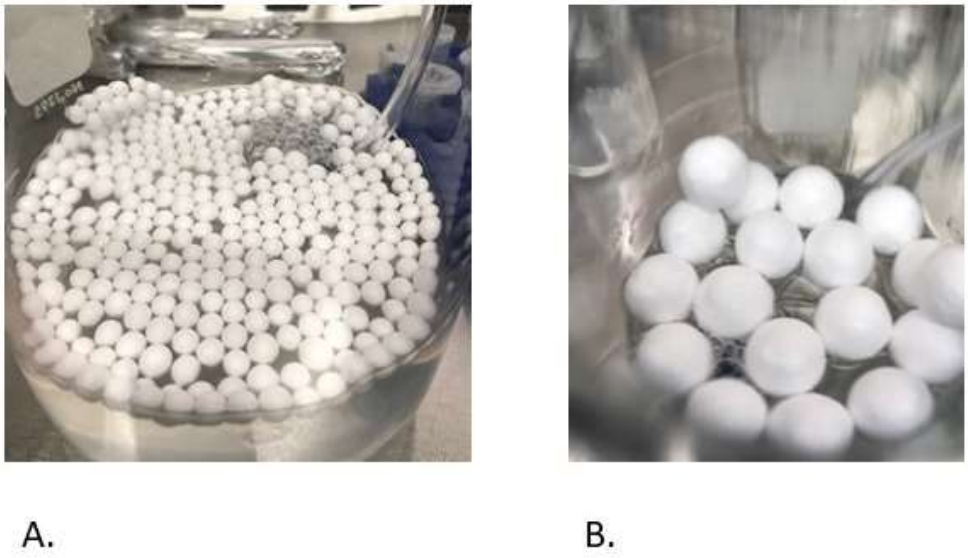

A. B.

Figure 14. Photographs of reactor bottle surface layers with FFCM added (a. Monolayer of 0.42 cm diameter expanded polystyrene spheres from experiment BGA34A, b. Monolayer of 1.91 cm diameter expanded polystyrene spheres from experiment BGA37A)

Percent coverage calculations were performed to compare the two different additives. The surface area of the water's surface within the reactor bottle was 71.42 cm^2. A monolayer of the small polystyrene spheres required 321 spheres (0.42 cm in diameter) would sum to a total area of 45.05 cm^2, observed in Figure 14A. Dividing this value by the total surface area of the water

surface and multiplying by 100 provides the percent coverage of the small spheres, calculated to be 63.08%. The same procedure was used to calculate percent coverage provided by the large spheres (1.91 cm in diameter), observed in Figure 14B. The total area of the large spheres was 51.42 cm^2, and the percent coverage of the large spheres was calculated to be 71.99%. Fewer larger gaps exist in the spaces between the floating large spheres, whereas more, smaller gaps exist in the spaces in between the floating small spheres.

4.4 Effect of Experimental Scale to Bioaerosol Capture

These experiments represented the medium-scale investigation into bioaerosol emissions, completed using 240 mL of BG and DI water solution in the reactor bottle. The small-scale experiments were completed in the same biosafety cabinet at AFIT by Dr. Adam Burdsall, and some of his unpublished data is included in this report for comparative purposes and for trend analysis. The large-scale experiments are, at the time of this writing, scheduled to be completed by the EPA at their pilot-scale facility in Cincinnati, Ohio. Observing trends between the small and medium-scale experiments can lead to better predictions being made about the large-scale experiments, as well as better hypotheses formed about applications at actual WWTPs. Figure 15 graphically depicts the average percent of BG captured in the BioSampler from the reactor bottle for the small-scale and medium-scale experiments. Four different experimental parameters were the same between the two different experimental scale sizes and were therefore the selected parameters for comparison. In Figure 15, the circle data markers indicate medium-scale experiments, and the square data markers indicate the small-scale experiments, with different colors indicating different experimental parameters. In general, the values for percent of BG captured in the BioSampler were similar when small and medium-scale results were compared for each of the four experimental parameters. The highest percent values in both scale sizes

occurred when the aeration rate was at the highest compared value (0.85 L/min) and no FFCM was added to the reactor bottle. The lowest percent values in both scale sizes occurred when the aeration rate was at the lowest compared value (0.50 L/min) and FFCM was added to the reactor bottle. Figure 15 represents an overall view of the trends associated with experimental scale. Statistical analysis will be provided in a subsequent section to better quantify the correlation between small and medium experimental scale.

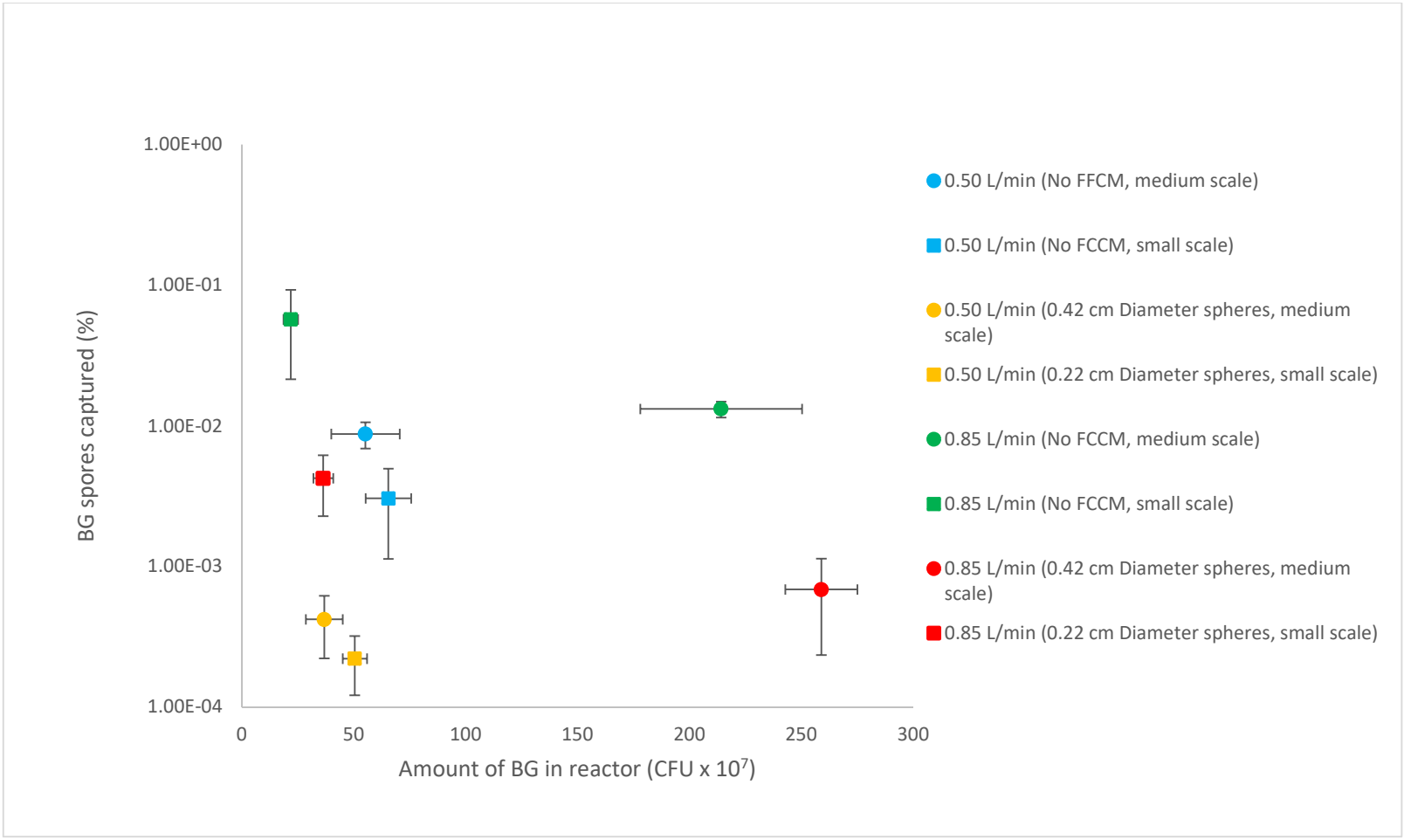

Figure 15. Scale-up comparison of average percent of BG captured in the BioSampler for experiments at comparable aeration rates and reactor bottle surface additives

It was hypothesized that similar values for the percent of the reactor bottle captured in the BioSampler would be observed between small and medium-scale experiments. Figure 16 graphically shows the percent of the BG in the reactor captured in the BioSampler as a function of small or medium experimental scale. The x-axis is divided into four groups of two bars each, with each group representing one of the four experimental parameters that were common to both the small and medium-scale experiments. In each group, one bar shows the percent of BG in the reactor captured in the BioSampler for the small-scale experiments at those parameters, and the adjacent bar shows the percent value for the medium-scale experiment conducted under the same parameters. At an aeration rate of 0.50 L/min and with no FFCM added, the small-experiments had an average percent capture of 0.0030%, and the medium-scale experiments had an average percent capture of 0.0088%, a 193.33% increase from small to medium-scale. When the flow rate was increased to 0.85 L/min and no FFCM was present, the small-scale experiments average a higher percent capture value of 0.057%, compared to the medium-scale experiments with an average percent capture value of 0.013%, a decrease of 77.19% from small to medium-scale. A similar pattern is observed when FFCM is added. At the 0.50 L/min aeration rate, the small-scale experiments averaged a percent capture of 0.00022%, while the medium-scale experiments saw an increased average percent capture value of 0.00042%, a 90.91% increase from small to medium-scale. When the aeration rate was increased to 0.85 L/min and FFCM was added, the small-scale value was the larger average percent capture value at 0.0042%, and the medium-scale value was 0.00069%, a decrease of 83.57% from small-scale to medium-scale.

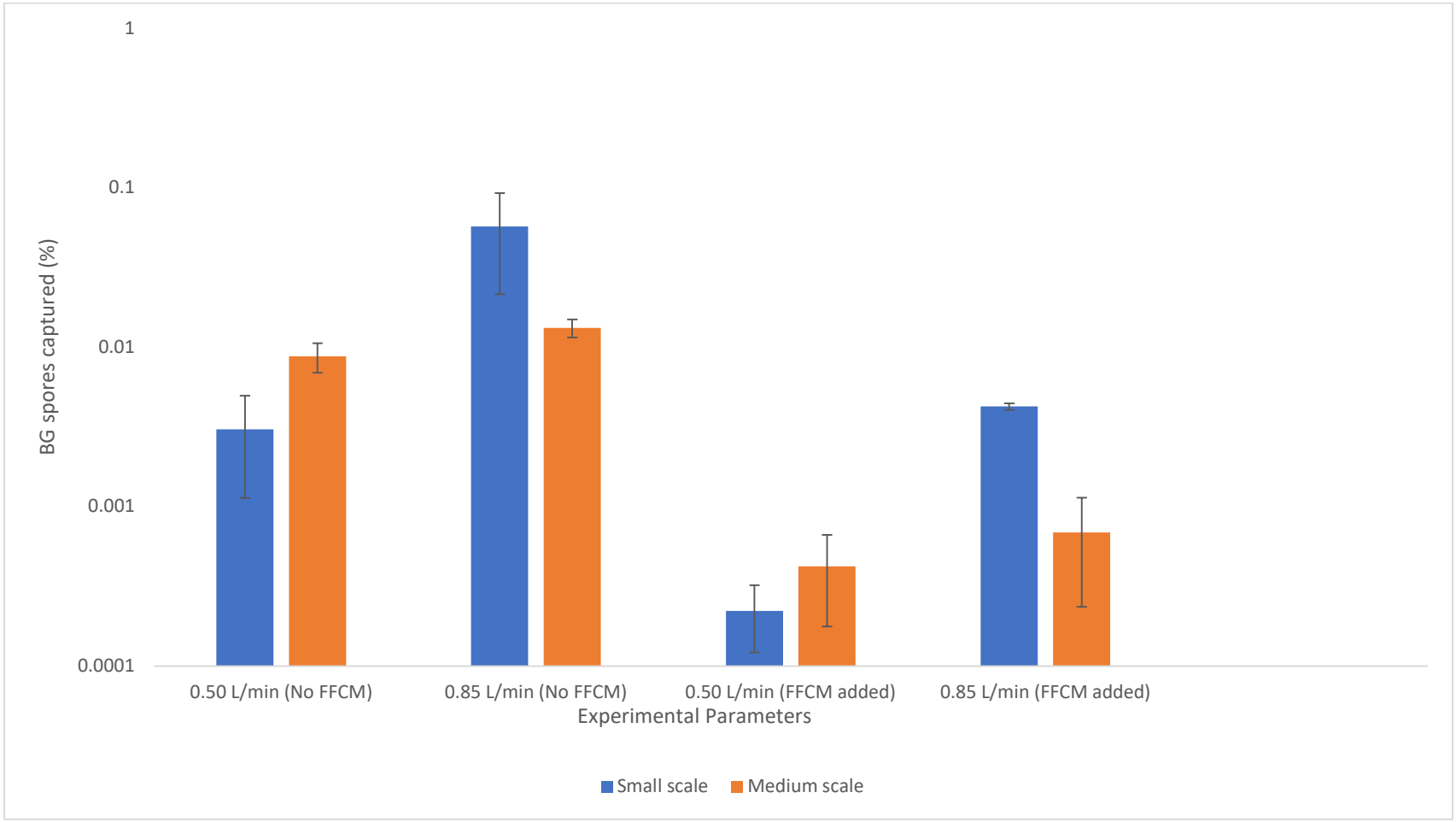

Figure 16. Percent of reactor captured in the BioSampler as a function of experimental scale (at four different experimental parameters) (small scale data provided by Burdsall et al.)

It is observed that scale does have an effect on the percent capture from the reactor bottle when analyzing aeration rate. If percent increase is calculated comparing each scale as aeration rate is increased from 0.50 to 0.85 L/min, it is observed that the small-scale increases more drastically than the medium-scale. With no FFCM added, the small-scale experiments see a percent increase of 1800.00% as the aeration rate increases, while the medium-scale experiments see a percent increase of only 47.73%. Similarly, when FFCM is added to the reactor bottle, the small-scale experiments experienced a percent increase of 1809.99% (nearly identical to the percent increase with no FFCM included), while the medium-scale experiments experienced a percent increase of 64.29%. Further analysis into the effect of experimental scale on the percent of BG spores captured in produced bioaerosols will be possible when more large-scale experiments are completed. Ultimately, trends observed in the study of the effect of experimental scale could be utilized in the development of a computational model to better predict bioaerosol emissions.

4.4.1 Statistical Analysis for the Effect of Experimental Scale on Percent Capture

Hypothesis testing using a two-tailed, unpaired T-Test was utilized to compare the percentage of the BG in the reactor captured in the BioSampler with differing the scale of the experiments. Hypotheses were made that stated that no statistically significant differences in percent capture of BG in BioSampler would be observed with a change from small-scale to medium-scale experiments. Table 5 summarizes the hypothesis testing conditions and results, with the α-value again nominally set to 0.05.

Table 5. Statistical Analysis of Experimental Scale

Test Performed: Two-tailed, unpaired T-Test on the percent of BG from the reactor bottle captured in the BioSampler

Aeration Rate (L/min)	Surface Additive (diameter reported)	Medium Scale FFCM Diameter (cm)	Small Scale FFCM Diameter (cm)	p-value	Compared α-value	Statistically Significant Difference
0.50	No FFCM	NA	NA	0.0180	0.05	Yes
0.50	polystyrene spheres	0.42	0.22	0.4813	0.05	No
0.85	No FFCM	NA	NA	0.0465	0.05	Yes
0.85	polystyrene spheres	0.42	0.22	0.0010	0.05	Yes

Four experimental conditions were common to the small-scale experiments conducted at AFIT by Dr. Adam Burdsall and the medium-scale experiments. When results of small and medium-scale experiments with an aeration rate of 0.85 L/min (regardless of whether FFCM was added or not) were compared, the results for percent capture in the BioSampler were calculated to be statistically different. At an aeration rate of 0.50 L/min and when no FFCM was added to the reactor bottles, the results for percent capture in the BioSampler were again calculated to be statistically different when the two scales were compared. However, at an aeration rate of 0.50 L/min and with FFCM present in the reactor, no statistically significant difference in percent capture in the BioSampler values was calculated. These results indicate that experimental scale has an effect on the percent of BG captured in the BioSampler following bubble aeration in the reactor bottle. This trend was observed when no FFCM was added to the reactor bottle. At the lowest aeration rate, 0.50 L/min, it was calculated that experimental scale may not significantly affect the percent capture when FFCM was added, but the statistical difference was once again calculated to exist when the aeration rate was increased to 0.85 L/min (a 70.00% increase) with the same FFCM added. It is also predicted that larger scale experiments (at a pilot plant or an actual WWTP) would utilize aeration rates greater than 0.50 L/min, although it would be necessary to normalize the value with respect to the volume of water being aerated. With these

facts, it would be hypothesized that experimental scale would affect the percent of BG captured in the BioSampler for large-scale experiments.

It is predicted that similar trends would be observed in the large-scale experiments: a significant reduction in bioaerosol capture is expected when FFCM is added to the reactor vessel, and a small percent increase in bioaerosol capture would be expected when increasing the aeration rate of the large-scale experiments by the same 70% factor (0.500 to 0.85 L/min in the small and medium-scale experiments).

4.4.2 Initial Results from Large-Scale Experiment at Pilot WWTP

An initial experiment was conducted using the EPA's pilot-scale activated sludge treatment system at their T&E Facility at the NHSRC. Differences in experimental design, particularly the use of synthetic wastewater in the aeration basin, precludes a direct comparison with the small and medium-scale experiments using DI water in the reactor bottles. While also including an aspect of realism with the use of the synthetic wastewater, the initial experiment itself provided unpublished data (courtesy of Dr. Adam Burdsall) that was compiled into Figure 17. In this plot, the y-axis value is the percent of BG spores from the aeration basin compartment captured in the BioSampler. Along the x-axis are bars for each of the six independent compartments in the aeration basin (A through F), organized into one of three groupings corresponding to experimental run-time (1, 7, and 24 hours). Many of the error bars, based on standard deviation of three plates per compartment per collection time, are too small to distinguish. Clearly all six bars are not present for all three time groups, indicating that all three plates from that compartment exhibited no growth of BG colonies.

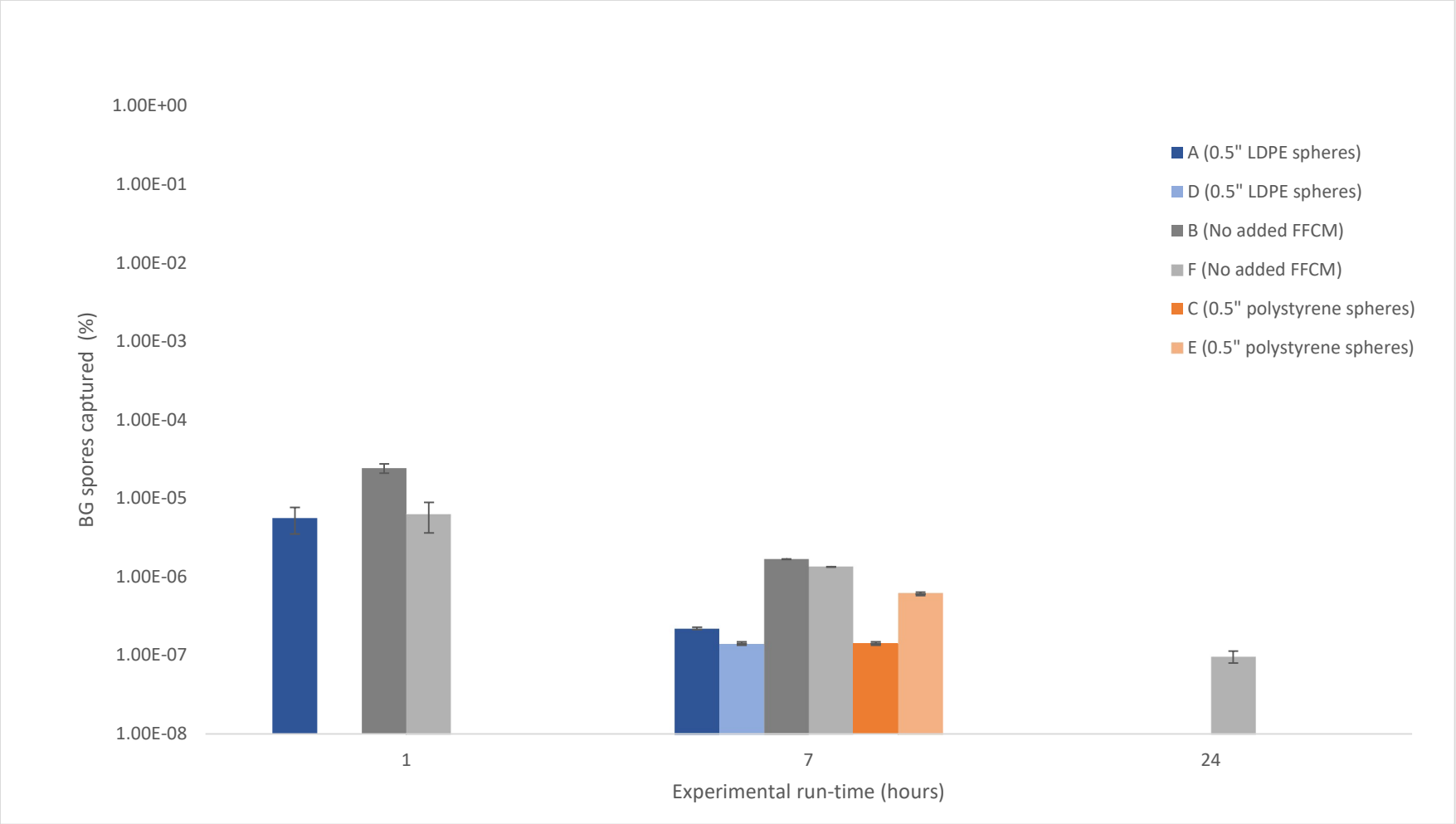

Figure 17. Initial large-scale experimental comparison of the percent of BG from the aeration basin captured in the Biosamplers at 1, 7, and 24 hours of run-time

Instances of zero growth on plates make it difficult to observe trends within the data, and this was due to the fact that the concentration of BG was being pumped into the experimental setup gradually, so that lower concentrations of BG were observed at 1 hour and 24 hours. The highest BG concentration (of the three groups) of $1.48x10^5$ CFU/mL occurred at 7 hours of run-time, and growth was observed on plates from all six compartments. Despite having the second highest average BG concentration of $1.02x10^5$ CFU/mL, the 24-hour collection time data saw the overall lowest growth of BG, and the most plates without a single colony. The compartments had a much lower mean BG concentration of $4.62x10^3$ CFU/mL after one hour of experimental run-time. Furthermore, all plates had eight or fewer CFUs, a fact that could weaken statistically based findings. It should also be reiterated that the experiment used synthetic wastewater in the aeration chambers, the presence of which has an unknown interaction with BG spores at this time.

Examining purely the data at the 7-hour run-time, Compartments B and F (the control groups with no FFCM added) had the highest percent of BG spores captured ($1.69x10^{-6}$% for Compartment B and $1.35x10^{-6}$% for Compartment F). The percent of BG spores captured decreased by 88.09% (a value also represented by the term "control efficiency") when the LDPE spheres were added to Compartments A and D and compared to the controls. Similarly, the percent of BG spores captured decreased by 75.30% when the polystyrene spheres were added to Compartments C and E and compared to the controls. These values were similar to the decreases observed in the medium-scale experiments when the 0.42 cm diameter spheres were added (average of 93.03% decrease in BG spores captured) and when the 1.91 cm diameter spheres were added (average of 83.95% decrease in BG spores captured). The range of values of percent of BG spores captured in this initial large-scale experiment were around two orders of magnitude

smaller than the range of values reported in the medium-scale experiments. As acknowledged, several differences exist between this experiment and the small and medium-scale experiments conducted in the laboratory setting. More data will eventually become available as more large-scale experiments are conducted. Still, the data from this initial experiment provides another set of results indicating a relationship between decreasing bioaerosol emissions in the form of BG spores when FFCM is added to the surface of an aerated volume of water.

4.6 Decreasing Concentration (Loss) of BG Spores Throughout an Experiment

Experiments were completed in triplicate with the same parameters of aeration rate and FFCM added (controls had no FFCM added). The concept of "loss" referred to the overall decreasing concentration of BG spores in the reactor bottle from the first experiment to the third experiment completed on the same day under the same parameters. BG spores were captured in the BioSampler following each thirty-minute bubble aeration iteration, and no new amount of BG spores was introduced to the reactor prior to the start of the second or third experiment. The water and BG spore solution in the reactor bottle was swirled every time before starting the collection in the BioSampler. Figure 18 graphically represents the concept of loss, with experiment number along the x-axis referring to whether the experiment was the first, second, or third in the triplicate for the given experimental parameters. The y-axis values represent the percent of the starting BG spore concentration within the reactor bottle, with that value equal to 100% for every first experiment of each experimental parameter investigated.

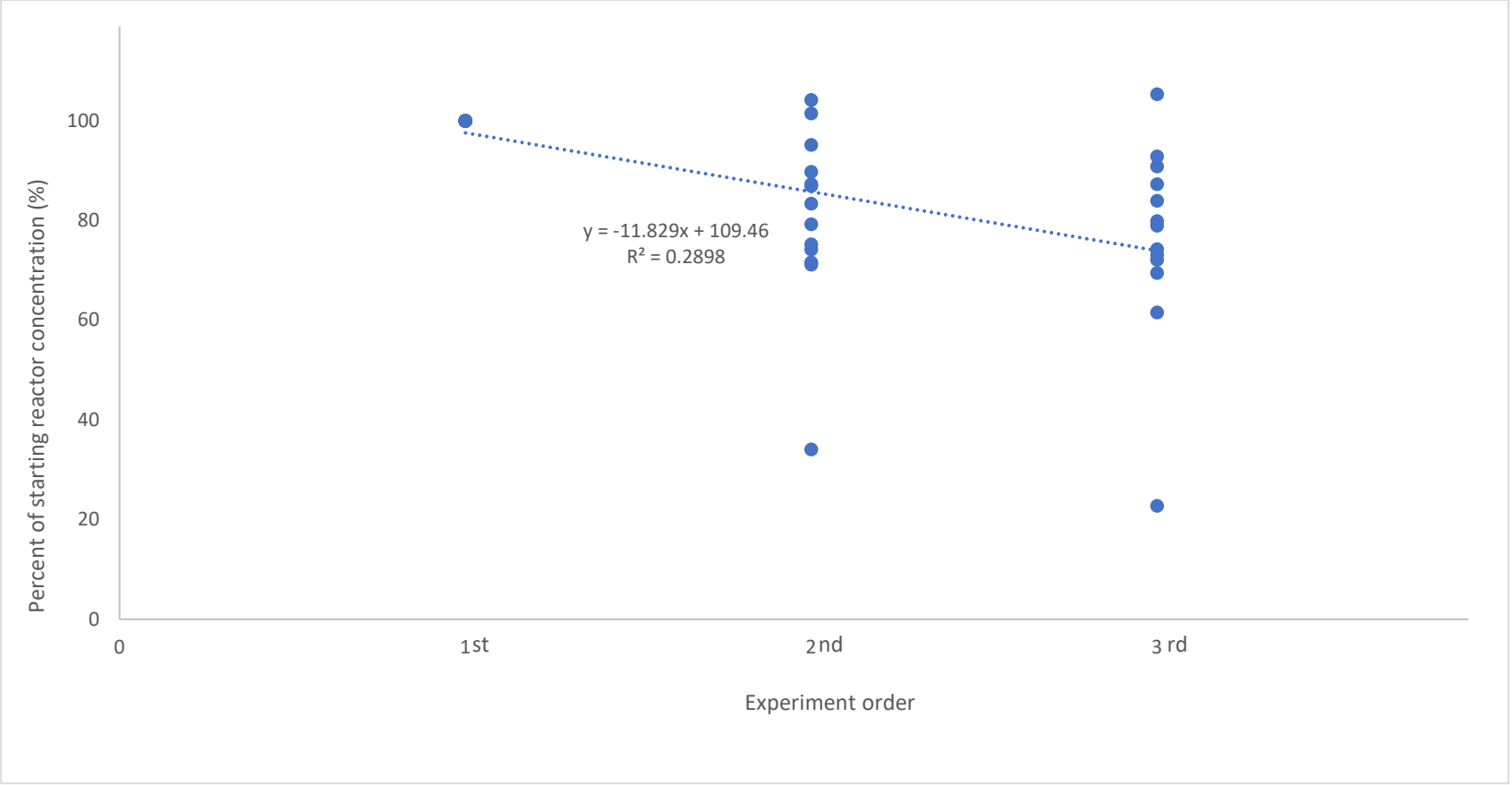

Figure 18. Overall loss in reactor vessel BG spore population during triplicate iterations of each experiment

The R^2 value of the calculated regression line suggests a correlation (although relatively weak) between experiment number and decreasing concentration of BG spores within the reactor bottle. The term "loss" refers to BG spores that are no longer found within the concentration of the reactor bottle but also not accounted for in the collection of BG spores within the BioSampler. Agar plates placed face up near the interfaces of tubing and the plastic fitting and BioSampler nozzle during the thirty-minute aeration period suggest that "loss" did not occur in the closed system as no BG colonies were observed after twenty-four hours of incubation. It is hypothesized that BG spores from the reactor that were not accounted for with the concentration of the BioSampler were transported and deposited on an interior surface of the apparatus. These surfaces would include the side walls of the reactor bottle, the underside of the plastic cap of the reactor bottle, inside the silicone tubing, and inside the inlet nozzle of the BioSampler. The attachment of the silicone tubing from the reactor bottle to the BioSampler directly had not been reported in previous research literature. While the length of tubing was kept to a minimum length, it is postulated that the slight bend in the tubing would result in additional spore deposition on the inside wall of the tubing as the aerosolized spores were drawn into the BioSampler. The experimental design and length of the tubing connecting the reactor bottle and the Inlet Nozzle of the BioSampler were kept consistent throughout all experiments, thereby maintaining comparability amongst experiments.

Figure 19 breaks down the data for "loss" based on the experimental parameter of aeration rate. The x-axis represents whether the experiment was the first, second, or third in the triplicate for the given experimental parameters. The y-axis values represent the percent of the starting BG spore concentration within the reactor bottle, with that value equal to 100% for every

first experiment of each experimental parameter investigated. The four different colors represent which of the four aeration rates (0.50, 0.65, 0.85, and 1.00 L/min) the experiment investigated.

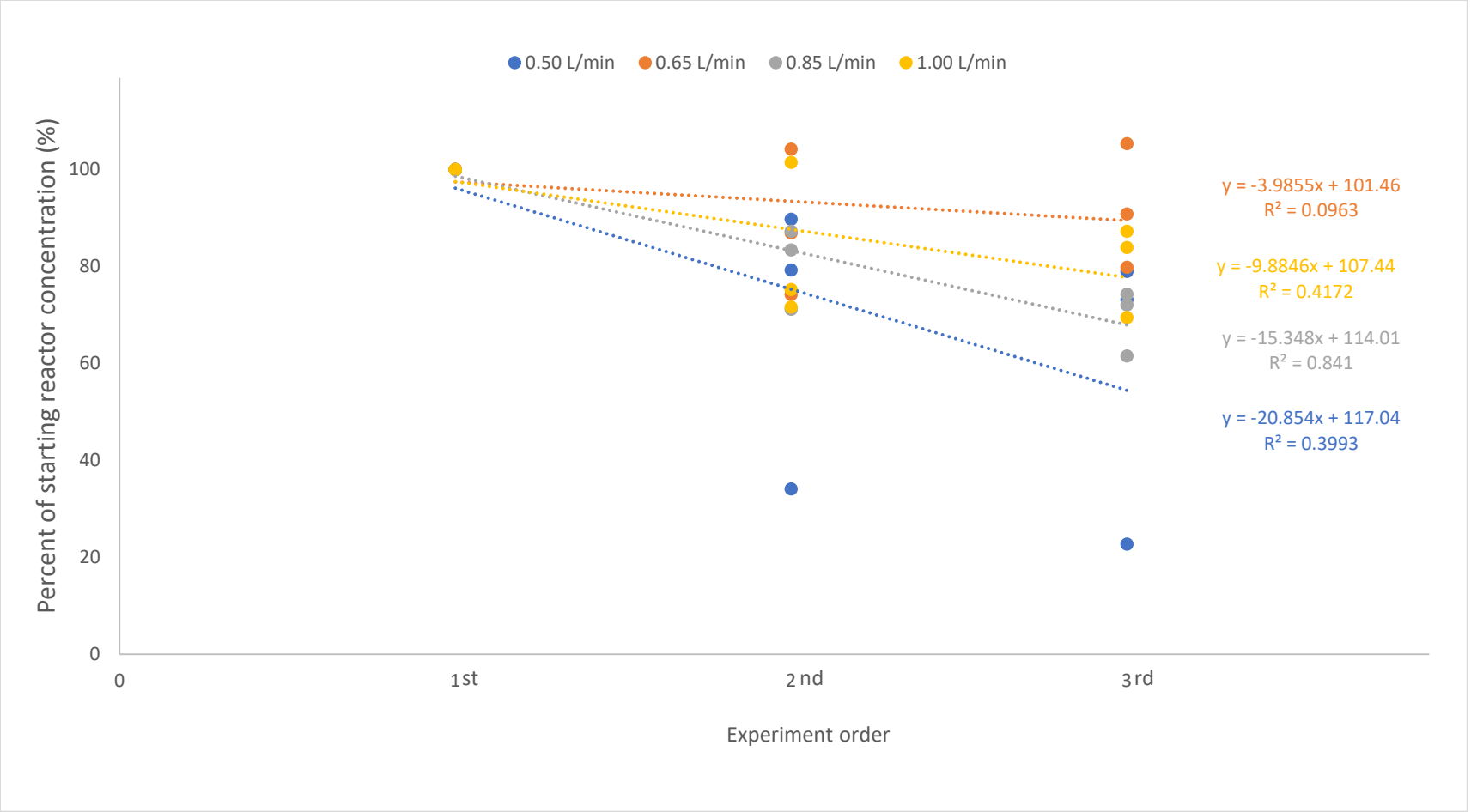

Figure 19. Overall loss in the reactor vessel BG spore population during experiments with varying the aeration rate (L/min)

The R^2 values of the associated regression line for each aeration rate range between 0.0963 and 0.8410, with all indicating some level of correlation to decreasing BG spore concentration inside the reactor bottle with each progressive experiment. A conclusion regarding the effect of aeration rate on the amount of loss of BG spores from the starting concentration could not necessarily be determined.

Figure 20 breaks down the data for "loss" based on the experimental parameter of FFCM added. The x-axis represents whether the experiment was the first, second, or third in the triplicate for the given experimental parameters. The y-axis values represent the percent of the starting BG spore concentration within the reactor bottle. That value is 100% for every first experiment of each experimental parameter investigated. The three different colors represent which of the three surface additive conditions (no FFCM added, small polystyrene spheres added, or large polystyrene spheres added) was investigated.

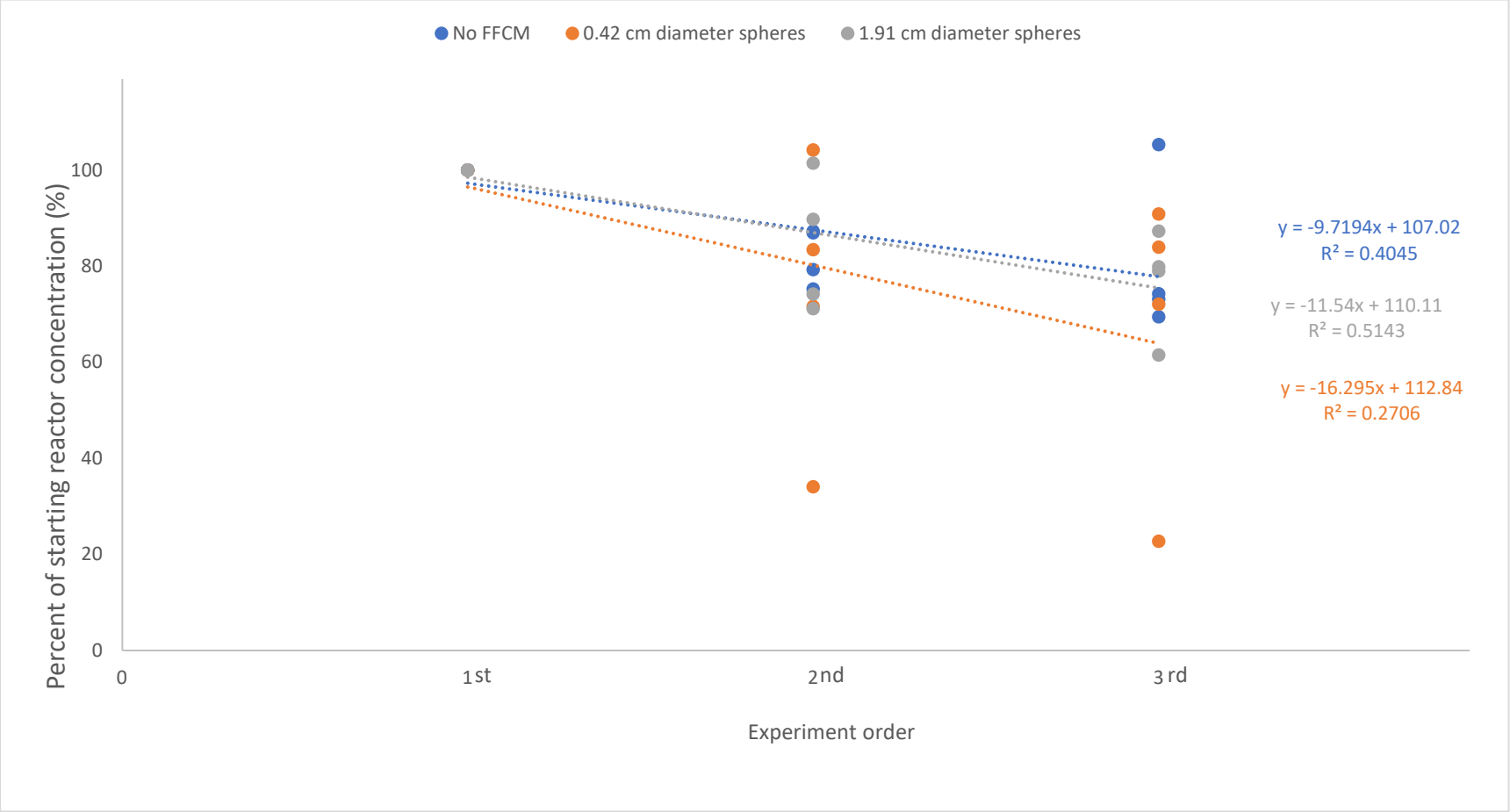

Figure 20. Overall loss in the reactor vessel BG spore population during experiments with different surface additives

The R^2 values of the associated regression line for each surface additive condition range between 0.2706 and 0.5143, with all indicating some level of correlation to decreasing BG spore concentration inside the reactor bottle with each progressive experiment. The slope of the regression line is represented in units of percent of the starting reactor concentration per triplicate experiment number (%/experiment). The slopes of the regression lines were nearly identical for the loss observed in experiments when no FFCM was added and for the loss observed in experiments when the large spheres were added (-9.7194 and -11.54 %/experiment respectively). The slope was significantly more negative, -16.295 %/experiment, in experiments when small spheres were added. However, previous data showed that the small spheres were more effective at attenuating the aerosolization of BG spores. A conclusion regarding the effect of adding FFCM to the surface of the reactor bottle water on the amount of loss of BG spores from the starting concentration could not necessarily be determined.

4.7 AFM

Understanding the physical properties of BG spore surfaces can lead to a better understanding of interactions involving BA spores. The intent of utilizing AFM in these experiments was to detect whether there are structural alterations or damage to exterior BG spore layers caused by aerosolization. BG spores from these experiments were qualitatively examined under light microscopy and the AFM. Length and width measurements were made on the AFM images of one hundred different spores (n=100), as depicted in Figure 21. Variability for all measurements are indicated by the respective standard deviation.

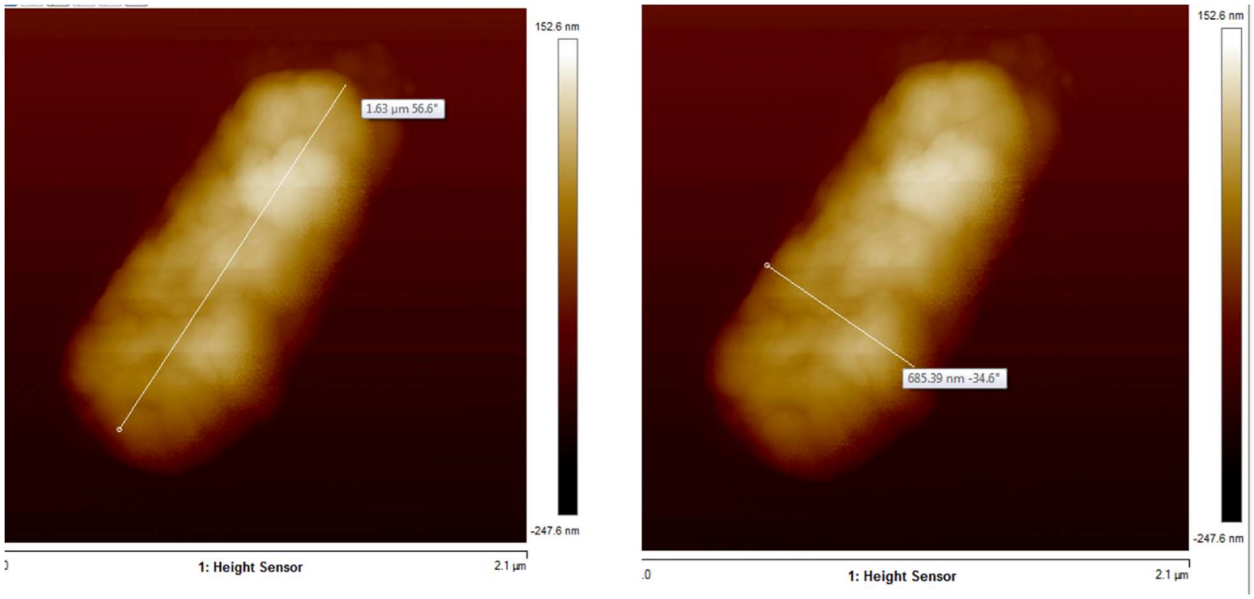

Figure 21. AFM Measurement of Spore Dimensions (n = 100 BG spores)

The aspect ratio was taken as the ratio between the major axis (length) and minor axis (width). The average BG spore length determined using the AFM was 1.396 ± 0.171 µm. The average spore width was 0.692 ± 0.090 µm, and the average aspect ratio for the ellipsoid-shaped spore was 2.044 ± 0.330 µm. These measurements were consistent with measurements taken via light microscopy at 100x magnification of a population of fifty spores (n=50). The average BG spore length determine through the use of the light microscope was 1.350 ± 0.177 µm. The average spore width was 0.793 ± 0.110 µm, and the average aspect ratio for the spores was 1.736 ± 0.376 µm. Carrera et al. described aspect ratios of 1.00 to 1.30 as near spherical, 1.31 to 1.50 as moderately elongated ellipsoids, 1.51 to 2.00 as pronouncedly elongated ellipsoids, and above 2.00 as extremely elongated ellipsoids (Carrera et al., 2007).

The above values, obtained through atomic force microscopy and light microscopy, were comparable with values obtained by Carrera et al. and within the value of the standard deviations. Carrera et al. reported a mean length value for *B. atrophaeus* spores of 1.22 ± 0.12

μm, mean width value of 0.65 ± 0.05 μm, and aspect ratio of 1.85 ± 0.19 μm using images obtained with a tunneling electron microscope (TEM) (Carrera et al., 2007). The variation provided for Carrera's measurements were all from the respective standard deviation. Plomp et al., 2005, reported mean lengths of 1.79 ± 0.19 μm and mean widths of 0.626 ± 0.027 μm for *B. atrophaeus* spores imaged with AFM. Spore measurements from all three imaging techniques (light microscopy, AFM, and TEM) were all comparable and within the tolerance of the calculated standard deviations.

BG spores examined with the AFM were observed to have pronounced ridges running along the major axis (length) of the individual spore. These same structures have been observed in previous investigations imaging *Bacillus* species spores with AFM (Ghosh et al., 2008; A. G. Li et al., 2016; Plomp et al., 2005b; Sahin et al., 2012; Xing, Li, Felker, & Burggraf, 2014; Zolock et al., 2006). Figure 22 shows an AFM image of BG spores from the stock solution (BGA3), with the aforementioned ridges observable.

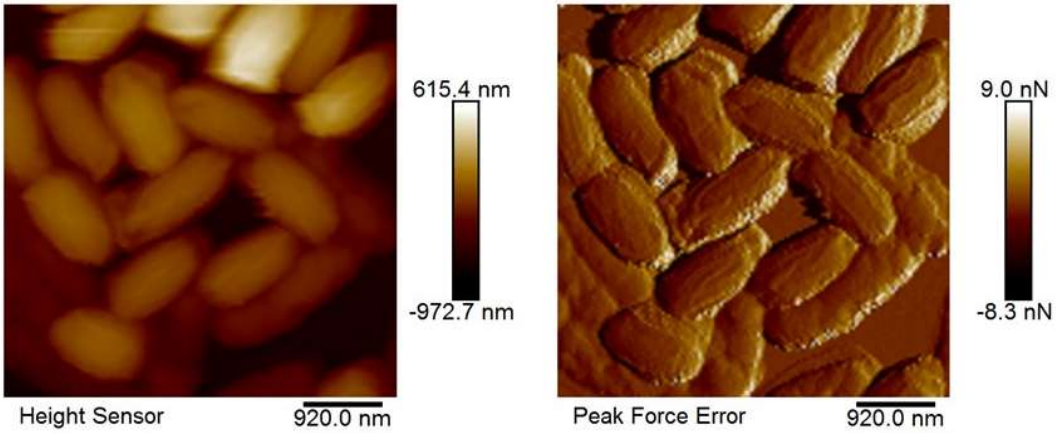

Figure 22. AFM image of BG spores from stock solution

The ridges are believed to be located in the spore coat and are believed to emerge during sporulation when water is expelled from the spore's core (Sahin et al., 2012), agreeing with

Zolock et al. that the features are likely inclusions underlying the spore's surface (Zolock et al., 2006). The visibility of the ridges is thought to change with changes in relative humidity, but the exact mechanisms for the formation of the ridges and how their topography is influenced by the spore coat's material properties are largely unknown (Sahin et al., 2012). Sahin et al. observed the ridges in *B. subtilis*, *B. atrophaeus*, and BA, and Zolock et al. concluded that the presence of ridges on the spore's surface observed through an imaging method such as AFM could not, in itself, identify a particular *Bacillus* species. Zolock et al. was successful at using AFM phase images, which rely on surface-probe interactions and surface viscoelasticity to map stiffness variations on the spore surface, to derive surface characteristics capable of differentiating four different *Bacillus* species spores when clustered in small groups (Zolock et al., 2006).

Spores in the stock solution were typically abundant in concentrations of the magnitude of 10^9 CFU/mL. The concentration of BG spores in the BioSampler following a 30-minute collection was typically of the magnitude of 10^4 CFU/mL. Spores were readily found and imaged on the AFM when the stock solution was sampled. When sampling from the BioSampler after a collection, spores could not be found on the mica disk when identically prepared. Even concentrating the sample by 100x with centrifugation did not yield visible results. Figure 23 shows the difference in how the disks appeared under the microscope of the AFM, with a sample of visible spores taken from the BG stock solution in Figure 23A, and a sample with no visible spores take from the BioSampler of experiment BGA35A in Figure 23B. The white circles highlight areas of interest on both images. In Figure 23A, the approximate number of BG spores on the mica disk was 4.00×10^7 CFU. In Figure 23B, the approximate number of BG spores on the mica disk was 8.95×10^4 CFU. Imaging with the microscope of the AFM is often used to visually identify regions of interest prior to engaging surface scanning with the AFM probe.

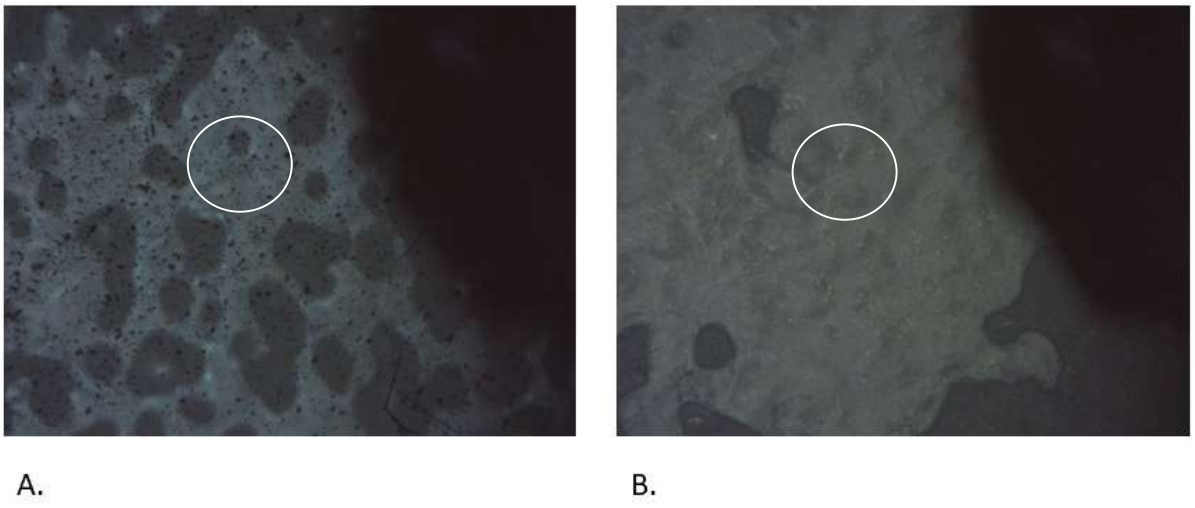

Figure 23. Comparative images of mica disk surfaces under the AFM's microscope where: A. BG spores are present and B. no spores present

The black specks observed in Figure 23A are spores and often groups of spores. Figure 23B is devoid of the black specks upon visual observation, and spores were not observed following multiple hours of scanning with the AFM probe.

Additional techniques were attempted to view BG spores sampled from the BioSampler on the mica disks used for the AFM. Following a 100x concentration using the centrifuge, 50 µL of solution was placed on a mica disk and allowed to evaporatively dry in 10 µL intervals. The surface of the mica disk had been altered using an Aqua Hold II barrier pen (Scientific Device Laboratory). The barrier pen applied a waxy, hydrophobic barrier on the surface of the mica disk, and the barrier was applied to cover three-quarters of the disk's surface. The wax barrier confined the 10 µL of solution to one-quarter of the disk's surface as it evaporatively dried. A comparison of an unaltered mica disk (left) and a disk with the added hydrophobic barrier (right) is depicted in Figure 24.

Figure 24. Comparison of an unaltered mica disk (left) and a mica disk with an added hydrophobic barrier (right)

On the unaltered mica disk, approximately 4.00×10^7 CFUs covered the surface of the mica disk (with an approximate surface area of 0.79 cm^2). On the mica disk with the open surface area restricted to approximately 0.19 cm^2, only 8.95×10^4 CFUs were approximated to be present. These techniques worked to further concentrate the number of spores on the mica surface from the starting concentration, however, no spores were visible on the AFM's microscope or with scans from the AFM probe. It was concluded that conventional techniques failed to yield high-quality AFM images because not enough spores were present on the mica disk to visually locate and initiate scanning. Future research efforts should endeavor to refine methods of concentrating spores collected in a BioSampler (or any type of impinger or impactor), as the overall number of spores in the collection apparatus is often several orders of magnitude lower than the starting number of spores prior to the production of the bioaerosols being studied.

V. Conclusions

Understanding the physical properties and behaviors of bioaerosols comprised of BG spores can potentially assist in the development of improved countermeasures and mechanisms to minimize or neutralize the effect of human pathogens released in facilities where bioaerosols are generated.

In exploring factors contributing to increased concentrations of BG spores collected following the sampling of generated bioaerosols, no strong correlation was observed between increasing the aeration rate and measuring increased BG spore concentrations in the BioSampler, within the investigated range. In the control condition experiments, the mean percent increase in the percent of the starting BG spore concentration captured in the BioSampler was 97.58% when the aeration rate was increased from 0.50 L/min to 1.00 L/min. In experiments with 0.42 cm diameter polystyrene spheres added as FFCM in a monolayer on the surface of the water in the reactor bottle, the mean percent increase was 129.57%. When the diameter of the spheres was increased to 1.91 cm, the resulting experiments had a calculated percent increase of 352.60%. Incremental increases in the collected BG spore concentration and increments increased of aeration rate (0.50, 0.65, 0.85, and 1.00 L/min) was only observed in experiments when the 1.91 cm diameter spheres were added, suggesting that experimental scale and the range of investigated aeration rates may have been too minimal to fully demonstrate a correlation. Smaller percent increases (30.77% or lower) in aeration rates resulted in fewer comparisons (1 out of 9) with a calculated statistically significant correlation to an increased percent capture of BG spores in the BioSampler. However, larger percent increases (53.85% or higher) in aeration rates resulted in many more comparisons (6 out 9) with a statistically significant correlation. These results reinforce the postulation that a greater range of aeration rate values in these experiments

would have likely resulted in a clearer positive correlation between increased aeration rate and increased percent of the starting BG spores starting in the reactor bottle collected in the BioSampler following aerosolization.

Through this research, it was determined that the addition of FFCM does merit further research as a means to attenuate bioaerosol emission. The addition of the polystyrene spheres, of either diameter investigated in these experiments, reduced the mean percent of capture of BG spores in the BioSampler by an order of magnitude or more. On average, the addition of 1.91 cm diameter spheres resulted in a control efficiency of the BG spores of 83.95%. The control efficiency was higher for the 0.42 cm spheres, which had an average of 93.03%. At all four different aeration rates, the smaller diameter spheres had a higher control efficiency than the larger diameter spheres. The high control efficiency of the smaller spheres agreed with unpublished data provided by Burdsall et al. who observed control efficiencies above 90% by polystyrene spheres with an average diameter of 0.22 cm. These results were further substantiated by the initial large-scale experiment where the pilot-scale treatment system was used. Control efficiencies were calculated at 88.09% when 1.27 cm diameter LDPE spheres were added and 75.30% when 1.27 cm diameter polystyrene spheres were added.

Polystyrene spheres could potentially offer an attainable and relatively easily applied option to add to turbulently mixed and aerated bio-contaminated water in order to reduce bioaerosol emissions. A wide range of different materials could potentially be used as FFCM and could possibly be shown to match or exceed the abilities of the polystyrene spheres at attenuation emissions in this research. A natural or otherwise biodegradable material would potentially be more desirable as FFCM than polystyrene spheres, as realistic challenges would exist to

physically keep polystyrene spheres contained in a large volume, open-air tank or basin at a WWTP.

With these experiments representing the middle of three different experimental scales involving the BG-containing bioaerosols, an opportunity existed to examine the effect of scale on the percent of BG collected in the BioSampler. Of the four experimental conditions compared between medium and small experimental scales (two with and two without FFCM), only one was determined to statistically support the hypothesis that scale would not have an effect on percent of BG captured. The small-scale experiments increased the average percent of BG captured when increasing the aeration rate from 0.50 to 0.85 L/min by 1771.72% and 1814.87%, without and with added FFCM, respectively. Under the same conditions with the medium-scale experiments, the average percent increase of BG captured were only 50.80% and 63.14% (with and without added FFCM, respectively). This data provides evidence that smaller experimental scales may result in more drastic changes in the percent of BG captured with changes made to aeration rate.

VI. Recommendations for Future Research

BG spores were used in this research as a surrogate for BA spores, one of the high-consequence pathogens concerning the EPA with regards to bioaerosol production in WWTP, but certainly not the only one. While belonging to the same genus, differences do in fact exist between the spores of BG and BA. Differences are known to exist in average length, average width, density, and the lack of exosporium on BG spores. Research of a similar nature using *Bacillus anthracis* Sterne (or simply the "Sterne strain") would perhaps provide an even closer surrogate regarding the behavior of the spores once aerosolized, while overall preserving research safety. Future research is also needed beyond BA on additional pathogens of interest, to include the use of MS2 virus as a surrogate for the Ebola virus. While it is difficult to plan for emerging biological threats or emerging pathogens, bacterial endospores, whole bacterial cells, and viruses would represent three main categories of pathogens that future research in bioaerosols could continue to investigate.

Future research would benefit from the development of foundational theory for the emission of bioaerosols. Disciplines including fluid mechanics and molecular dynamics can be applied to understanding and predicting bioaerosol emissions as a function of mixing intensity. Improving the accuracy of theoretical models for bioaerosol formation could lead to the development of mathematical models for bioaerosol production and distribution, which in turn could influence the development of regulations and procedures at WWTPs and other facilities that generate bioaerosols.

Experiments investigating the role of FFCM as a means of attenuating bioaerosol emissions have not, to the author's knowledge, quantitatively or qualitatively assessed the number of biological particles deposited on the FFCM. The expanded polystyrene utilized in

these experiments was porous, allowing high amounts of available surface area for spores to be deposited. However, some repulsion was expected between the hydrophobic spores and the hydrophobic polystyrene. Investigations into coatings for polystyrene spheres and different FFCM altogether would greatly benefit endeavors to safely, effectively, and feasibly reduce bioaerosol emissions following turbulent mixing and aeration regimes.

Polystyrene was the only type of FFCM utilized in these experiments, but the material used could be one of numerous options. Cost, environmental impact, and ease of application would all need to be considered for practical reasons. More research and understanding of bioaerosol formation and transport is necessary to aid in the selection of the most effective FFCM material and size. Understanding the chemical and mechanical considerations involved would ultimately reduce the time and effort required to investigate the effectiveness of various materials.

Particle size was not measured or determined in this research. The experimental setup was designed to reduce the number of non-aerosolized biological particles (BG spores in this research) collected in the BioSampler. Particle size distribution data would provide pertinent information about the threat of potential pathogens being transported in bioaerosols. Other studies have used a different bioaerosol collection apparatus to determine size distribution. Hung et al. utilized an Andersen six-stage cascade impactor, and thereby distinguished between groupings with aerodynamic cut-off sizes ranging from 0.65 to 7.0 μm. Size-fractionated sample collection would be additionally useful in samples with multiple contaminants or pathogens of interest, to include medical waste.

Maintaining a constant aeration rate was of paramount importance in these experiments. Similar studies, to include Hung et al., 2010, and Lin et al., 2016, used experimental setups in

which all supplied air flowed through an in-line rotameter or another type of air flowmeter. This allowed for constant, real-time monitoring of the aeration rates and is a recommended practice for future research efforts to decrease a potential source of variability.

The concept of "loss", the BG spores leaving the reactor bottle as evidenced by decreasing BG spore concentrations within the reactor between experiments one to three but not collected in the BioSampler, prompted the question of where the unaccounted spores were collecting. Further investigation as to what portions of the apparatus the BG spores were collecting (if one place more than another) would assist in producing better estimates of aerosolized BG spore behavior in larger-scale experiments. The information could also be used to design more efficient apparatus to better collect the BG spores.

The first large-scale experimental conditions at the pilot-scale water treatment plant included the use of synthetic wastewater. The mixture used included dissolved salts in the synthetic wastewater. It would be beneficial if future large-scale experiments utilized DI water in order to allow for closer comparisons to the small and medium-scale studies. However, future work could also be conducted with the small and medium-scale apparatus with similar experimental conditions as previously utilized and with the addition of synthetic wastewater. Synthetic wastewater of the same composition could be made or transported to AFIT. The inclusion of synthetic wastewater in even the bench-top scale experiments could potentially provide even more usable data, as the water in WWTPs will contain an array of chemicals, biological organisms, and various debris.

Bibliography

Abou-Elela, S. I., Ibrahim, H. S., Kamel, M. M., & Gouda, M. (2014). Application of Nanometal Oxides In Situ in Nonwoven Polyester Fabric for the Removal of Bacterial Indicators of Pollution from Wastewater. *The Scientific World Journal*, *2014*, 1–7.

Arias, F. J., Martin, L., Matilde, A., Girotti, A., & Rodriguez-Cabello, J. C. (2009). Synthesis and Characterization of Macroporous Thermosensitive Hydrogels from Recombinant Elastin-Like Polymers. *Biomacromolecules*, *10*(11), 3015–3022.

Bartrand, T. A., Weir, M. H., & Haas, C. N. (2008). Dose-Response Models for Inhalation of Bacillus anthracis Spores: Interspecies Comparisons. *Risk Analysis*, *28*(4), 1115–1124. https://doi.org/10.1111/j.1539-6924.2008.01067

Bauer, H., Fuerhacker, M., Zibuschka, F., Schmid, H., & Puxbaum, H. (2002). Bacteria and fungi in aerosols generated by two different types of wastewater treatment plants. *Water Research*, *36*(16), 3965–3970. https://doi.org/10.1016/S0043-1354(02)00121-5

Berger, J. A., & Marr, A. G. (1960). Sonic Disruption of Spores of Bacillus cereus. *Journal of General Microbiology*, *22*, 147–157.

Bioterrorism Agents/Disease. (2018). Retrieved from Centers for Disease Control and Prevention website: https://emergency.cdc.gov/agent/agentlist-category.asp#a

Bishop, A. H., & Stapleton, H. L. (2016). Aerosol and surface deposition characteristics of two surrogates for Bacillus anthracis spores. *Applied and Environmental Microbiology*, *82*(22), 6682–6690. https://doi.org/10.1128/AEM.02052-16

Boone, T., & Driks, A. (2016). Protein synthesis during germination: Shedding new light on a classical question. *Journal of Bacteriology*, *198*(24), 3251–3253. https://doi.org/10.1128/JB.00721-16

Boone, T. J., Mallozzi, M., Nelson, A., Thompson, B., Khemmani, M., Lehmann, D., … Driks, A. (2018). Coordinated Assembly of the Bacillus anthracis Coat and Exosporium during Bacterial Spore Outer Layer Formation. *Molecular Biology and Physiology*, *9*(6), 1–16. https://doi.org/10.1128/mBio.01166-18

Buttner, M. P., Cruz-Perez, P., & Stetzenbach, L. D. (2001). Enhanced Detection of Surface-Associated Bacteria in Indoor Environments by Quantitative PCR. *Applied and Environmental Microbiology*, *67*(6), 2564–2570. https://doi.org/10.1128/AEM.67.6.2564-2570.2001

Campbell, G. A., & Mutharasan, R. (2007). Method of Measuring Bacillus anthracis Spores in the Presence of Copious Amounts of Bacillus thuringiensis and Bacillus cereus. *Analytical Chemistry*, *79*(3), 1145–1152. Retrieved from https://doi.org/10.1021/ac060982b

Carducci, A., Tozzi, E., Rubulotta, E., Casini, B., Cantiani, L., Rovini, E., … Pacini, R. (2000). Assessing Airborne Biological Hazard from Urban Wastewater Treatment. *Water Research*, *34*(4), 1173–1178.

Carrera, M., Zandomeni, R. O., Fitzgibbon, J., & Sagripanti, J. L. (2007). Difference Between the Spore Sizes of Bacillus Anthracis and Other Bacillus Species. *Journal of Applied Microbiology*, *102*(2), 303–312. https://doi.org/10.1111/j.1365-2672.2006.03111

Chemical , Biological , Radiological , and Nuclear Threats and Hazards (TM 3-11.91). (2017). Washington D.C.

Chen, G., Driks, A., Tawfiq, K., Mallozzi, M., & Patil, S. (2010). Bacillus anthracis and Bacillus subtilis spore surface properties and transport. *Colloids and Surfaces B: Biointerfaces*, *76*(2), 512–518. https://doi.org/10.1016/j.colsurfb.2009.12.012

Clark, C. S. (1984). Health Effects Associated with Wastewater Treatment and Disposal. *Journal*

(Water Pollution Control Federation), *56*(6), 625–627. Retrieved from https://www.jstor.org/stable/25042311

Coleman, M. E., Thran, B., Morse, S. S., Hugh-Jones, M., & Massulik, S. (2008). Inhalation Anthrax: Dose Response and Risk Analysis. *Biosecurity and Bioterrorism: Biodefense Strategy, Practice, and Science*, *6*(2), 147–160. https://doi.org/10.1089/bsp.2007.0066

Cooper, C. W., Aithinne, K. A. N., Floyd, E. L., Stevenson, B. S., & Johnson, D. L. (2019). A comparison of air sampling methods for Clostridium difficile endospore aerosol. *Aerobiologia*, *35*(3), 411–420. https://doi.org/10.1007/s10453-019-09566-2

DHS' Progress in Federal Incident Management Planning. (2010). Retrieved from https://www.oig.dhs.gov/assets/Mgmt/OIGr_10-58_Feb10.pdf

Druett, H. A., Henderson, D. W., Packman, L., & Peacock, S. (1953). *Studies On Respiratory Infection: I . The Influence of Particle Size on Respiratory Infection With Anthrax Spores*. 359–371.

El-Serehy, H. A., Bahgat, M. M., Al-Rasheid, K., Al-Misned, F., Mortuza, G., & Shafik, H. (2014). Cilioprotists as Biological Indicators for Estimating the Efficiency of Using Gravel Bed Hydroponics System in Domestic Wastewater Treatment. *Saudi Journal of Biological Sciences*, *21*(3), 250–255. https://doi.org/10.1016/j.sjbs.2013.11.003

EPA: How Wastewater Treatment Works... The Basics. (1998). Washington D.C.

EPA: Progress on Water Sector Decontamination Recommendations & Proposed Strategic Plan. (2015). Washington D.C.

Fannin, K. F., Vana, S. C., & Jakubowski, W. (1985). Effect of an Activated Sludge Wastewater Treatment Plant on Ambient Air Densities of Aerosols Containing Bacteria and Viruses. *Applied and Environmental Microbiology*, *49*(5), 1191–1196.

Farrell, S., Halsall, H. B., & Heineman, W. R. (2005). Immunoassay for B. globigii spores as a model for detecting B. anthracis spores in finished water. *Analyst*, *130*(4), 489–497. https://doi.org/https://doi.org/10.1039/B413652G

Fernando, N. L., & Fedorak, P. M. (2005). Changes at an activated sludge sewage treatment plant alter the numbers of airborne aerobic microorganisms. *Water Research*, *39*(19), 4597–4608. https://doi.org/10.1016/j.watres.2005.08.010

Fiester, S. E., Helfinstine, S. L., Redfearn, J. C., Uribe, R. M., & Woolverton, C. J. (2012). Electron Beam Irradiation Dose Dependently Damages the Bacillus Spore Coat and Spore Membrane. *International Journal of Microbiology*, *2012*. https://doi.org/10.1155/2012/579593

Fracchia, L., Pietronave, S., Rinaldi, M., & Giovanna, M. (2006). Site-related airborne biological hazard and seasonal variations in two wastewater treatment plants. *Water Research*, *40*(10), 1985–1994. https://doi.org/10.1016/j.watres.2006.03.016

Franco, C., & Bouri, N. (2010). Environmental Decontamination Following a Large-Scale Bioterrorism Attack: Federal Progress and Remaining Gaps. *Biosecurity and Bioterrorism: Biodefense Strategy, Practice, and Science*, *8*(2), 107–117.

Garcia, R., & DesRochers, B. (1979). Toxicity of Bacillus Thuringiensis var Israelensis to Some California Mosquitoes Under Different Conditions. *Mosquito News*, *September*, 541–544.

Ghosh, S., Setlow, B., Wahome, P. G., Cowan, A. E., Plomp, M., Malkin, A. J., & Setlow, P. (2008). Characterization of Spores of Bacillus subtilis That Lack Most Coat Layers. *Journal of Bacteriology*, *190*(20), 6741–6748. https://doi.org/10.1128/JB.00896-08

Haas, C. N. (2002). On the Risk of Mortality to Primates Exposed to Anthrax Spores. *Risk Analysis*, *22*(2), 189–193.

Han, Y., Li, L., & Liu, J. (2013). Characterization of the airborne bacteria community at different distances from the rotating brushes in a wastewater treatment plant by 16S rRNA gene clone libraries. *Journal of Environmental Sciences*, *25*(1), 5–15. https://doi.org/10.1016/S1001-0742(12)60018-7

Han, Y., Wang, Y., Li, L., Xu, G., Liu, J., & Yang, K. (2018). Science of the Total Environment Bacterial population and chemicals in bioaerosols from indoor environment : Sludge dewatering houses in nine municipal wastewater treatment plants. *Science of the Total Environment*, *618*, 469–478. https://doi.org/10.1016/j.scitotenv.2017.11.071

Hawkins, L. S. (2008). *Micro-etched Platforms for Thermal Inactivation of Bacillus Anthracis and Bacillus Thuringiensis Spores*. Masters Thesis - Air Force Institute of Technology.

Heinonen-Tanski, H., Reponen, T., & Koivunen, J. (2009). Airborne Enteric Coliphages and Bacteria in Sewage Treatment Plants. *Water Research*, *43*(9), 2558–2566. https://doi.org/10.1016/j.watres.2009.03.006

HSPD 8 Annex 1. (2017). Retrieved from US Department of Homeland Security website: https://www.dhs.gov/hspd-8-annex-1

Hung, H. F., Kuo, Y. M., Chien, C. C., & Chen, C. C. (2010). Use of floating balls for reducing bacterial aerosol emissions from aeration in wastewater treatment processes. *Journal of Hazardous Materials*, *175*, 866–871. https://doi.org/10.1016/j.jhazmat.2009.10.090

Jung, J. H., Lee, J. E., Lee, C. H., Kim, S. S., & Lee, B. U. (2009). Treatment of Fungal Bioaerosols by a High-Temperature , Short-Time Process in a Continuous-Flow System. *Applied and Environmental Microbiology*, *75*(9), 2742–2749. https://doi.org/10.1128/AEM.01790-08

Kang, S. M., Heo, K. J., & Lee, B. U. (2015). Why Does Rain Increase the Concentrations of

Environmental Bioaerosols during Monsoon? *Aerosol and Air Quality Research*, *15*, 2320–2324. https://doi.org/10.4209/aaqr.2014.12.0328

Karra, S., & Katsivela, E. (2007). Microorganisms in Bioaerosol Emissions from Wastewater Treatment Plants During Summer at a Mediterranean Site. *Water Research*, *41*(6), 1355–1365. https://doi.org/10.1016/J.WATRES.2006.12.014

Kesavan, J., Schepers, D., & Mcfarland, A. R. (2010). Sampling and Retention Efficiencies of Batch-Type Liquid-Based Bioaerosol Samplers. *Aerosol Science and Technology*, *44*(10), 817–829. https://doi.org/10.1080/02786826.2010.497513

Khan, M. M. T., Chapman, T., Cochran, K., & Schuler, A. J. (2013). Attachment surface energy effects on nitrification and estrogen removal rates by biofilms for improved wastewater treatment. *Water Research*, *47*(7), 2190–2198. https://doi.org/10.1016/j.watres.2013.01.036

Korsten, L., & De Jager, E. E. (1995). Mode of Action of Bacillus subtilis for Control of Avocado Post-harvest Pathogens. *South African Avocado Growers' Association Yearbook*, *18*, 124–130.

Lee, B. U. (2011). Life comes from the air: A short review on bioaerosol control. *Aerosol and Air Quality Research*, *11*(7), 921–927. https://doi.org/10.4209/aaqr.2011.06.0081

Lee, B. U., Lee, G., Heo, K. J., & Jung, J. (2019). Concentrations of Atmospheric Culturable Bioaerosols at Mountain and Seashore Sites. *International Journal of Environmental Research and Public Health*, *16*(4323), 1–6.

Lee, J.-H., & Wu, C.-Y. (2006). *Evaluation of the Performance of Iodine-Treated Biocide Filters Challenged with Bacterial Spores and Viruses*. https://doi.org/AFRL-ML-TY-TR-2007-4510

Li, A. G., Burggraf, L. W., & Xing, Y. (2016). Nanomechanical Characterization of Bacillus

anthracis Spores by Atomic Force Microscopy. *Applied and Environmental Microbiology*, *82*(10), 2988–2999. https://doi.org/10.1128/aem.00431-16

Li, J., Zhou, L., Zhang, X., Xu, C., Dong, L., & Yao, M. (2016). Bioaerosol emissions and detection of airborne antibiotic resistance genes from a wastewater treatment plant. *Atmospheric Environment*, *124*, 404–412. https://doi.org/10.1016/j.atmosenv.2015.06.030

Li, Y., Zhang, H., Qiu, X., Zhang, Y., & Wang, H. (2013). Dispersion and risk assessment of bacterial aerosols emitted from rotating-brush aerator during summer in a wastewater treatment plant of xi'an, china. *Aerosol and Air Quality Research*, *13*(6), 1807–1814. https://doi.org/10.4209/aaqr.2012.09.0245

Lin, K., & Marr, L. C. (2017). Aerosolization of Ebola Virus Surrogates in Wastewater Systems. *Environmental Science and Technology*, *51*(5), 2669–2675. https://doi.org/10.1021/acs.est.6b04846

Lin, T. H., Chiang, C. F., Lin, S. T., & Tsai, C. T. (2016). Effects of small-size suspended solids on the emission of Escherichia coli from the aeration process of wastewater treatment. *Aerosol and Air Quality Research*, *16*(9), 2208–2215. https://doi.org/10.4209/aaqr.2015.04.0232

Lundholm, M., & Rylander, R. (1983). Work related symptoms among sewage workers. *British Journal of Industrial Medicine*, *40*, 325–329.

Mandal, J., & Brandl, H. (2011). Bioaerosols in Indoor Environment - A Review with Special Reference to Residential and Occupational Locations. *The Open Environmental & Biological Monitoring Journal*, *4*, 83–96.

Marti, E., Monclús, H., Jofre, J., Rodriguez-roda, I., Comas, J., & Luis, J. (2011). Bioresource Technology Removal of microbial indicators from municipal wastewater by a membrane

bioreactor (MBR). *Bioresource Technology*, *102*(8), 5004–5009. https://doi.org/10.1016/j.biortech.2011.01.068

Medema, G., Wullings, B., Roeleveld, P., & van der Kooij, D. (2004). Risk Assessment of Legionella and Enteric Pathogens in Sewage Treatment Works. *Water Science and Technology*, *4*(2), 125–132.

Metcalf & Eddy, I. (2013). *Wastewater Engineering: Treatment and Reuse* (4th ed.). New York: McGraw-Hill.

Michałkiewicz, M. (2018). Comparison of wastewater treatment plants based on the emissions of microbiological contaminants. *Environmental Monitoring and Assessment*, *190*(11). https://doi.org/10.1007/s10661-018-7035-2

Miles, M. (1997). Scanning Probe Microscopy: Probing the Future. *Science*, *277*(5333), 1845–1847. Retrieved from https://science-sciencemag-org.afit.idm.oclc.org/content/277/5333/1845

Morawska, L. (2001). *Environmental Aerosol Physics*. Retrieved from https://biophysics.sbg.ac.at/transcript/aerosol2.pdf

Murray, Patrick R.; Rosenthal, Ken S.; Pfaller, M. A. (2005). *Medical Microbiology* (5th ed.). Philadelphia, PA: Elsevier Inc.

Mwilu, S. K., Aluoch, A. O., Miller, S., Wong, P., Sadik, O. A., Fatah, A. A., & Arcilesi, R. D. (2009). Identification and Quantitation of Bacillus globigii Using Metal Enhanced Electrochemical Detection and Capillary Biosensor. *Analytical Chemistry*, *81*(18), 7561–7570.

Nagler, K., & Moeller, R. (2015). Systematic investigation of germination responses of Bacillus subtilis spores in different high-salinity environments. *Federation of European*

Microbiological Societies (FEMS) Microbiology Ecology, *91*(5), 1–10. https://doi.org/10.1093/femsec/fiv023

Nakamura, L. K. (1989). Taxonomic relationship of black-pigmented Bacillus subtilis strains and a proposal for Bacillus atrophaeus sp. nov. *International Journal of Systematic Bacteriology*, *39*(3), 295–300. https://doi.org/10.1099/00207713-39-3-295

Office of Research and Development Homeland Security Research Program. (2018). *Exposure Pathways to High-Consequence Pathogens in the Wastewater Collection and Treatment Systems Exposure Pathways to High-Consequence Pathogens in the Wastewater Collection and Treatment Systems*.

Omotade, T. O., Bernhards, R. C., Klimko, C. P., Matthews, M. E., Hill, A. J., Hunter, M. S., … Cote, C. K. (2014). The impact of inducing germination of Bacillus anthracis and Bacillus thuringiensis spores on potential secondary decontamination strategies. *Journal of Applied Microbiology*, *117*, 1614–1633. https://doi.org/10.1111/jam.12644

Orsini, M., Laurenti, P., Boninti, F., Arzani, D., Ianni, A., & Romano-Spica, V. (2002). A molecular typing approach for evaluating bioaerosol exposure in wastewater treatment plant workers. *Water Research*, *36*(5), 1375–1378. https://doi.org/10.1016/S0043-1354(01)00336-0

Paidhungat, M., Setlow, B., Daniels, W. B., Hoover, D., Papafragkou, E., & Setlow, P. (2002). Mechanisms of Induction of Germination of Bacillus subtilis Spores by High Pressure. *Applied and Environmental Microbiology*, *68*(6), 3172–3175. https://doi.org/10.1128/AEM.68.6.3172

Pascual, L., Pérez-Luz, S., Yáñez, M. A., Santamaría, A., Gibert, K., Salgot, M., … Catalán, V. (2003). Bioaerosol emission from wastewater treatment plants. *Aerobiologia*, *19*(3), 261–

270. https://doi.org/10.1023/B:AERO.0000006598.45757.7f

Plomp, M., Leighton, T. J., Wheeler, K. E., & Malkin, A. J. (2005a). Architecture and High-Resolution Structure of Bacillus thuringiensis and Bacillus cereus Spore Coat Surfaces. *Langmuir*, *21*(17), 7892–7898. https://doi.org/10.1021/la050412r

Plomp, M., Leighton, T. J., Wheeler, K. E., & Malkin, A. J. (2005b). The high-resolution architecture and structural dynamics of Bacillus spores. *Biophysical Journal*, *88*(1), 603–608. https://doi.org/10.1529/biophysj.104.049312

Reponen, T., Willeke, K., Grinshpun, S., & Nevalainen, A. (2011). Biological Particle Sampling. In P. Kulkarni, P. A. Baron, & K. Willeke (Eds.), *Aerosol Measurement: Principles, Techniques, and Applications* (3rd ed.). https://doi.org/10.1002/9781118001684.ch24

Roadmap to a Secure and Resilient Water and Wastewater Sector. (2017).

Sahin, O., Yong, E. H., Driks, A., & Mahadevan, L. (2012). Physical basis for the adaptive flexibility of Bacillus spore coats. *Journal of the Royal Society Interface*, *9*, 3156–3160.

Sánchez-Monedero, M. A., Aguilar, M. I., Fenoll, R., & Roig, A. (2008). Effect of the aeration system on the levels of airborne microorganisms generated at wastewater treatment plants. *Water Research*, *42*(14), 3739–3744. https://doi.org/10.1016/j.watres.2008.06.028

Sella, S. R. B. R., Vandenberghe, L. P. S., & Soccol, C. R. (2014). Life cycle and spore resistance of spore-forming Bacillus atrophaeus. *Microbiological Research*, *169*(12), 931–939. https://doi.org/10.1016/j.micres.2014.05.001

Setlow, B., Cowan, A. E., & Setlow, P. (2003). Germination of spores of Bacillus subtilis with dodecylamine. *Journal of Applied Microbiology*, *95*, 637–648. https://doi.org/10.1046/j.1365-2672.2003.02015.x

Shreve, M. J., & Brennan, R. A. (2019). Trace organic contaminant removal in six full-scale

integrated fixed-film activated sludge (IFAS) systems treating municipal wastewater. *Water Research*, *151*, 318–331. https://doi.org/10.1016/j.watres.2018.12.042

SKC BioSampler Specification Sheet. (2019). Retrieved from SKC Inc. website: https://www.skcinc.com/catalog/pdf/instructions/1603.pdf

Smith, M., Stuntz, S., Xing, Y., Magnuson, M., Phillips, R., & Harper, Jr., W. F. (2019). *Functional Resilience of Activated Sludge Exposed to Bacillus globigii and Bacteriophage MS2*.

Spencer, R. C. (2003). Bacillus anthracis. *Journal of Clinical Pathology*, *56*, 182–187.

Stensel, H. D., & Reiber, S. (1983). Industrial Wastewater Treatment with a New Biological Fixed-Film System. *Environmental Progress*, *2*(2), 110–115.

Stewart, G. C. (2015). The Exosporium Layer of Bacterial Spores: A Connection to the Environment and the Infected Host. *Microbiology and Molecular Biology Reviews*, *79*(4), 437–457. https://doi.org/10.1128/MMBR.00050-15

Szabo, J. G., Muhammad, N., Heckman, L., Rice, E. W., & Hall, J. (2012). Germinant-Enhanced Decontamination of Bacillus Spores Adhered to Iron and Cement-Mortar Drinking Water Infrastructures. *Applied and Environmental Microbiology*, *99*, 2449–2451. https://doi.org/10.1128/AEM.07242-11

Torok, T. J., Tauxe, R. V., Wise, R. P., Sokolow, R., Mauvais, S., Birkness, K. A., … Foster, L. R. (1997). A Large Community Outbreak of Salmonellosis Caused by Intentional Contamination of Restaurant Salad Bars. *Journal of the American Medical Association*, *278*(5), 389–395.

Tsai, C. T., Lai, J. S., & Lin, S. T. (1998). Quantification of pathogenic micro-organisms in the sludge from treated hospital wastewater. *Journal of Applied Microbiology*, *85*, 171–176.

Tufts, J. A. M., Calfee, M. W., Lee, S. D., & Ryan, S. P. (2014). Bacillus thuringiensis as a surrogate for Bacillus anthracis in aerosol research. *World Journal of Microbiology and Biotechnology*, *30*(5), 1453–1461. https://doi.org/10.1007/s11274-013-1576-x

Turner, W. C., Kausrud, K. L., Beyer, W., Easterday, W. R., Barandongo, Z. R., Blaschke, E., … Getz, W. M. (2016). Lethal exposure : An integrated approach to pathogen transmission via environmental reservoirs. *Scientific Reports*, *6*(23711), 1–13. https://doi.org/10.1038/srep27311

US EPA. (2016). *Clean Watersheds Needs Survey 2012: Report to Congress*.

Wang, Y., Li, L., Xiong, R., Guo, X., & Liu, J. (2019). Effects of aeration on microbes and intestinal bacteria in bioaerosols from the BRT of an indoor wastewater treatment facility. *Science of the Total Environment*, *648*, 1453–1461. https://doi.org/10.1016/j.scitotenv.2018.08.244

Weber, D. J., Sickbert-Bennett, E., Gergen, M. F., & Rutala, W. A. (2003). Efficacy of Selected Hand Hygiene Agents Used to Remove Bacillus atrophaeus (a Surrogate of Bacillus anthracis) From Contaminated Hands. *JAMA*, *289*(10), 1274–1277. https://doi.org/10.1001/jama.289.10.1274

White, C. P., Popovici, J., Lytle, D. A., & Rice, E. W. (2014). Endospore surface properties of commonly used Bacillus anthracis surrogates vary in aqueous solution. *Antonie van Leeuwenhoek, International Journal of General and Molecular Microbiology*, *106*(2), 243–251. https://doi.org/10.1007/s10482-014-0187-3

Wiencek, K. M., Klapes, N. A., & Foegedingl, P. M. (1990). Hydrophobicity of Bacillus and Clostridium Spores. *Applied and Environmental Microbiology*, *56*(9), 2600–2605.

Willeke, K., Lin, X., & Grinshpun, S. A. (2007). Improved Aerosol Collection by Combined

Impaction and Centrifugal Motion Impaction and Centrifugal. *Aerosol Science*, *28*(5), 439–456. https://doi.org/10.1080/02786829808965536

Withers, M. R. (2014). *USAMRIID's Medical Management of Biological Casualties Handbook* (8th Editio; M. R. Withers, Ed.). Fort Detrick, MD: USAMRIID.

Xing, Y., Li, A., Felker, D. L., & Burggraf, L. W. (2014). Nanoscale Structural and Mechanical Analysis of Bacillus anthracis Spores Inactivated with Rapid Dry Heating. *Applied and Environmental Microbiology*, *80*(5), 1739–1749. https://doi.org/10.1128/aem.03483-13

Xu, Z., Wu, Y., Shen, F., Chen, Q., Tan, M., & Yao, M. (2011). Bioaerosol science, technology, and engineering: Past, present, and future. *Aerosol Science and Technology*, *45*(11), 1337–1349. https://doi.org/10.1080/02786826.2011.593591

Zhao, L., Schaefer, D., & Marten, M. R. (2005). Assessment of Elasticity and Topography of Aspergillus nidulans Spores via Atomic Force Microscopy. *Applied and Environmental Microbiology*, *71*(2), 955–960. https://doi.org/10.1128/AEM.71.2.955

Zhen, H., Han, T., Fennell, D. E., & Mainelis, G. (2014). A Systematic Comparison of Four Bioaerosol Generators: Affect on Culturability and Cell Membrane Integrity When Aerosolizing Escherichia coli Bacteria. *Journal of Aerosol Science*, *70*, 67–79. https://doi.org/10.1016/j.jaerosci.2014.01.002

Zheng, Y., & Yao, M. (2017). Liquid impinger BioSampler's performance for size-resolved viable bioaerosol particles. *Journal of Aerosol Science*, *106*(September 2016), 34–42. https://doi.org/10.1016/j.jaerosci.2017.01.003

Zolock, R. A., Li, G., Bleckmann, C., Burggraf, L., & Fuller, D. C. (2006). Atomic force microscopy of Bacillus spore surface morphology. *Micron*, *37*(4), 363–369. https://doi.org/10.1016/J.MICRON.2005.11.006

Appendix A: Additional Graphical Representations

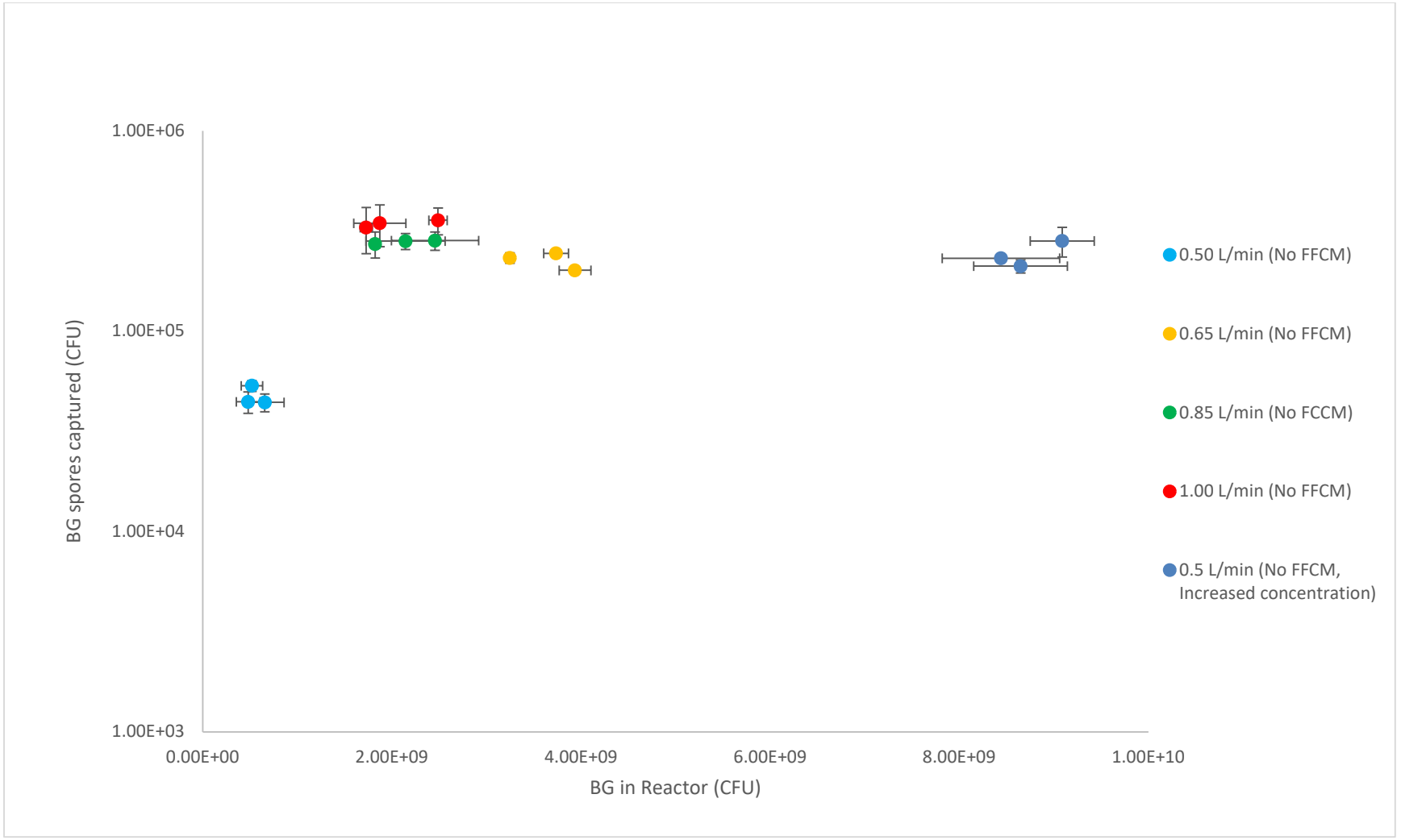

Figure 25. Number of CFU captured in the BioSampler versus starting amount of BG in the reactor (in CFU) (log scale) (controls only displayed)

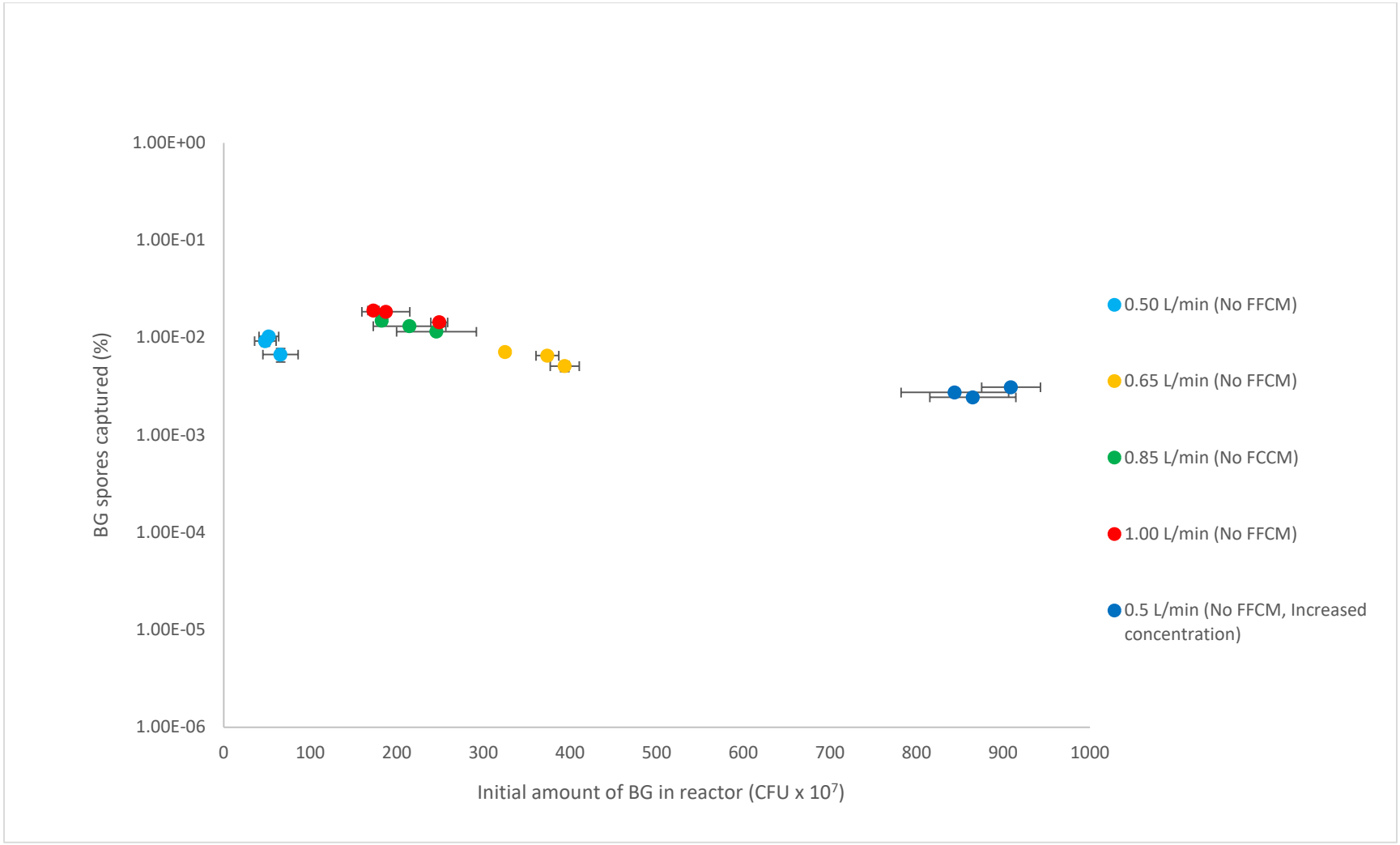

Figure 26. Percent of reactor captured in the BioSampler versus starting amount of BG in the reactor (controls only displayed)

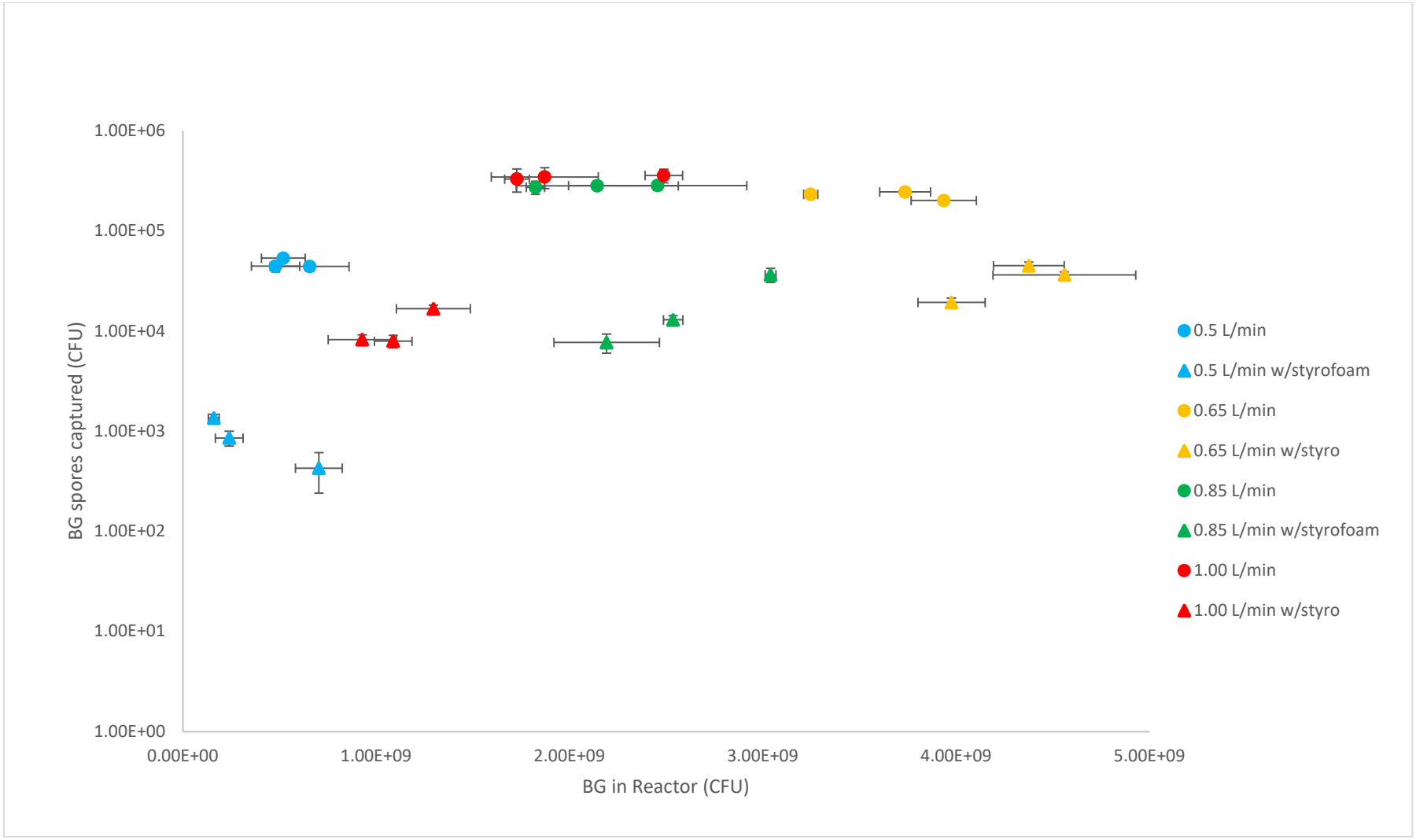

Figure 27. Number of CFU captured in the BioSampler versus the starting amount of BG in the reactor (in CFU) (log scale) (0.42 cm diameter spheres added)

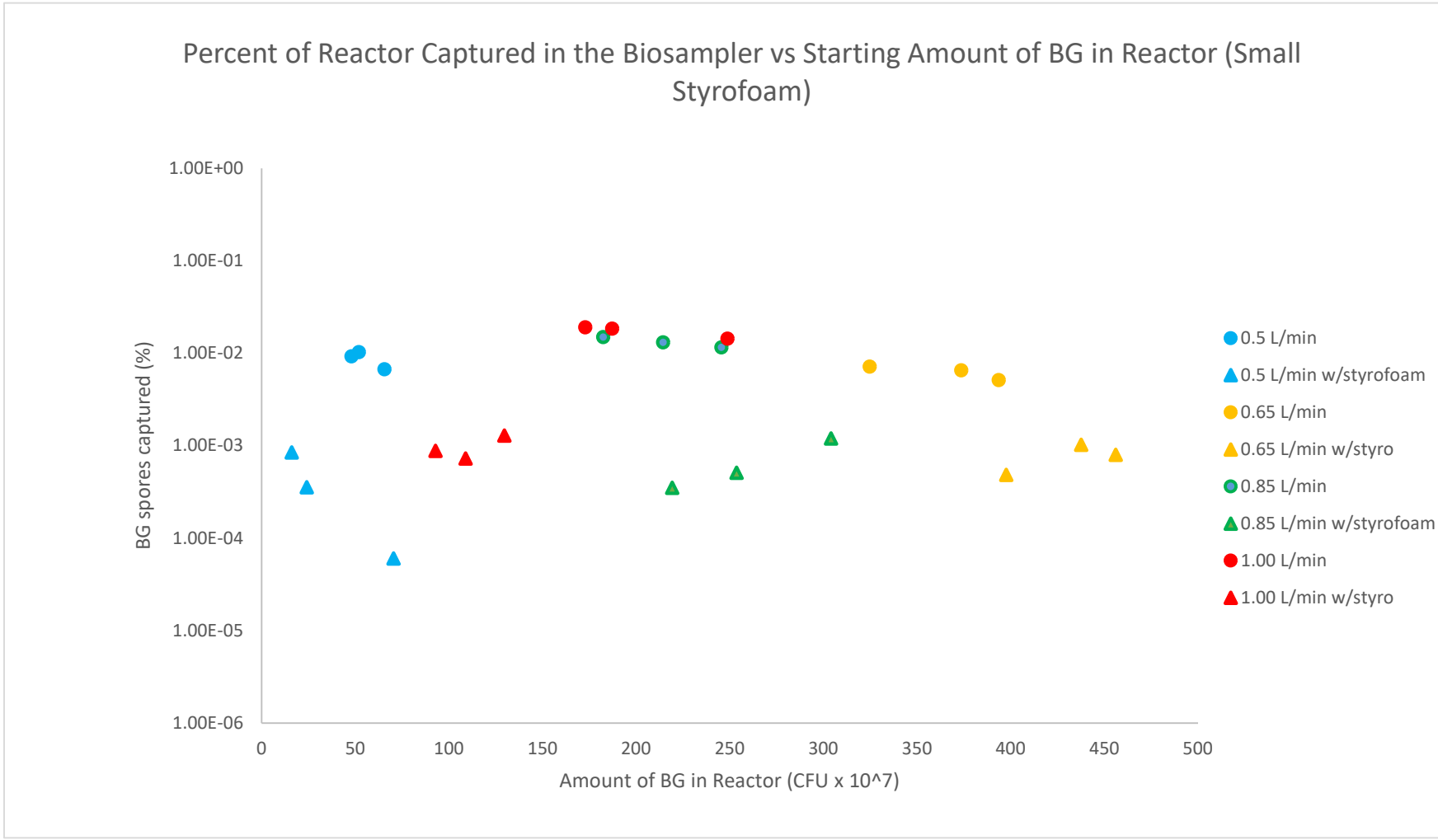

Figure 28. Percent of the reactor captured in the BioSampler versus starting amount of BG in the reactor (0.42 cm diameter spheres added)

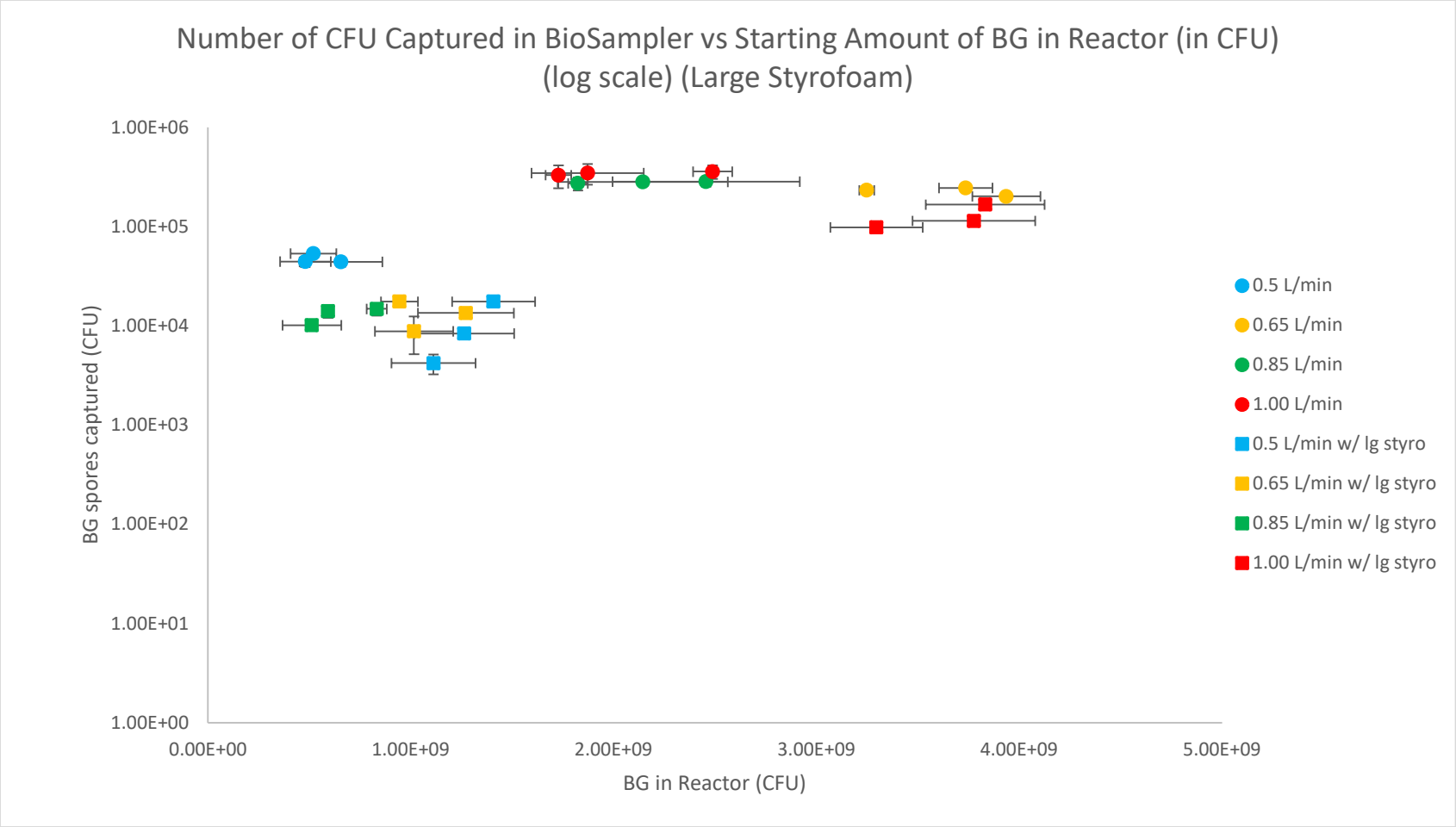

Figure 29. Number of CFU captured in BioSampler versus starting amount of BG in the reactor (CFU) (log scale) (1.91 cm diameter spheres added)

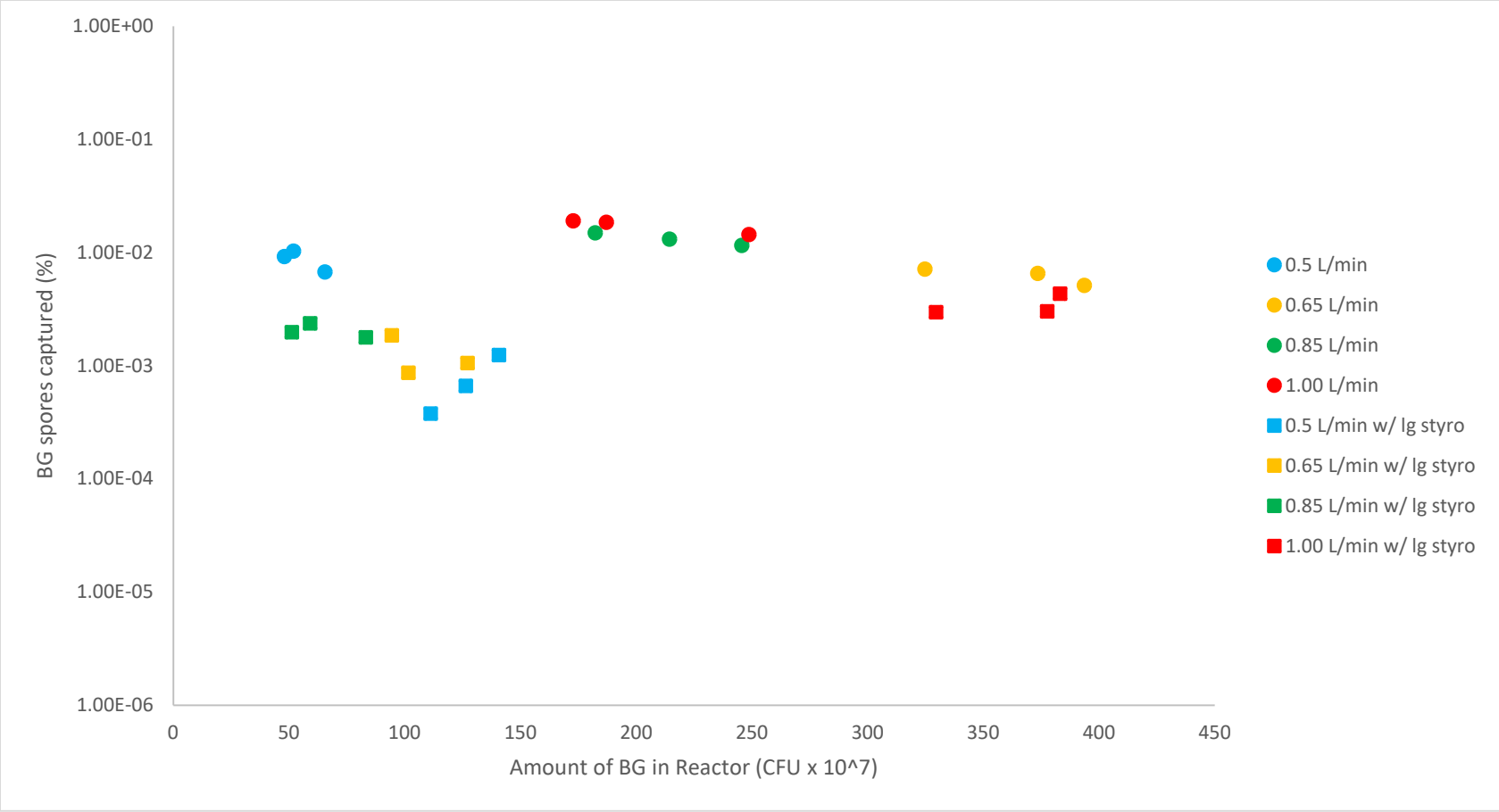

Figure 30. Percent of reactor captured in the BioSampler versus the starting amount of BG in the reactor (1.9 cm diameter spheres added)

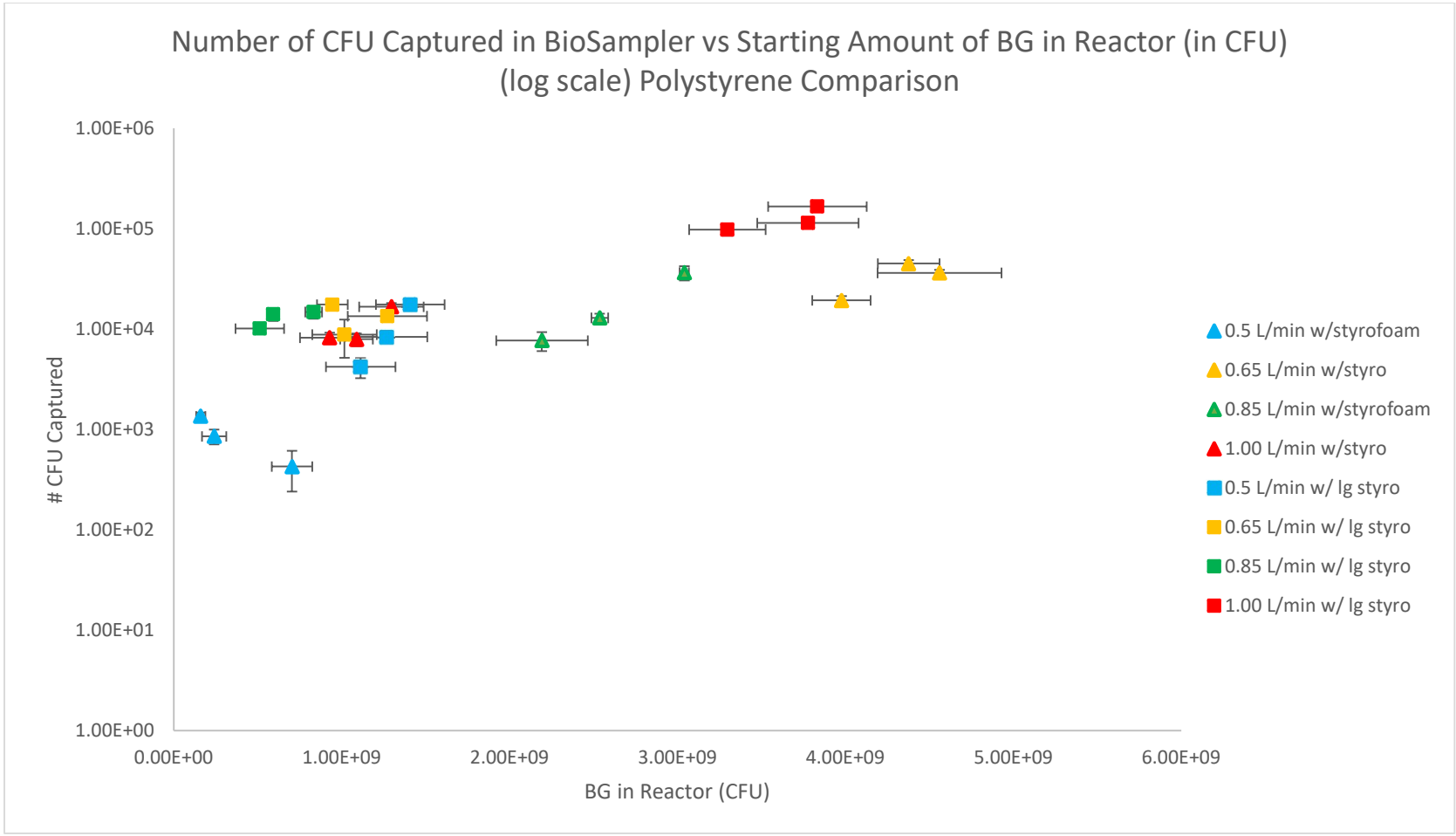

Figure 31. Number of CFU captured in BioSampler versus starting amount of BG in the reactor (CFU) (log scale) (comparison of 0.42 and 1.91 cm diameter spheres)

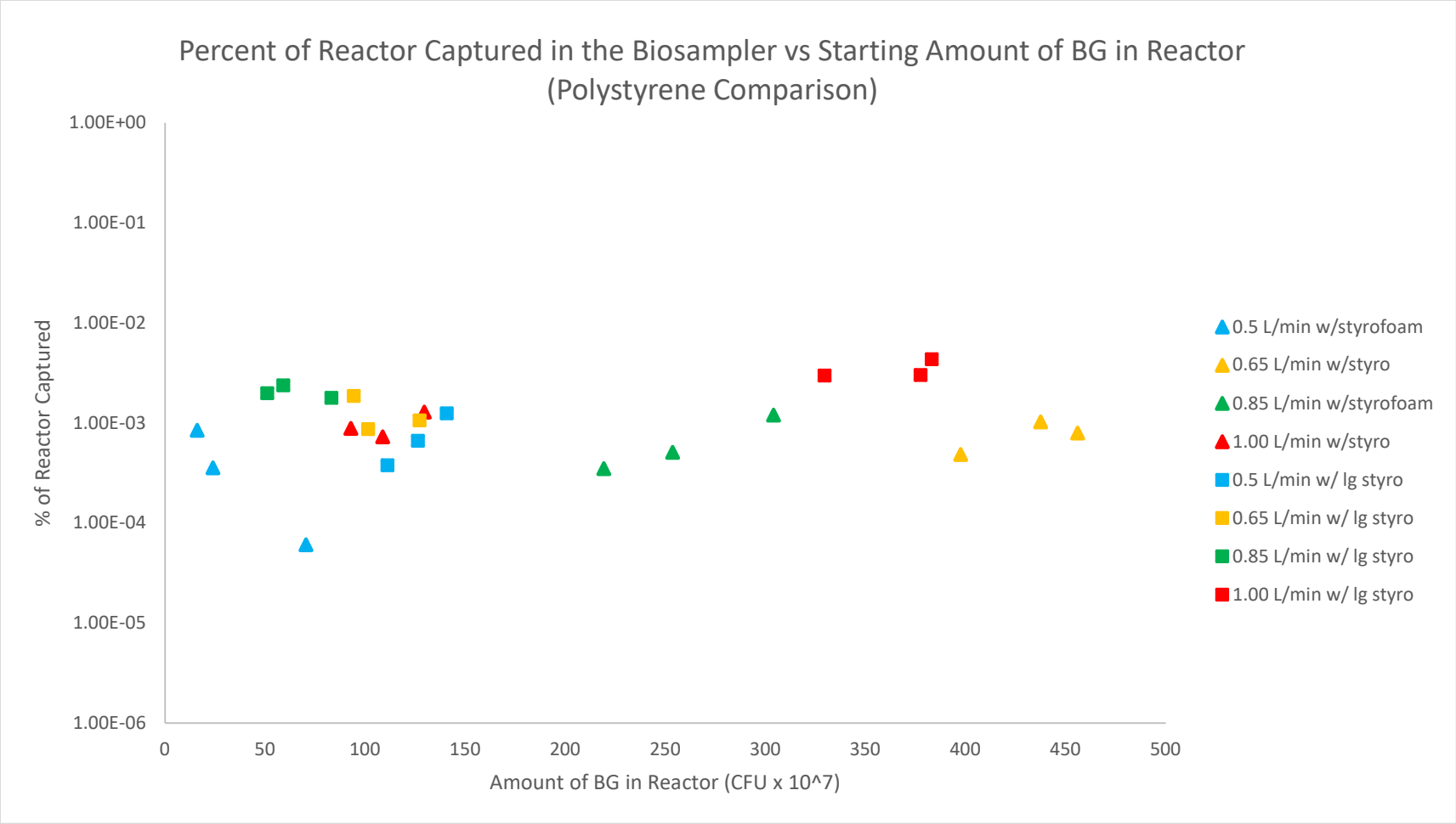

Figure 32. Percent of reactor captured in the BioSampler versus starting amount of BG in the reactor (comparision of 0.42 and 1.91 cm diameter spheres)

Appendix B: Field Rotameter Calibration

SKC Field Rotameter Calibration

Primay Calibration Standard: Bios Defender 510

Defender 510 Flow Rate (L/min)	Defender 510 Average (L/min)	SKC Field Rotameter Flow Rate (L/min)	Std Dev
1.0773			
1.0667			
1.0746			
1.0672			
1.0711	1.07138	1.05	0.004606
0.50603			
0.50669			
0.50553			
0.50495			
0.50675	0.50599	0.45	0.000769
0.64090			
0.64029			
0.63952			
0.63965			
0.63869	0.63981	0.55	0.000834
0.84323			
0.83830			
0.84294			
0.83889			
0.84376	0.841424	0.80	0.002608
1.2046			
1.2044			
1.2155			
1.2047			
1.2046	1.20676	1.25	0.004887

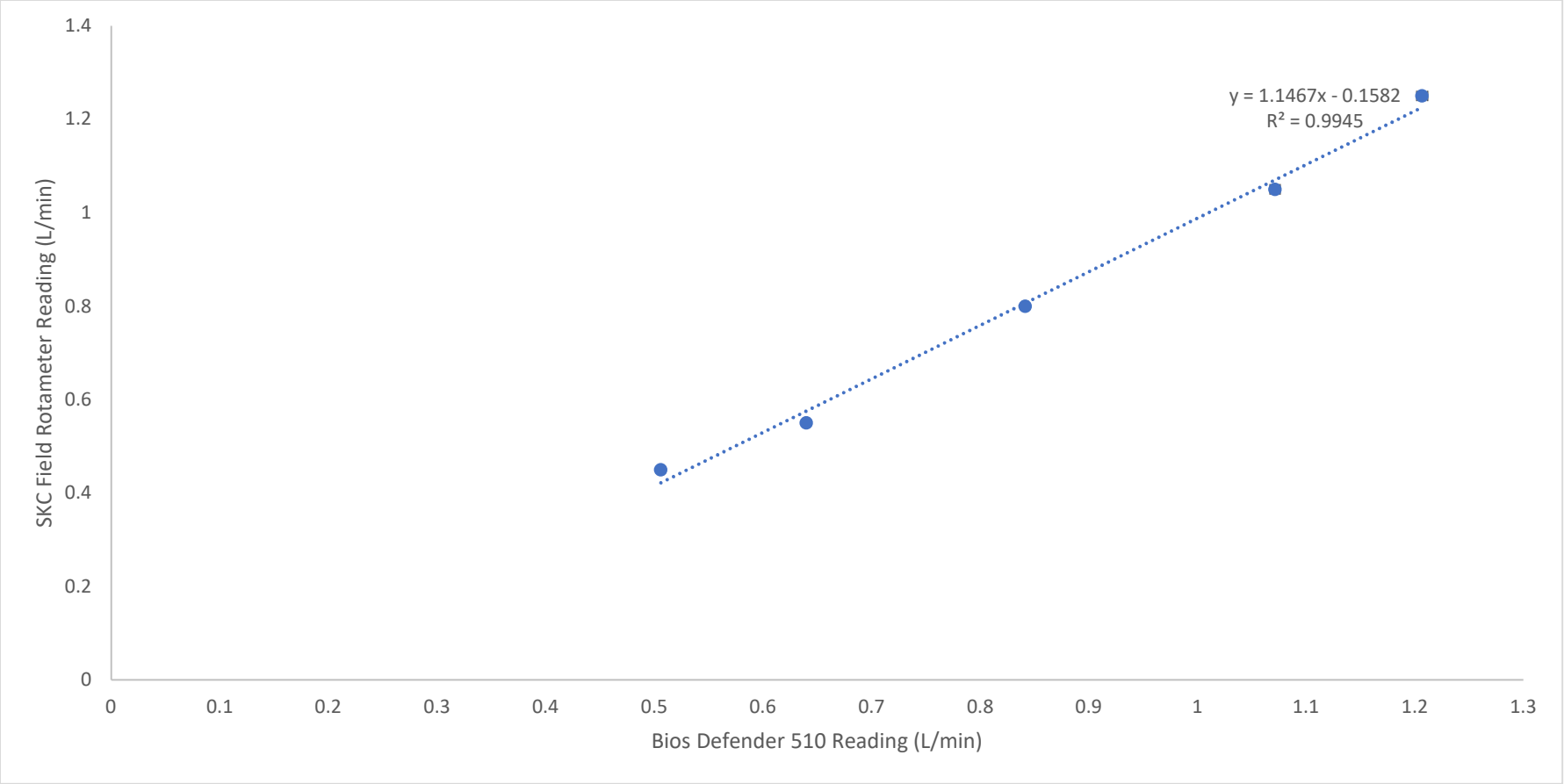

Figure 33. SKC Field Rotameter Calibration Curve

Appendix C: Literature Review WWTP Summary

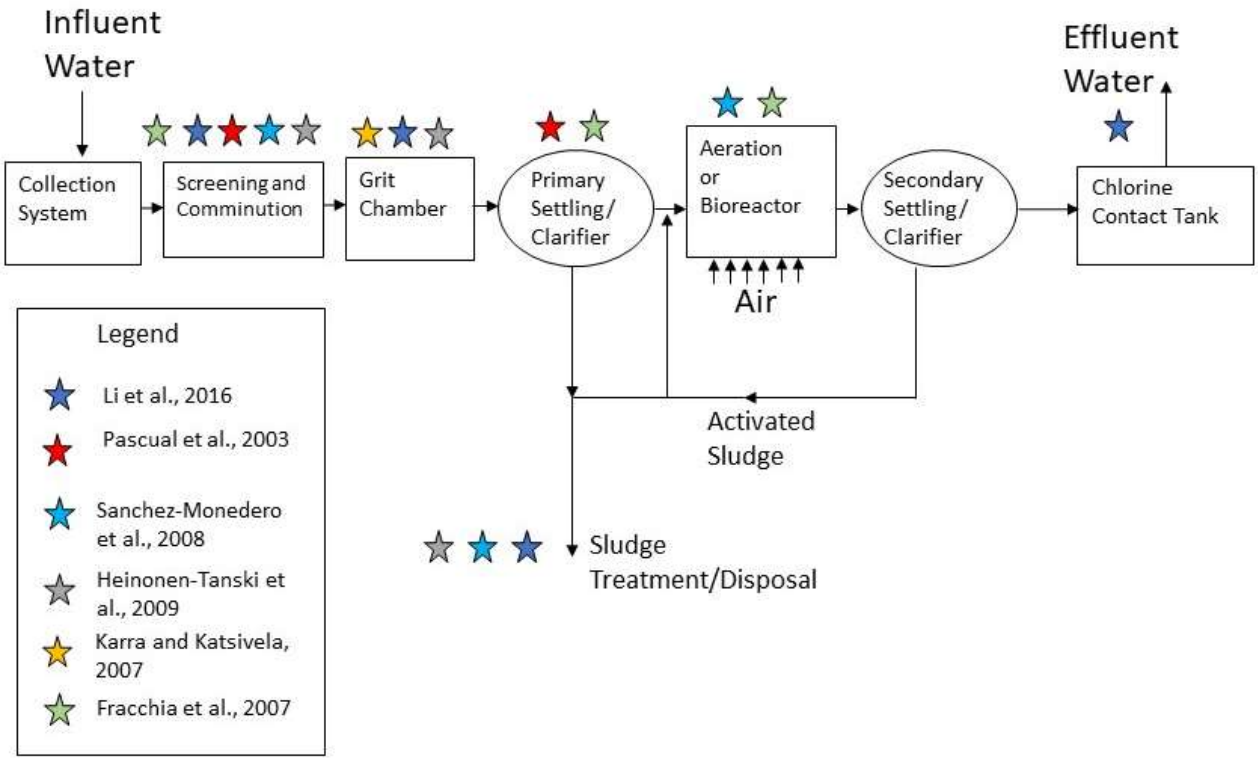

Figure 34. Literature Review summary of WWTP locations with highest observed microorganism concentrations due to bioaerosol production

Appendix D: Comparison of Endospore Physical Characteristics of BG and BA (Sterne strain)

Table 6. Comparison of endospore physical characterisitcs of BG and BA (Sterne strain) (*Data from Carrera et al., 2007, **Data from Chen et al., 2010)

Parameter	BG	BA (Sterne strain)
Average Spore Length *	1.22 ± 0.12 µm	1.49 ± 0.17 µm
Average Spore Width *	0.65 ± 0.5 µm	0.85 ± 0.08 µm
Average Spore Aspect Ratio *	1.85 ± 0.19	1.75 ± 0.20
Average Volume *	0.273 ± 0.046 μm^3	0.569 ± 0.140 μm^3
Average Density (wet) *	1.201 ± 0.0030 g/mL	1.162 ± 0.0023 g/mL
Average Density (dry) *	1.45 ± 0.02 g/mL	1.42 ± 0.01 g/mL
Weight *	328 fg	661 fg
Outermost Layer **	Spore Coat	Exosporium
Polarity **	Monopolar	Monopolar
Charge **	Negative	Negative

REPORT DOCUMENTATION PAGE

Form Approved
OMB No. 074-0188

PLEASE DO NOT RETURN YOUR FORM TO THE ABOVE ADDRESS.

1. REPORT DATE *(DD-MM-YYYY)*	2. REPORT TYPE	3. DATES COVERED *(From – To)*
26-03-2020	Master's Thesis	October 2018 – March 2020

TITLE AND SUBTITLE

The Effect of Aeration Rate and Free-Floating Carrier Media on the Emission of *Bacillus globigii* in Bioaerosols

5a. CONTRACT NUMBER

5b. GRANT NUMBER
DW-057-92440901-3

5c. PROGRAM ELEMENT NUMBER

6. AUTHOR(S)

Owens, Andrew J., Major, USA

5d. PROJECT NUMBER

5e. TASK NUMBER

5f. WORK UNIT NUMBER

7. PERFORMING ORGANIZATION NAMES(S) AND ADDRESS(S)

Air Force Institute of Technology
Graduate School of Engineering Physics (AFIT/ENP)
2950 Hobson Way, Building 640
Wright-Patterson AFB OH 45433-8865

8. PERFORMING ORGANIZATION REPORT NUMBER
AFIT-ENP-MS-20-M-110

9. SPONSORING/MONITORING AGENCY NAME(S) AND ADDRESS(ES)

Matthew L. Magnuson, PhD
Environmental Protection Agency
Office of Research and Development/National Homeland Security Research Center Water Infrastructure Protection Division MS NG-16
26 W. Martin Luther King Drive
Cincinnati, OH 45268

10. SPONSOR/MONITOR'S ACRONYM(S)
US EPA

11. SPONSOR/MONITOR'S REPORT NUMBER(S)

12. DISTRIBUTION/AVAILABILITY STATEMENT

Distribution Statement A. Approved for Public Release; Distribution Unlimited.

13. SUPPLEMENTARY NOTES

14. ABSTRACT

Aerosols produced by turbulent mechanical mixing and bubble aeration at Waste Water Treatment Plants (WWTPs) become bioaerosols with the entrainment of biological materials. Bioaerosols become a public health risk when human pathogens are present. This study evaluated bioaerosols containing *Bacillus globigii* (BG) spores, and the effects that aeration rate and the addition of Free-Floating Carrier Media (FFCM) had on the amount of BG spores collected following aerosolization. A series of laboratory-scale experiments investigated two different sizes of floating polystyrene spheres as FFCM and four different aeration rates. When the differences in compared aeration rates were sufficiently large, a positive correlation was observed between increasing aeration rate and increasing bioaerosol production. The maximum increase from 0.50 to 1.00 L/min resulted in a 97.58% increase in the percent of starting BG spores captured after aerosolization. The addition of FFCM of both sizes reduced the amount of BG spores captured when compared to the control. Smaller spheres (0.42 cm diameter) consistently attenuated BG bioaerosol emissions more effectively than those with larger (1.91 cm) diameters, with a mean control efficiency of 93.03% compared to 83.95%. Statistical analysis showed a significant increase in the ability of smaller diameter FFCM to attenuate bioaerosol production at the two higher investigated aeration rates. This study was the first, to the author's knowledge, to investigate multiple effects on bioaerosol production where the aerosol contained strictly bacterial endospores. As a part of a larger investigation including laboratory scale and pilot-scale WWTP research, this study is the first in a series of studies intended to investigate the effect of experimental scale on bioaerosol production. Results related to effects due to scale can be applied to better predict bioaerosol behaviors in operating treatment plants.

15. SUBJECT TERMS

Bioaerosol, BG, Anthrax, aeration rate, Free-floating carrier media, WWTP

16. SECURITY CLASSIFICATION OF:			17. LIMITATION OF ABSTRACT	18. NUMBER OF PAGES	19a. NAME OF RESPONSIBLE PERSON
a. REPORT	b. ABSTRACT	c. THIS PAGE			Dr. Larry W. Burggraf, AFIT/ENP
U	U	U	UU	153	19b. TELEPHONE NUMBER *(Include area code)* (937) 255-6565, x4507 larry.burggraf@afit.edu

Standard Form 298 (Rev. 8-98)
Prescribed by ANSI Std. Z39-18